Design, Synthesis, and Biological Evaluation of 1,2,4-Oxadiazole Derivatives Containing an Aryl Carboxylic Acid Moiety as Potent Sarbecovirus Papain-like Protease Inhibitors

Bo Qin,[⊥] Chengwei Wu,[⊥] Binbin Zhao,[⊥] Gang Li, Baolian Wang, Mengdie Ou, Ziheng Li, Xuli Lang, Peng Li,* Jiangning Liu,* Sheng Cui,* and Haihong Huang*
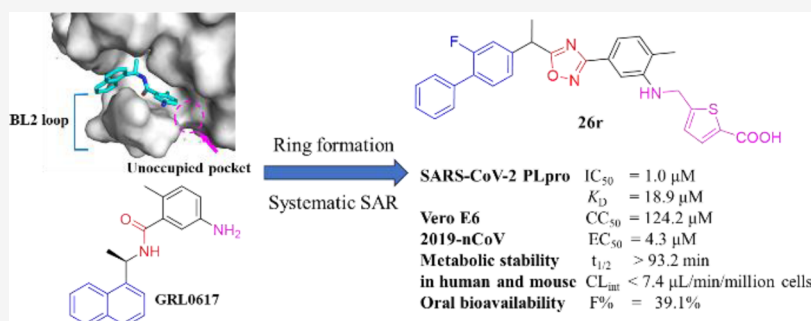
ACCESS | Metrics & More | Article Recommendations | SI Supporting Information

ABSTRACT: Papain-like protease (PLpro) is a promising therapeutic target for its pivotal role in the life cycle of SARS-CoV-2. A series of 1,2,4-oxadiazole derivatives was designed and synthesized via a ring formation strategy based on SARS-CoV-2 PLpro−GRL0617 complex structure. Systematic structure−activity relationship studies revealed that introducing oxadiazole and aryl carboxylic acid moieties to GRL0617 enhanced the enzymatic inhibition activity, affinity, and deubiquitination capacity toward PLpro. 1,2,4-Oxadiazole compounds **13f** and **26r**, which had PLpro inhibition activity (IC$_{50}$ = 1.8 and 1.0 μM) and antiviral activity against SARS-CoV-2 (EC$_{50}$ = 5.4 and 4.3 μM), exhibited good metabolic stability ($t_{1/2}$ > 93.2 min) and higher plasma exposure (AUC$_{0-t}$ = 17,380.08 and 24,289.76 ng·h/mL) in mice. Especially, compound **26r** with moderate oral bioavailability of 39.1% and potent antiviral activity is worthy of further studies *in vivo*. Our findings provide a new insight for the discovery of antiviral agents targeting PLpro.

INTRODUCTION

COVID-19 is not the largest epidemic in history, but it has caused the most fatalities in the past century. Since December 2019, over 760 million cases and 6.9 million deaths have been recorded worldwide, although the actual figures are presumed to be higher.[1] Despite the World Health Organization declaring the end of the emergency phase of COVID-19 in May 2023, the persisting challenges of long COVID[2] and immunity debt[3] resulting from this epidemic are expected to endure into the foreseeable future.

Although vaccination is key in early preventive therapy,[4,5] the prompt and appropriate use of antiviral agents is crucial in reducing both morbidity and mortality, restoring healthcare capacity, and facilitating a return to the new normal. Present antiviral therapies for COVID-19 include neutralizing monoclonal antibodies[6] and direct antiviral agents, like molnupiravir,[7] which targets RNA-dependent RNA polymerase, and nirmatrelvir,[8] which targets 3-chymotrypsin like protease. To avoid single-drug-induced resistance,[9−12] the focus has shifted toward identifying additional potential drug targets among

various nonstructural SARS-CoV-2 proteins[13,14] because these proteins have well-defined binding sites and vital roles in the viral life cycle. One such protein is papain-like protease (PLpro),[15] which is pivotal in viral replication, maturation, and immune evasion. Apart from its role in site-specific hydrolysis of viral polyproteins, PLpro can also hydrolyze and remove several post-translational modifications from host proteins involved in the innate immune response.[16] This dual functionality makes PLpro an enticing therapeutic target.

Considerable progress has been made in discovering and characterizing small-molecule inhibitors that target SARS-CoV PLpro.[17−20] Structural analysis shows that most reported SARS-CoV/SARS-CoV-2 PLpro inhibitors have the *N*-
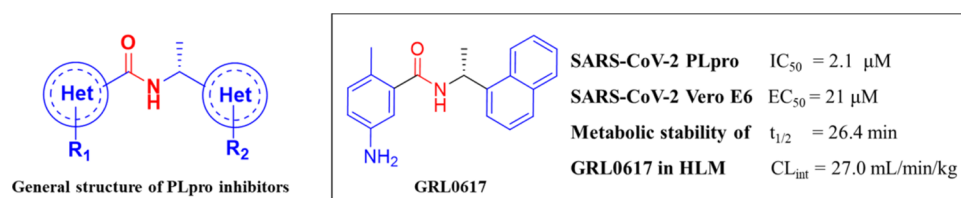
Figure 1. General structure of PLpro inhibitors and biological activities of GRL0617.
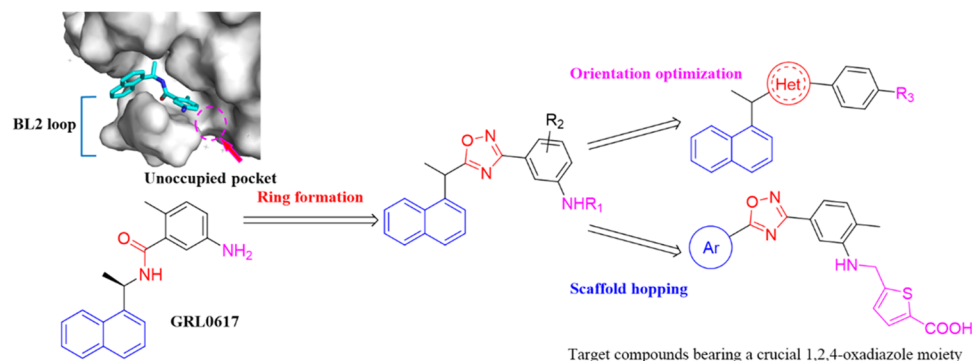

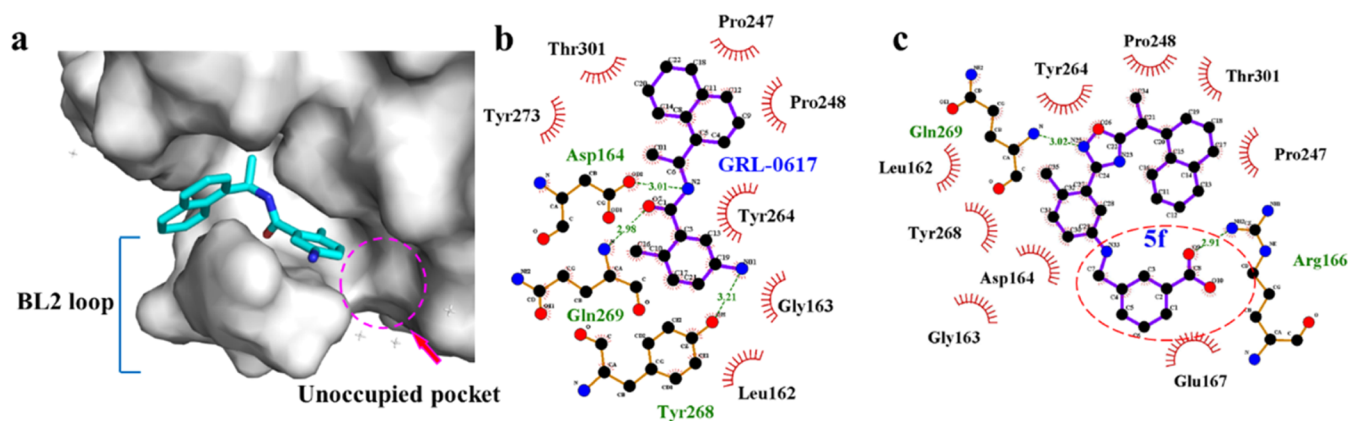**Figure 2.** Design strategy for target compounds.

Figure 3. Design of model compound **5f** based on the analysis of the cocrystal structure of the SARS-CoV-2 PLpro−GRL0617 complex. (a) Crystal structure of SARS-CoV-2 PLpro complexed with GRL0617 (PDB: 7CMD). (b) Noncovalent interactions of GRL0617 with PLpro. (c) Docking model of **5f** in the binding site of PLpro (PDB: 7CMD).

benzylbenzamide backbone (Figure 1).[21,22] GRL0617, a naphthylmethylbenzamide compound, remains one of the most potent PLpro inhibitors reported,[19,23] despite multiple high-throughput screening[24] and medicinal chemistry optimization campaigns. GRL0617 was originally developed as a deubiquitinase inhibitor and was later identified as a SARS-CoV PLpro inhibitor by high-throughput screening.[17] Because SARS-CoV-2 and SARS-CoV PLpro share a sequence identity of 83% and similarity of 90%,[25,26] GRL0617 has also been repurposed for SARS-CoV-2 PLpro, and multiple studies have reported that it inhibits SARS-CoV-2 PLpro with an IC$_{50}$ value of approximately 2.1 μM and SARS-CoV-2 viral replication with an EC$_{50}$ value of around 21 μM.[27] However, the poor metabolic stability of GRL0617 has prompted us to explore the *N*-benzylbenzamide backbone further and improve the druggability (Figure 1).[28]

Herein, we designed and synthesized a series of 1,2,4-oxadiazole derivatives through a ring formation strategy focusing on improving metabolic stability. Further optimization around the unoccupied pocket based on the crystal

structure of the SARS-CoV-2 PLpro−GRL0617 complex[29] led to the discovery of terminal aryl carboxylic acid moieties. The subsequent *in vitro* enzymatic activity evaluation and systematic step-by-step structure−activity relationship (SAR) exploration mostly focusing on the amine in the phenyl ring and the naphthyl group resulted in a series of target compounds with superior potency compared with GRL0617 (Figure 2). Various biochemical assays were performed, including melting temperature assessments, binding activity, and deubiquitination. Ultimately, we developed 1,2,4-oxadiazole derivatives **13f** and **26r** that exhibited potent PLpro inhibitory activities with improved metabolic stability and lower EC$_{50}$ values against different SARS-CoV-2 variants of concern. Collectively, these findings provide critical insights for further structure-based drug design against PLpro to explore higher-potency inhibitors for human therapeutics.

■ RESULTS AND DISCUSSION

Exploring the Ring Formation Strategy for Molecular Design. Our previous work on the cocrystal structure of

Scheme 1. General Synthetic Route to Target Compounds with 1,2,4-Oxadiazole Scaffold 5a−p[a]
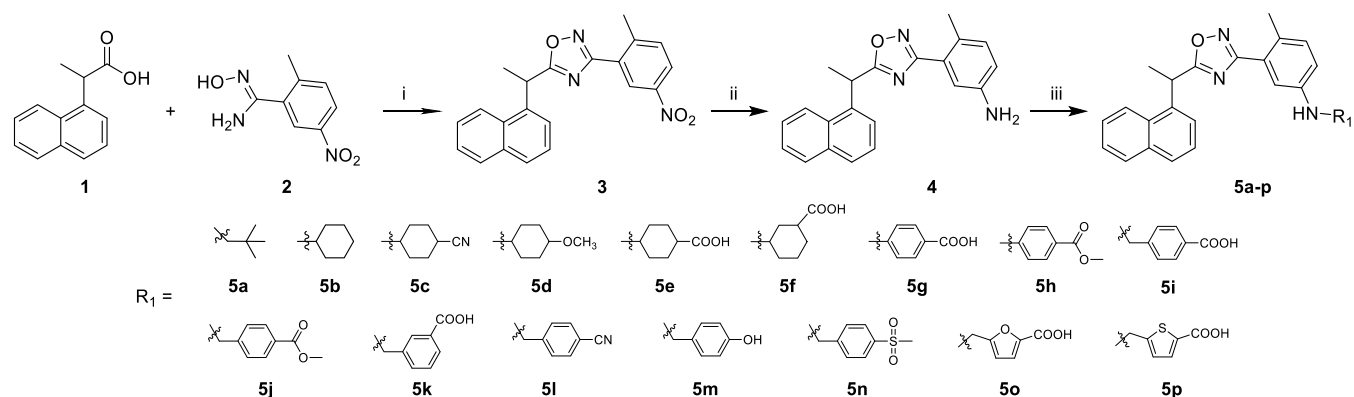
[a]Reagents and conditions: (i) NMM, CDMT, 1,4-dioxane, rt, 1 h, then, reflux, 6 h, 66%; (ii) Zn, NH$_4$Cl, ethanol/H$_2$O, rt, 2 h, 61%; (iii) corresponding aldehyde, AcOH, NaBH(OAc)$_3$, 1,2-dichloroethane, rt, 3 h, 43−84%; or substituted bromobenzene, Pd(OAc)$_2$, BINAP, Cs$_2$CO$_3$, toluene, Ar, 100 °C, 12 h, 72−73% (for **5g**, **5h**).

Scheme 2. General Synthetic Route to Target Compounds Containing Aryl Carboxylic Acid Moiety 9a−i[a]
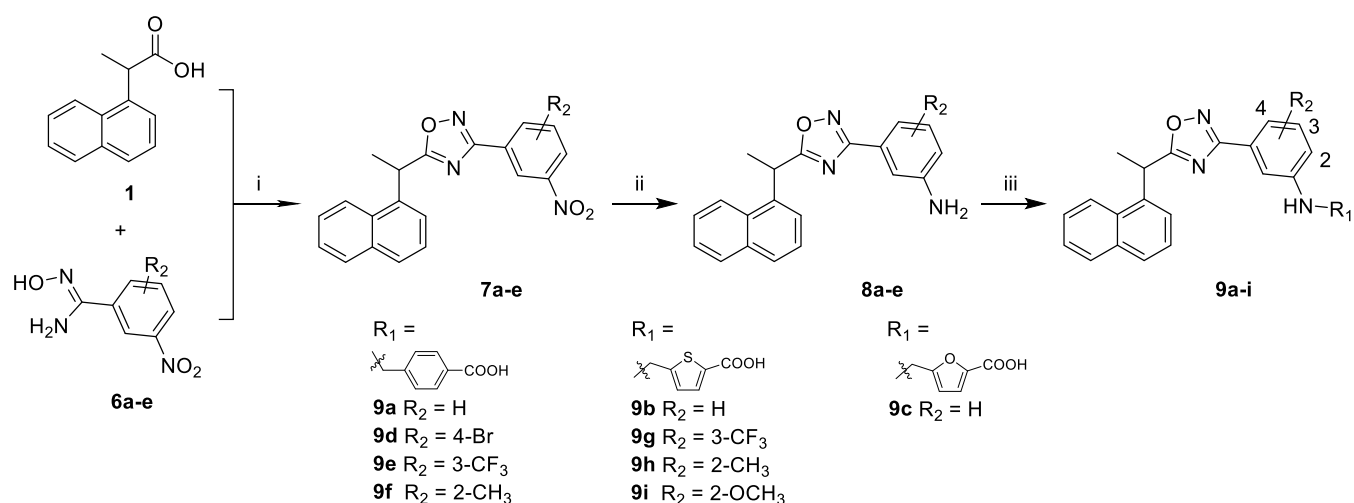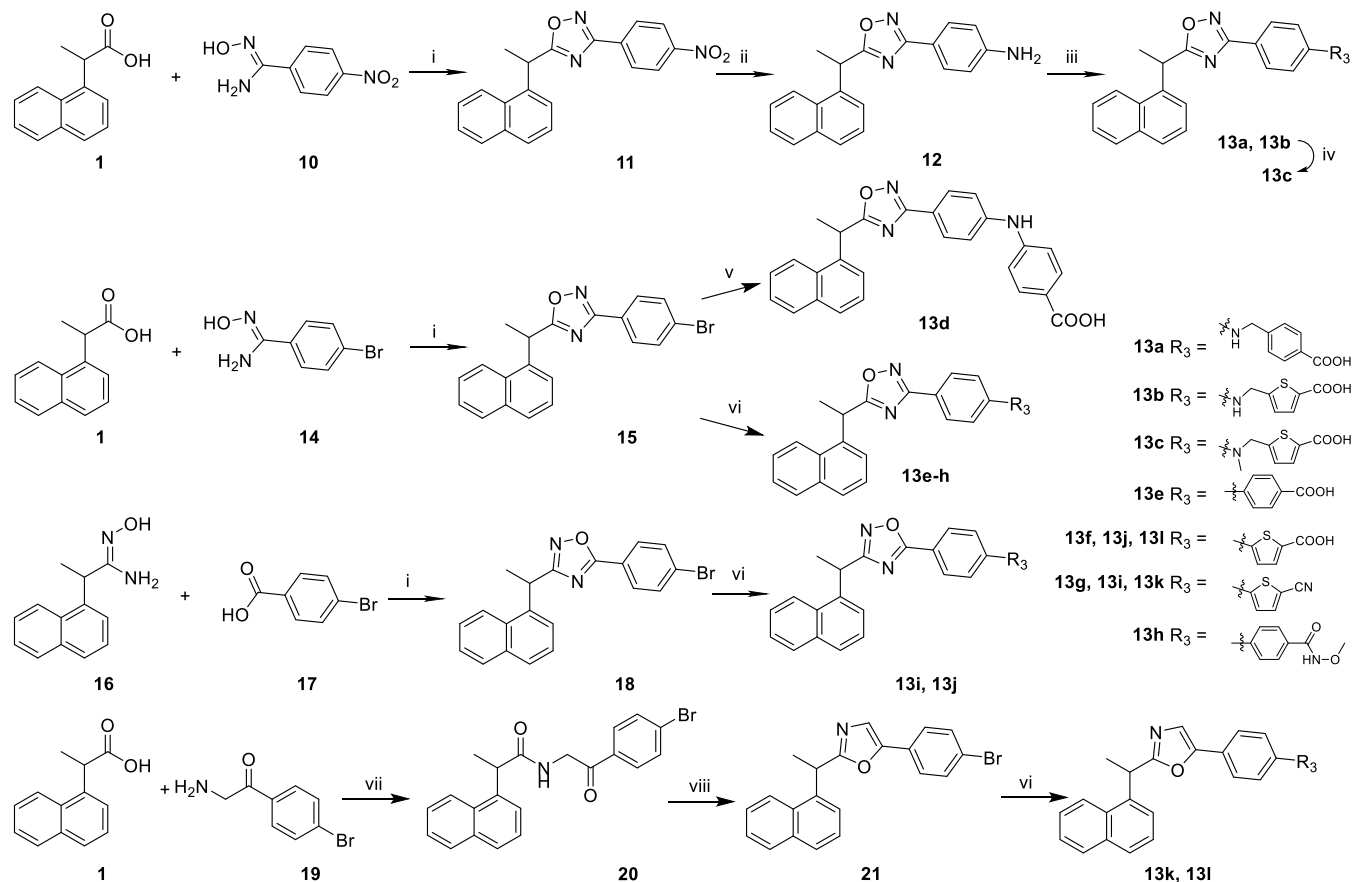

[a]Reagents and conditions: (i) NMM, CDMT, 1,4-dioxane, rt, 1 h, then, reflux, 6 h, 46−62%; (ii) Zn, NH$_4$Cl, ethanol/H$_2$O, rt, 2 h, 59−75%; (iii) corresponding aldehyde, AcOH, NaBH(OAc)$_3$, 1,2-dichloroethane, rt, 3 h, 55−88%.

SARS-CoV-2 PLpro with GRL0617 indicated that the interaction of the BL2 loop is crucial in inhibiting the protease activity of PLpro.[29] GRL0617 not only occupies the substrate pockets but also seals the entrance to the substrate binding cleft (Figure 3a). The benzamide group of GRL0617 forms two hydrogen bond interactions with key residues Gln269 and Asp164 in PLpro, thereby closing the BL2 loop (Figure 3b). We noticed that GRL0617 does not penetrate deep into the binding pocket due to its length. Introducing a suitable functional moiety in the unoccupied pocket may provide additional reinforcing interactions and increase the binding affinity.

We began our study with molecular modeling to understand the binding mode of the template compound **5f** and exploit interactions with the BL2 loop in SARS-CoV-2 PLpro (Figure 3c). The docking results show that compound **5f** fits well with the binding site around the BL2 loop. The nitrogen of the oxadiazole ring can form a hydrogen bond with Gln269 on the BL2 loop. There are T-shaped π−π interactions between **5f** and Tyr268, similar to the binding mode of GRL0617. Furthermore, the introduction of the cyclohexane carboxylic acid fragment in the unoccupied pocket creates an additional

hydrogen bond with Arg166, which may increase the binding affinity (Figure 3c). This predicted docking model, which was consistent with our design strategy, prompted us to explore the SAR of the oxadiazole compounds with other carboxylic acid moiety further.
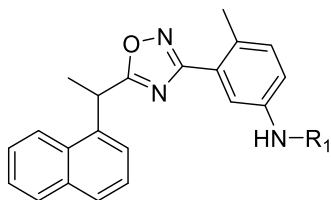
Chemistry. To explore the structure−activity relationship (SAR) of the 1,2,4-oxadiazole derivatives, the synthesis of target compounds is outlined in Scheme 1. The 1,2,4-oxadiazole scaffold was obtained through triazine-based coupling followed by cyclization. 2-(1-Naphthyl)propionic acid[30] **1** was treated with 2-chloro-4,6-dimethoxy-1,3,5-triazine (CDMT) and N-methylmorpholine (NMM) in 1,4-dioxane at room temperature. The corresponding activated ester was subsequently treated with nitroaromatic amidoxime[31] **2** to afford nitroaromatic 1,2,4-oxadiazole **3**.[32] Zinc-ammonium chloride-mediated reduction of compound **3** afforded aniline derivative **4**.[33] Compounds **5a−p** were prepared by reductive intermediate **4** with aldehyde in the presence of sodium triacetoxyborohydride in 1,2-dichloroethane at room temperature except for compounds **5g** and **5h** which were obtained through palladium-mediated C−N coupling. Similarly, the target compounds **9a−i** were synthesized using the same route

Scheme 3. General Synthetic Route to Target Compounds Bearing Various Oxazoles 13a–l[a]

[a]Reagents and conditions: (i) NMM, CDMT, 1,4-dioxane, rt, 1 h, then, reflux, 6 h, 43–66%; (ii) Zn, NH_4Cl, ethanol/H_2O, rt, 2 h, 75%; (iii) corresponding aldehyde, AcOH, NaBH(OAc)_3, 1,2-dichloroethane, rt, 3 h, 60–62%; (iv) CH_3I, K_2CO_3, acetone, reflux, 2 h, 62%; (v) 4-aminobenzoic acid, Pd(OAc)_2, BINAP, Cs_2CO_3, toluene, Ar, 100 °C, 12 h, 62%; (vi) Aryl boronic acids, Pd(PPh_3)_4, K_2CO_3, 1,4-dioxane/H_2O, Ar, 100 °C, 6 h, 30–68%; (vii) CDI, N,N-diisopropylethylamine (DIPEA), CH_2Cl_2, Ar, rt, 1 h, 67%; (viii) POCl_3, pyridine, rt, 2 h, 63%.

Scheme 4. General Synthetic Route to 2-Thiophene Carboxylic Acid Compounds 26a–t[a]
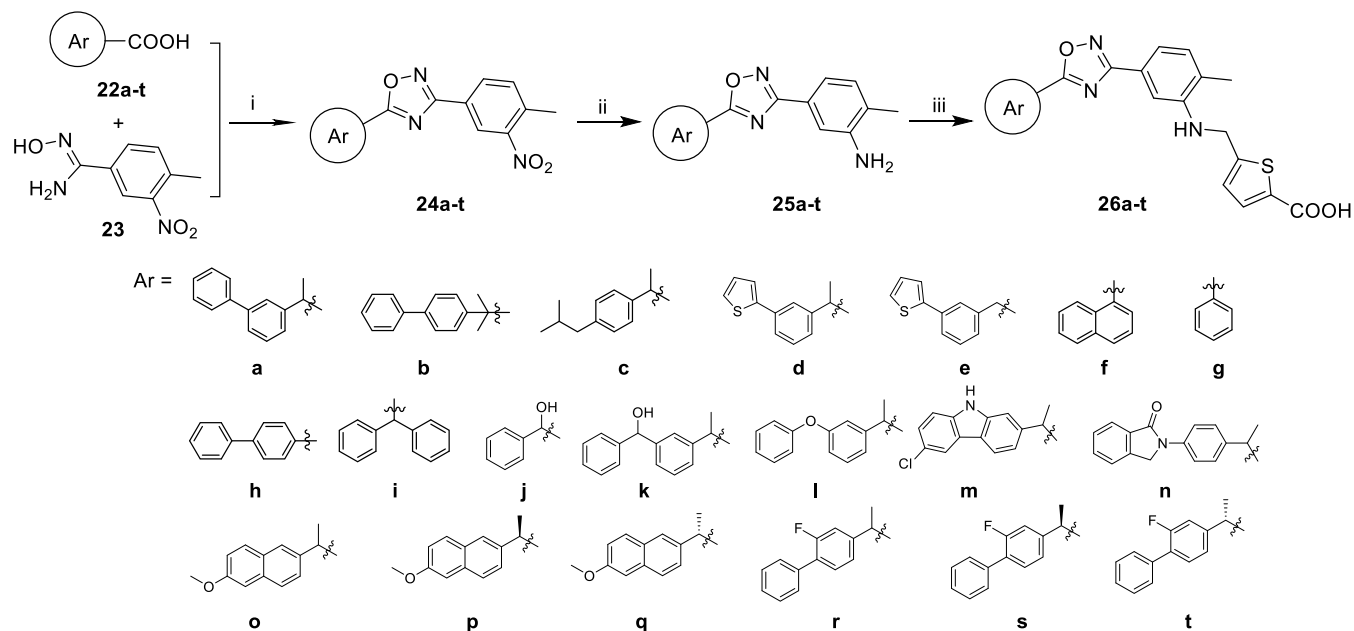
[a]Reagents and conditions: (i) NMM, CDMT, 1,4-dioxane, rt, 1 h, then, reflux, 6 h, 35–82%; (ii) Zn, NH_4Cl, ethanol/H_2O, rt, 2 h, 50–85%; (iii) 5-formylthenoic acid, AcOH, NaBH(OAc)_3, 1,2-dichloroethane, rt, 3 h, 21–73%.

Table 1. Exploration of Privileged R_1 Substituents on 1,2,4-Oxadiazole Compounds

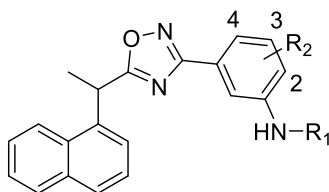| Compounds	R_1	IC_{50} (μM)
4	H	>200
5a		>200
5b		100.6
5c	CN	>200
5d	OCH_3	113.8
5e	COOH	22.7
5f	COOH	35.1
5g	COOH	10.7
5h		70.9
5i	COOH	11.2
5j		>200
5k	COOH	11.1
5l	CN	>200
5m	OH	176.5
5n		59.2
5o	COOH	14.4
5p	COOH	10.4
GRL0617		1.7

with different nitroaromatic amidoximes **6a**−**e** as the starting reagents (Scheme 2).

The synthetic route for the target compounds **13a**−**l** is shown in Scheme 3. The target compounds **13a**−**b** were synthesized using the same method as in Scheme 1. Under alkaline conditions, compound **13c** was obtained by *N*-methylation of compound **13b** with iodomethane. The brominated intermediate **15** was synthesized through triazine-based coupling using brominated amidoxime as the starting material, followed by reaction with *p*-aminobenzoic acid to yield compound **13d**. Suzuki coupling of intermediate **15** with various aromatic boric acids obtained the target compounds **13e**−**h**. Amidoxime compound **16** was synthesized

according to the literature method.[31] It reacted with 4-bromobenzoic acid **17** to yield the reversal 1,2,4-oxadiazole compound **18**, which then transformed to the target compounds **13i** and **13j** by Suzuki coupling reaction, respectively. Naphthylacetamide compound **20** was formed through CDI-mediated amide coupling between 2-(1-naphthyl)propionic acid **1** and amine compound **19**. Oxazole compound **21** was synthesized under the action of phosphorus oxychloride. The target compounds **13k** and **13l** were also obtained through Suzuki coupling reaction.

According to the same route shown in Scheme 1, the 2-thiophene carboxylic acid target compounds **26a**−**t** were

Table 2. SAR of R$_2$ Substituents with R$_1$ Containing Aryl Carboxylic Acids

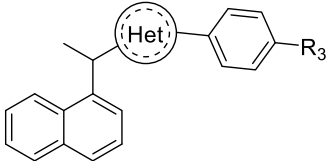| Compound	R$_1$	R$_2$	IC$_{50}$ (μM)
9a	benzene-COOH	H	7.5
9b	thiophene(S)-COOH	H	7.6
9c	furan(O)-COOH	H	96.5
9d	benzene-COOH	4-Br	2.1
9e	benzene-COOH	3-CF$_3$	0.2
9f	benzene-COOH	2-CH$_3$	0.2
9g	thiophene(S)-COOH	3-CF$_3$	0.1
9h	thiophene(S)-COOH	2-CH$_3$	0.1
9i	thiophene(S)-COOH	2-OCH$_3$	1.3
GRL0617			1.7

synthesized using different aryl carboxylic acids **22a**−**t** as the starting materials (Scheme 4).

SAR Optimization Strategy. Although lead compound GRL0617 has good inhibitory activity toward PLpro, its disadvantages of low antiviral potency and metabolic stability hinder its further *in vivo* pharmacokinetic and pharmacodynamic evaluation (Figure 1). By analyzing the structural characteristics and binding mode of GRL0617 in PLpro, we began with the modification of the amide group to obtain a series of 1,2,4-oxadiazole derivatives via a ring formation strategy and introduced suitable functional moieties in the unoccupied pocket. The target compounds were evaluated for their activities via fluorescence-based PLpro enzymatic inhibition assays in Tables 1−4 and GRL0617 was used as the reference compound for the PLpro inhibitory activity assay.

Privileged Fragment Identification via SAR Exploration of R$_1$ Substituents on Amine. Based on the cocrystal structure of GRL0617 and binding model of the template compound **5f** in PLpro, we concluded that the binding pocket in this active site was deep and not fully occupied. Therefore, R$_1$ functional fragments with different physical and chemical properties could be introduced to improve the activity and druggability profile further. Compound **4** with H as R$_1$ showed a loss of potency and the introduction of a bulky alkyl group (**5a**) led to no activity (Table 1). To our delight, compound **5b** bearing a cycloalkane group (IC$_{50}$ = 100.6 μM) exhibited some activity. To improve the affinity in this binding pocket, various polar groups, such as cyano (**5c**), methoxy (**5d**), and carboxyl (**5e**) groups, were introduced into the cyclohexane fragment. Compared with cyano and methoxy groups, the compound with 4-COOH group (**5e**, IC$_{50}$ = 22.7 μM) exhibited improved PLpro inhibitory activity. Changing the 4-

COOH group to 3-COOH (**5f**, IC$_{50}$ = 35.1 μM) resulted in the comparative potency compared with **5e**. Replacing the cycloalkane with an aromatic core increased the inhibitory activity (**5g**, IC$_{50}$ = 10.7 μM) compared with compound **5e**. To improve the flexibility of the terminal fragment, a methylene group was inserted between the nitrogen and aromatic substituent, and compound **5i** showed similar inhibitory activity to **5e**. Adjusting the position of the carboxyl group (**5k**) maintained the activity compared with **5i**, and the replacement of the carboxyl group (**5i**) with cyano (**5l**), hydroxyl (**5m**), and methylsulfonyl (**5n**) groups decreased the potency. Replacing benzoic acid (**5i**) with 2-furoic acid (**5o**, IC$_{50}$ = 14.4 μM) and 2-thiophene carboxylic acid (**5p**, IC$_{50}$ = 10.4 μM) resulted in good inhibitory activity for all. In addition, esterification of **5g** and **5i** to corresponding compounds **5h** and **5j**, respectively, decreased the activity. Accordingly, we concluded that introducing an aryl carboxylic acid moiety was tolerated at the R$_1$ site.

Optimization of R$_2$ Substituents with R$_1$ Containing Aryl Carboxylic Acids. Based on the preliminary identification of the aryl carboxylic acid moiety R$_1$, subsequently, we investigated the position and electrical properties of R$_2$ substituents on the benzene ring (Table 2). First, keeping the amino group in the ortho position, the effects of different R$_2$ substituents were explored. When substituent R$_2$ was H, the inhibitory activities of compound **9a** (IC$_{50}$ = 7.5 μM) with R$_1$ containing 4-benzoic acid and compound **9b** (IC$_{50}$ = 7.6 μM) with R$_1$ containing 2-thiophene carboxylic acid were improved substantially, whereas compound **9c** (IC$_{50}$ = 96.5 μM) with R$_1$ containing 2-furoic acid was decreased. There were no obvious differences in the inhibitory activity when we introduced the electron-withdrawing group CF$_3$ and the electron-donating

Table 3. SAR of R_3 Substituents with Various Oxazole Scaffolds

Compound	Het	R_3	IC_{50} (µM)
13a			50.2
13b			0.2
13c			4.0
13d			4.2
13e			11.7
13f			1.8
13g			0.6
13h			0.9
13i			31.4
13j			2.1
13k			20.8
13l			7.7
GRL0617			1.7

group CH_3 with R_1 containing 4-benzoic acid (**9e** vs **9f**) or 2-thiophene carboxylic acid (**9g** vs **9h**). The compound with a 4-bromo substituent when R_1 containing 4-benzoic acid (**9d**, IC_{50} = 2.1 µM) or with a 2-methoxy substituent when R_1-containing 2-thiophene carboxylic acid (**9i**, IC_{50} = 1.3 µM) showed similar activity to GRL0617. It was noted that the 2-thiophene carboxylic acid compounds (**9g** and **9h**, IC_{50} = 0.1 and 0.1 µM, respectively) displayed a 10-fold increase in potency relative to GRL0617 (IC_{50} = 1.7 µM). The results further indicated that 2-thiophene carboxylic acid may be the privileged fragment suitable for the unoccupied pocket.

Optimization of the Terminal Substituent Orientation and Center Oxazole Ring. To adjust the orientation of the terminal aryl carboxylic acid or polar moiety in the unoccupied pocket, a series of *para*-substituted on the benzene ring target compounds **13a−l** related to the *meta*-substituted compounds such as **5** series in Table 1 and **9** series in Table 2 was designed and synthesized (Table 3). *para*-Substituted compound **13a** showed lower activity than the corresponding *meta*-substituted compound **9a** (IC_{50} = 50.2 vs 7.5 µM), whereas compound **13b** with a 2-thiophene carboxylic acid moiety showed better activity than *meta*-substituted compound **9b** (IC_{50} = 0.2 vs 7.6 µM). The *N*-methylation compound

(**13c**) decreased the potency compared with **13b** (IC_{50} = 4.0 vs 0.2 µM). Removing methylene (**13d**) increased the potency compared with **13a** (IC_{50} = 4.2 vs 50.2 µM). Compared with compounds **13a** and **13b**, compounds **13e** and **13f** without the aminomethyl linker still maintained good activities. Replacing COOH (**13f**) with CN (**13g**) or $CONHOCH_3$ (**13h**) increased the potency slightly. Finally, we explored whether the 1,2,4-oxadiazole scaffold is best tolerated. The replacement with various oxazole scaffolds led to decreased potency, exemplified as compounds **13i** and **13k** compared with **13g** (IC_{50} = 31.4 and 20.8 µM vs 0.6 µM) and compounds **13j** and **13l** compared with **13f** (IC_{50} = 2.1 and 7.7 µM vs 1.8 µM). Therefore, the 1,2,4-oxadiazole and 2-thiophene carboxylic acid moieties were confirmed as the privileged fragments for further exploration.

Further Optimization of the Naphthalene Moiety. Based on the SAR results, naphthyl compound **9h**, which had privileged 1,2,4-oxadiazole and 2-thiophene carboxylic acid moieties and displayed the potent PLpro inhibitory activity, was selected as the model compound to explore the optimal aromatic fragment through scaffold hopping strategy (Table 4). Replacing the naphthalene ring with biphenyl (**26a**) gave good inhibitory activity compared with GRL0617 (IC_{50} = 4.3

Table 4. Optimization of the Naphthalene Moiety with Privileged 1,2,4-Oxadiazole and 2-Thiophene Carboxylic Acid Fragments

Compound	Ar	IC$_{50}$ (μM)	Compound	Ar	IC$_{50}$ (μM)
26a		4.3	26l		4.4
26b		35.4	26m		1.9
26c		3.6	26n		3.9
26d		4.1	26o		5.9
26e		6.8	26p		10.5
26f		11.6	26q		5.8
26g		59.0	26r		1.0
26h		25.5	26s		4.0
26i		9.0	26t		3.4
26j		435.4	GRL0617		1.7
26k		11.1			
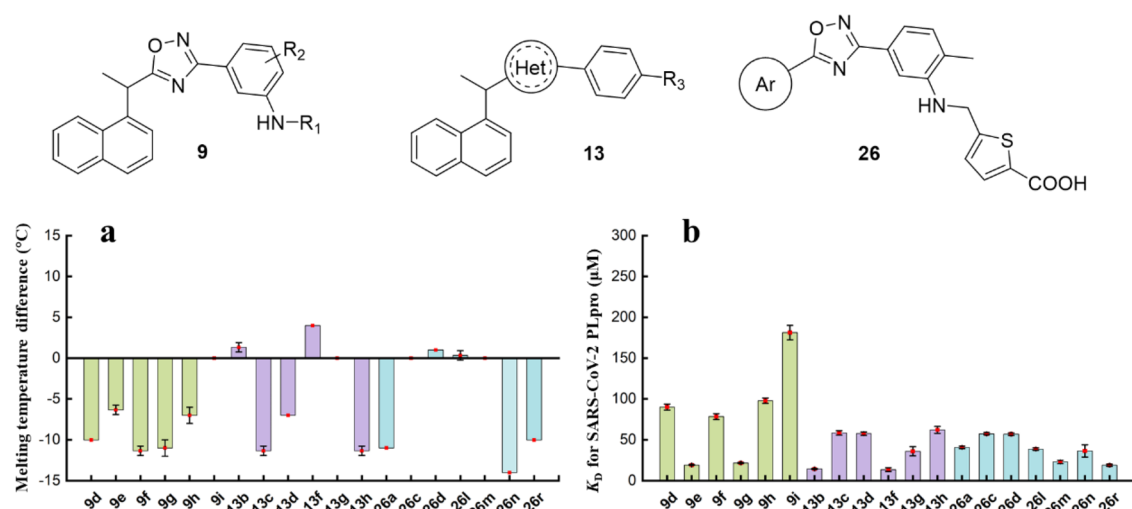
Figure 4. Screening and identification of effective compounds by melting temperature assay and biolayer interferometry. (a) Melting temperature assay. (b) Binding affinity activity.

vs 1.7 μM), whereas compound **26b** with a linear biphenyl moiety and additional methyl group had lower activity. A substituted phenyl scaffold with isobutyl (**26c**) and thienyl (**26d**) groups maintained the activity (IC$_{50}$ = 3.6 and 4.1 μM,

respectively). Removing the methyl to eliminate chirality (**26e**) resulted in similar activity compared with **26d** (IC$_{50}$ = 6.8 vs 4.1 μM). Subsequent modifications to remove the methylene did not increase the potency (**26f−i**, IC$_{50}$ = 9.0−59.0 μM).
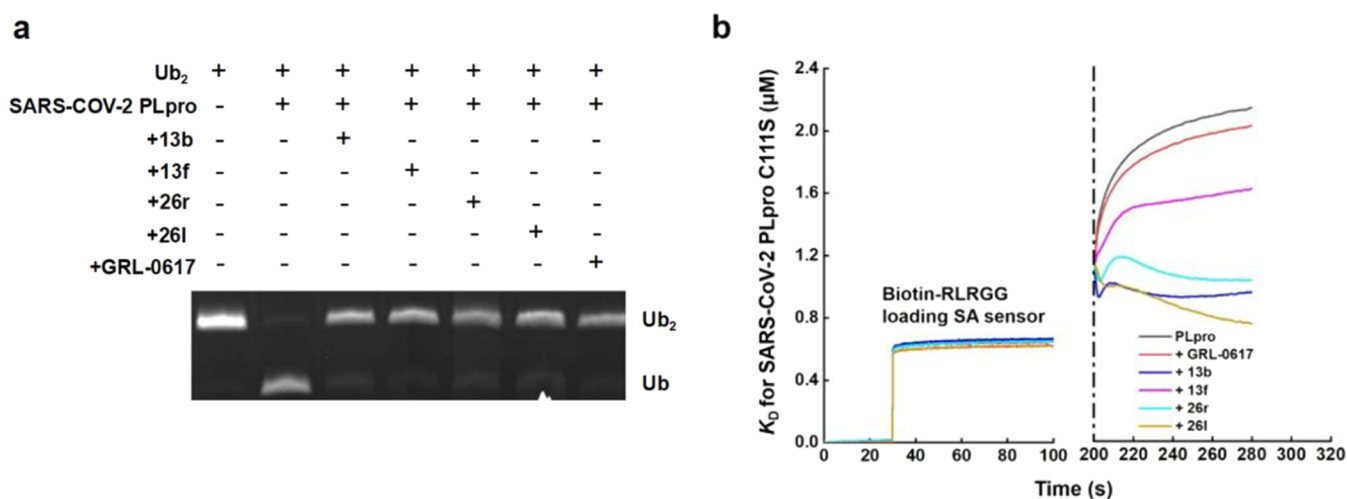
Figure 5. Deubiquitination and RLRGG competitive binding activity assays of four hit compounds **13b**, **13f**, **26l**, **26r**, and GRL0617 as the control. (a) Cleavage activity assay of K48-linked diubiquitin chains (2Ub-K48) by SARS-CoV-2 PLpro. Hit compounds impaired the interaction between peptide substrate RLRGG and SARS-CoV-2 PLpro. (b) Four hit compounds impaired the interaction between the RLRGG substrate peptide and SARS-CoV-2 PLpro C111S. Ub$_2$: diubiquitin; Ub: ubiquitin; SA: streptavidin.

The introduction of hydroxymethylene (**26j**) dramatically decreased the potency (IC$_{50}$ = 435.4 μM). Various aromatic rings were introduced (**26k–n**) and the inhibitory activities toward PLpro were measured accordingly. The results indicated that compounds containing benzylbenzene (**26k**), diphenyl ether (**26l**), carbazole (**26m**), and benzolactam (**26n**) displayed potent activity (IC$_{50}$ = 1.9–11.1 μM). Finally, we chose racemic compounds **26o** and **26r** with good potency to investigate the effect of the chirality of the benzyl methyl group on the activity. Distinct chiral isomers **26p** and **26q** as well as **26s** and **26t** maintained good potency (IC$_{50}$ = 3.4–10.5 μM), and the isomers exhibited no obvious differences compared with the corresponding racemates (**26o** and **26r**, IC$_{50}$ = 5.9 and 1.0 μM). Therefore, the more accessible racemates were promoted to evaluate the in vitro biological assay.

Validation of Effective Compounds Using Thermal Shift Assay and Biolayer Interferometry. Target compounds displaying good PLpro inhibition with IC$_{50}$ values below 5 μM (Supporting Information Figure S58) were selected for the binding activity assessment. First, these compounds were incubated with SARS-CoV-2 PLpro for 1 h on ice and the melting temperatures (T_m) of the complex with and without compounds were measured. Values obtained by subtracting the control temperature with dimethyl sulfoxide (DMSO) are shown in Figure 4a. T_m values of most compounds were less than that of the control, although those of **13b**, **13f**, **26d**, and **26l** were higher. Next, to identify the binding activity of the selected compounds with SARS-CoV-2 PLpro, the dissociation constant (K_D) values were obtained and compared using biolayer interferometry (Figure 4b and Supporting Information Figure S59). Most of the K_D values were at the micromolar level, especially for compounds **9e**, **9g**, **13b**, **13f**, **26m**, and **26r** (K_D = 13.6–23.1 μM). Based on the parameters including T_m and K_D, compounds **13b**, **13f**, **26l**, and **26r** were selected for further assessment.

Assays of Deubiquitination Activity and Competitive Binding Activity to RLRGG by Gel and Biolayer Interferometry. The SARS-CoV-2 PLpro cleavage activity of K48-linked diubiquitin to single ubiquitin with or without compounds **13b**, **13f**, **26l**, **26r**, and GRL0617 as the control

was measured by sodium dodecyl sulfate polyacrylamide gel electrophoresis (SDS-PAGE) (Figure 5a). All five compounds affected the cleavage activity of SARS-CoV-2 PLpro toward the linker peptide between the two ubiquitins. Therefore, a competitive binding assay was conducted between linker peptide RLRGG and the selected compounds, including GRL0617 as a control. The four compounds disrupted the interaction between RLRGG and PLpro to varying degrees (Figure 5b). Additionally, the enzymatic inhibitory activity of four compounds against SARS-CoV PLpro and Middle East respiratory syndrome coronavirus (MERS-CoV) PLpro indicated that these compounds exhibited broad-spectrum enzymatic inhibitory activity against sarbecovirus PLpro (Supporting Information Figure S60).

In Vitro Metabolic Stability Assay and In Vivo Pharmacokinetic Evaluation. To assess the metabolic stability of the selected compounds including GRL0617 as a control, we performed an in vitro metabolic stability assay in human and mouse. Compounds **9e** and **9g** showed moderate to good metabolic stability in hepatocytes. Compound **9g** was more stable than GRL0617. It was noted that compounds **13b**, **13f**, **26l**, and **26r** exhibited superior metabolic stability in liver microsomes with much longer half-life ($t_{1/2}$ > 93.2 min) and lower intrinsic clearance (CL$_{int}$ < 7.4 μL/min/million cells) (Table 5). The results indicated that our ring formation strategy was important in improving metabolic stability.

Spurred on by the potent PLpro inhibit activities, high binding activity, increased stability, and broad-spectrum enzymatic inhibitory activity, the pharmacokinetic properties of **13f** and **26r** were evaluated further. These two compounds were administered to mice through intravenous injection at a dose of 5 mg/kg or orally at a dose of 50 mg/kg (Table 6). The in vivo pharmacokinetic analysis indicated that **13f** had a favorable half-life ($t_{1/2}$ = 6.5 h) with medium plasma exposure (AUC$_{(0-t)}$ = 17,380.08 ng·h/mL) and lower plasma concentration (C_{max} = 3672.19 ng/mL). Compound **26r** had a moderate half-life ($t_{1/2}$ = 2.53 h), higher plasma exposure (AUC$_{(0-t)}$ = 24,289.76 ng·h/mL), and higher plasma concentration (C_{max} = 10,179.88 ng/mL). The mean residence time (MRT$_{0-t}$) of **13f** was much longer than that of **26r**, but the oral bioavailability was very low (F = 4.8%). Compound

Table 5. Metabolic Stability Assay in Human and Mouse[a]

Compound	$t_{1/2}$ (min) Human	$t_{1/2}$ (min) Mouse	CL_{int} (μL/min/million cells) Human	CL_{int} (μL/min/million cells) Mouse	Remaining[b] (%) Human	Remaining[b] (%) Mouse
9e	36.5	16.7	19.0	41.5	56.6	28.8
9g	92.4	53.9	7.5	12.9	79.8	68.0
13b	>93.2	>93.2	<7.4	<7.4	102.2	93.8
13f	>93.2	>93.2	<7.4	<7.4	82.1	100.7
26l	>93.2	>93.2	<7.4	<7.4	87.0	80.0
26r	>93.2	>93.2	<7.4	<7.4	100.9	99.1
GRL0617	45.0	7.6	15.4	91.5	63.0	6.4

[a]GRL0617, 9e, and 9g were measured in hepatocytes, and 13b, 13f, 26l, and 26r were measured in liver microsomes. [b]Substrate concentrations were determined in incubations after 30 min and normalized to concentrations at time zero.

Table 7. Antiviral Activity of Selected Compounds against SARS-CoV-2

Compound	CC_{50} (μM)	2019-nCoV EC_{50} (μM)	2019-nCoV Selectivity index[a]	Omicron BA.1 EC_{50} (μM)	Omicron BA.1 Selectivity index[a]
13f	170.0	5.4	31.5	25.2	6.7
26r	124.2	4.3	28.9	79.8	1.6
GRL0617	253.2	44.1	5.7	80.8	3.1

[a]Selectivity index = CC_{50}/EC_{50}.

inhibitory activities. Biochemical assays, including a thermal shift assay, biolayer interferometry, and deubiquitination, were conducted to validate the mode of action via PLpro. In particular, compared to the lead compound GRL0617, the representative compounds 13f and 26r with improved metabolic stability displayed potent antiviral activity against SARS-CoV-2 2019-nCoV and omicron BA.1 in cells. Compound 26r, which had an acceptable oral bioavailability, merited further *in vivo* efficacy studies along with compound 13f, which had a favorable half-life. Our efforts are ongoing to evaluate the druggability profiles of this series of 1,2,4-oxadiazole compounds with the aim of developing further promising candidates as antiviral agents targeting PLpro.

26r had acceptable oral bioavailability (F = 39.1%). Both compounds merited further antiviral evaluation.

Antiviral Activity of Representative PLpro Inhibitors against SARS-CoV-2. To evaluate the antiviral activity of 1,2,4-oxadiazole derivatives 13f and 26r against 2019-nCoV and omicron BA.1 in cells (Table 7), the cell viability in Vero E6 cells was tested. Then, the number of viral RNA copies in the cellular supernatant with diluted compound concentrations was measured using quantitative real-time polymerase chain reaction (qRT-PCR). Compounds 13f and 26r had low cytotoxicity and an 8-fold greater antiviral activity compared with GRL0617 (EC_{50} = 5.4 and 4.3 μM vs 44.1 μM). The selectivity index values toward the 2019-nCoV strain were higher than that of GRL0617. Compound 13f showed a 3-fold greater potency toward omicron BA.1 than GRL0617 (EC_{50} = 25.2 vs 80.8 μM). The results indicate that these 1,2,4-oxadiazole PLpro inhibitors with improved potency and pharmacokinetic properties have the potential to treat SARS-CoV-2.

◼ CONCLUSIONS

We designed, synthesized, and performed a biological evaluation of new 1,2,4-oxadiazole derivatives as PLpro inhibitors based on our previously reported crystal structure of the SARS-CoV-2 PLpro–GRL0617 complex. Systematic SAR studies provided new insight into the structural requirements for potent inhibitors discovery. Most derivatives with an aryl carboxylic acid moiety showed potent PLpro

◼ EXPERIMENTAL SECTION

General Chemistry Methods. Chemicals and solvents were purchased from commercial sources and were used as received. Dry solvents were purchased in Sure Seal bottles stored over molecular sieves. Thin-layer chromatography (TLC) was performed on silica gel plates (GF254) with visualization of components by UV light (254 nm). Column chromatography was carried out on silica gel (200−300 mesh). The structural characterizations of the prepared compounds were confirmed by ^{1}H NMR and ^{13}C NMR spectroscopy and high-resolution mass spectrometry (HR-MS). ^{1}H NMR spectra were obtained on an ECZ-400 spectrometer (JEOL, Tokyo, Japan) at 400 MHz, Bruker AVANCE 500 (Bruker, Rheinstetten, Germany) at 500 MHz, and Bruker AVANCE NEO (Bruker, Rheinstetten, Germany) at 700 MHz. ^{13}C NMR spectra were obtained on a Bruker AVANCE 500 (Bruker, Rheinstetten, Germany) at 125 MHz and a Bruker AVANCE NEO (Bruker, Rheinstetten, Germany) at 175 MHz. Chemical shift values were referenced to the residual solvent peak and reported in ppm (δ scale), and all coupling constant (J) values were given in Hz. CDCl$_3$ or DMSO-d_6 were used as the standard NMR solvents. The following multiplicity abbreviations are used: (s) singlet, (d) doublet, (t) triplet, (q) quartet, (m) multiplet, and (brs) broad singlet. HR-MS (ESI) data were measured on a Thermo Exactive Orbitrap plus spectrometer. All target compounds were purified by

Table 6. Mouse Pharmacokinetic Properties of Compounds 13f and 26r

Parameters	Units	13f po	13f iv	26r po	26r iv
Dose	mg/kg	50	5	50	5
$t_{1/2}$[a]	h	6.50	5.80	2.53	4.20
t_{max}	h	0.88	0.17	1.25	0.05
C_{max}	ng/mL	3672.19	14,193.89	10,179.88	10,586.04
AUC_{0-t}	ng·h/mL	17,380.08	36,274.38	24,289.76	6,206.05
$AUC_{0-\infty}$[b]	ng·h/mL	17,462.43	36,335.51	24,446.36	6,258.13
MRT_{0-t}	h	8.05	5.04	2.19	2.74
$MRT_{0-\infty}$[c]	h	8.29	5.12	2.72	2.96
Clearance	mL/min/kg		140.89		808.12
F[d]	%	4.8		39.1	

[a]Plasma elimination half-life. [b]Plasma exposure. [c]Mean residence time. [d]Oral bioavailability. po: oral administration; iv: intravenous administration.

chromatography and have a purity of >95% as determined by UPLC analysis conducted on Waters ACQUITY UPLC H-Class and ACQUITY QDa system, using a reversed-phase C18 column (ACQUITY UPLC BEH C18 1.7 μm 2.1 mm × 100 mm) with a gradient of 5−95% CH_3CN in water (0.1% HCOOH) in 8 min with a flow rate of 0.3 mL·min^{-1}.

General Procedure A to Synthesize 3-Nitroaromatic-1,2,4-oxadiazoles. To a stirred solution of NMM (15.0 mmol) in 1,4-dioxane (20.0 mL), CDMT (5.0 mmol) was added and stirred for 5 min. To the white suspension containing 4-(4,6-dimethoxy-1,3,5-triazin-2-yl)-4-methylmorpholinium chloride, a solution of carboxylic acid (5.0 mmol) was added and stirred at room temperature for 5 min. Then, the corresponding amidoxime (5.0 mmol), synthesized according to the literature method,[31] was added to the above reaction mixture and stirred at room temperature for 1 h and then refluxed for 6 h. After the completion of the reaction (monitored by TLC), the reaction mixture was cooled to room temperature, 100 mL of water was added, and extracted with 50 mL of ethyl acetate twice. The organic layer was combined, washed with brine, dried over Na_2SO_4, and concentrated under vacuum to afford the crude compound. The crude compound was purified with silica gel column chromatography using (hexane/EtOAc = 20:1) as eluents to afford the pure product.

3-(2-Methyl-5-nitrophenyl)-5-(1-(naphthalen-1-yl)ethyl)-1,2,4-oxadiazole (3). Following general procedure A, the target compound was afforded (1.18 g) as a yellow solid, yield 66%. ^{1}H NMR (400 MHz, CDCl$_3$) δ 8.94 (d, J = 2.5 Hz, 1H), 8.21 (dd, J = 8.5, 2.5 Hz, 1H), 8.16 (d, J = 8.3 Hz, 1H), 7.90 (d, J = 8.8 Hz, 1H), 7.82 (d, J = 8.9 Hz, 1H), 7.61−7.56 (m, 1H), 7.55−7.51 (m, 1H), 7.51−7.45 (m, 3H), 5.31 (q, J = 7.2 Hz, 1H), 2.73 (s, 3H), 2.00 (d, J = 7.2 Hz, 3H).

General Procedure B to Synthesize 3-Aniline-1,2,4-oxadiazoles. To a stirred solution of 3-nitroaromatic-1,2,4-oxadiazoles (2.0 mmol) in ethanol (10.0 mL) and NH$_4$Cl aq. (2.0 mL) was added zinc powder (10.0 mmol). The reaction mixture was stirred at room temperature for 2.0 h. The reaction mixture was filtered, and the filtrate was concentrated *in vacuo*. The residue was purified with silica gel column chromatography using (hexane/EtOAc = 3:1) as eluents to afford the target compounds.

4-Methyl-3-(5-(1-(naphthalen-1-yl)ethyl)-1,2,4-oxadiazol-3-yl)-aniline (4). The target compound was afforded following general procedure B. White solid 400 mg, yield 61%. ^{1}H NMR (500 MHz, CDCl$_3$) δ 8.15 (d, J = 8.5 Hz, 1H), 7.89 (d, J = 8.1 Hz, 1H), 7.81 (d, J = 9.3 Hz, 1H), 7.57 (t, J = 7.7 Hz, 1H), 7.51 (t, J = 7.4 Hz, 1H), 7.47 (d, J = 7.0 Hz, 2H), 7.38 (s, 1H), 7.09 (d, J = 8.1 Hz, 1H), 6.73 (d, J = 8.2 Hz, 1H), 5.27 (q, J = 7.3 Hz, 1H), 2.49 (s, 3H), 1.97 (d, J = 7.2 Hz, 3H).

General Procedure C to Synthesize 5a−f, 5i−p, 9a−i, 13a, 13b, and 26a−t. To a solution of 3-aniline-1,2,4-oxadiazoles (0.4 mmol) in 1,2-dichloroethane (10.0 mL) at room temperature under Ar atmosphere were added the corresponding aldehyde (0.8 mmol), acetic acid (2.4 mmol), and sodium triacetoxyborohydride (2.4 mmol). The reaction mixture was stirred at room temperature for 3 h. The mixture was added to 10 mL of water and extracted with 20 mL of CH$_2$Cl$_2$. The organic extract was washed with brine and dried over anhydrous Na$_2$SO$_4$. The solvent was removed by evaporation, and the crude product was purified by flash chromatography on silica gel (MeOH(0.1% acetic acid)/CH$_2$Cl$_2$ = 0−2:100) to afford the target compounds.

4-Methyl-3-(5-(1-(naphthalen-1-yl)ethyl)-1,2,4-oxadiazol-3-yl)-N-neopentylaniline (5a). White solid, 134 mg, yield 84%, mp 85−86 °C. ^{1}H NMR (400 MHz, CDCl$_3$) δ 8.16 (d, J = 8.4 Hz, 1H), 7.89 (d, J = 9.6 Hz, 1H), 7.81 (dd, J = 6.8, 2.3 Hz, 1H), 7.60−7.54 (m, 1H), 7.53−7.50 (m, 1H), 7.50−7.43 (m, 2H), 7.37−7.30 (m, 1H), 7.07 (d, J = 8.2 Hz, 1H), 6.73 (s, 1H), 5.28 (q, J = 7.2 Hz, 1H), 2.93 (s, 2H), 2.46 (s, 3H), 1.97 (d, J = 7.2 Hz, 3H), 1.01 (s, 9H). ^{13}C NMR (100 MHz, CDCl$_3$) δ 180.6, 169.1, 145.3, 136.2, 134.0, 132.2, 132.1, 130.9, 129.1, 128.3, 126.6, 126.5, 125.8, 125.6, 124.7, 122.8, 120.4, 115.2, 34.2, 31.8, 27.7, 21.0, 19.6. HRMS (ESI): m/z [M + H]$^+$ calcd for C$_{26}$H$_{30}$N$_3$O 400.2383; found 400.2385.

N-Cyclohexyl-4-methyl-3-(5-(1-(naphthalen-1-yl)ethyl)-1,2,4-ox-adiazol-3-yl)aniline (5b). White solid, 138 mg, yield 67%, mp 111−

112 °C. ^{1}H NMR (400 MHz, CDCl$_3$) δ 8.16 (d, J = 8.5 Hz, 1H), 7.89 (d, J = 8.9 Hz, 1H), 7.80 (dd, J = 7.4, 2.1 Hz, 1H), 7.59−7.43 (m, 4H), 7.25 (d, J = 2.8 Hz, 1H), 7.07 (d, J = 8.2 Hz, 1H), 6.65 (dd, J = 8.4, 2.6 Hz, 1H), 5.27 (q, J = 7.2 Hz, 1H), 3.32−3.23 (m, 1H), 2.46 (s, 3H), 2.10−2.01 (m, 2H), 1.96 (d, J = 7.2 Hz, 3H), 1.79−1.70 (m, 2H), 1.40−1.30 (m, 2H), 1.28−1.09 (m, 4H). ^{13}C NMR (100 MHz, CDCl$_3$) δ 180.6, 169.2, 145.1, 141.0, 136.2, 134.0, 132.2, 130.9, 129.1, 128.2, 126.6, 126.6, 125.8, 125.6, 124.7, 122.8, 115.5, 115.3, 52.1, 34.2, 33.3, 25.9, 25.0, 20.9, 19.6. HRMS (ESI): m/z [M + H]$^+$ calcd for C$_{27}$H$_{30}$N$_3$O 412.2389; found 412.2383.

4-((4-Methyl-3-(5-(1-(naphthalen-1-yl)ethyl)-1,2,4-oxadiazol-3-yl)phenyl)amino)cyclohexane-1-carbonitrile (5c). White solid, 155 mg, yield 71%, mp 117−118 °C. ^{1}H NMR (500 MHz, CDCl$_3$) δ 8.16 (d, J = 8.5 Hz, 1H), 7.89 (d, J = 8.1 Hz, 1H), 7.81 (d, J = 7.6 Hz, 1H), 7.56 (t, J = 8.4 Hz, 1H), 7.54−7.41 (m, 3H), 7.25 (s, 1H), 7.09 (d, J = 8.3 Hz, 1H), 6.65 (d, J = 8.3 Hz, 1H), 5.27 (q, J = 7.1 Hz, 1H), 3.40−3.28 (m, 1H), 2.89 (t, J = 4.3 Hz, 1H), 2.47 (s, 3H), 2.12−2.01 (m, 4H), 1.97 (d, J = 7.2 Hz, 3H), 1.76−1.66 (m, 2H), 1.61−1.54 (m, 2H). ^{13}C NMR (100 MHz, CDCl$_3$) δ 180.7, 169.1, 144.6, 136.2, 134.0, 132.3, 130.9, 129.1, 128.3, 126.7, 126.6, 125.8, 125.6, 124.7, 122.8, 121.7, 115.7, 115.1, 50.6, 34.2, 29.3, 27.2, 26.8, 20.9, 19.6. HRMS (ESI): m/z [M + H]$^+$ calcd for C$_{28}$H$_{29}$N$_4$O 437.2336; found 437.2339.

N-(4-Methoxycyclohexyl)-4-methyl-3-(5-(1-(naphthalen-1-yl)-ethyl)-1,2,4-oxadiazol-3-yl)aniline (5d). White solid, 140 mg, yield 63%, mp 90−91 °C. ^{1}H NMR (400 MHz, CDCl$_3$) δ 8.16 (d, J = 8.4 Hz, 1H), 7.89 (dd, J = 7.9, 1.9 Hz, 1H), 7.80 (dd, J = 7.3, 2.1 Hz, 1H), 7.60−7.42 (m, 4H), 7.30 (s, 1H), 7.08 (d, J = 8.2 Hz, 1H), 6.70 (s, 1H), 5.27 (q, J = 7.2 Hz, 1H), 3.42−3.34 (m, 2H), 3.31 (s, 3H), 2.46 (s, 3H), 1.96 (d, J = 7.2 Hz, 3H), 1.89−1.75 (m, 4H), 1.64−1.52 (m, 4H). ^{13}C NMR (100 MHz, CDCl$_3$) δ 180.6, 169.1, 137.7, 136.2, 134.0, 132.2, 130.9, 129.1, 128.2, 126.7, 126.6, 125.8, 125.6, 124.7, 122.8, 116.2, 115.7, 75.0, 55.6, 51.0, 34.2, 27.9, 27.4, 21.0, 19.6. HRMS (ESI): m/z [M + H]$^+$ calcd for C$_{28}$H$_{32}$N$_3$O$_2$ 442.2489; found 442.2494.

4-((4-Methyl-3-(5-(1-(naphthalen-1-yl)ethyl)-1,2,4-oxadiazol-3-yl)phenyl)amino)cyclohexane-1-carboxylic Acid (5e). White solid, 98 mg, yield 43%, mp 161−162 °C. ^{1}H NMR (500 MHz, CDCl$_3$) δ 8.15 (d, J = 8.5 Hz, 1H), 7.88 (d, J = 8.1 Hz, 1H), 7.80 (d, J = 7.6 Hz, 1H), 7.56 (t, J = 7.6 Hz, 1H), 7.53−7.42 (m, 3H), 7.23 (d, J = 2.6 Hz, 1H), 7.08 (d, J = 8.2 Hz, 1H), 6.67−6.58 (m, 1H), 5.27 (q, J = 7.2 Hz, 1H), 3.28 (t, J = 11.0 Hz, 1H), 2.46 (s, 3H), 2.38−2.27 (m, 1H), 2.20 (d, J = 12.0 Hz, 2H), 2.09 (d, J = 12.0 Hz, 2H), 1.96 (d, J = 7.2 Hz, 3H), 1.59 (q, J = 13.0 Hz, 2H), 1.14 (q, J = 13.4 Hz, 2H). ^{13}C NMR (100 MHz, CDCl$_3$) δ 181.1, 180.6, 169.1, 145.0, 136.2, 134.0, 132.3, 130.9, 129.1, 128.3, 126.8, 126.6, 125.8, 125.6, 124.7, 122.8, 115.6, 115.2, 51.5, 42.4, 34.2, 32.4, 27.8, 20.9, 19.6. HRMS (ESI): m/z [M + H]$^+$ calcd for C$_{28}$H$_{30}$N$_3$O$_3$ 456.2282; found 456.2285.

3-((4-Methyl-3-(5-(1-(naphthalen-1-yl)ethyl)-1,2,4-oxadiazol-3-yl)phenyl)amino)cyclohexane-1-carboxylic Acid (5f). White solid, 135 mg, yield 59%, mp 150−151 °C. ^{1}H NMR (500 MHz, CDCl$_3$) δ 8.14 (d, J = 8.5 Hz, 1H), 7.88 (d, J = 8.0 Hz, 1H), 7.80 (d, J = 7.7 Hz, 1H), 7.55 (t, J = 6.9 Hz, 1H), 7.52−7.43 (m, 3H), 7.30 (s, 1H), 7.09 (d, J = 8.2 Hz, 1H), 6.70 (d, J = 8.2 Hz, 1H), 5.26 (q, J = 7.2 Hz, 1H), 3.69−3.62 (m, 1H), 2.79−2.70 (m, 1H), 2.47 (s, 3H), 2.22−2.11 (m, 1H), 1.96 (d, J = 7.2 Hz, 3H), 1.87−1.78 (m, 2H), 1.77−1.55 (m, 5H). ^{13}C NMR (100 MHz, CDCl$_3$) δ 180.6, 180.0, 169.1, 136.2, 134.0, 132.3, 130.9, 129.1, 129.0, 128.3, 128.2, 126.6, 126.6, 125.8, 125.6, 125.3, 124.7, 122.8, 115.6, 67.1, 48.2, 38.4, 34.2, 32.7, 29.7, 27.6, 21.0, 19.6. HRMS (ESI): m/z [M + H]$^+$ calcd for C$_{28}$H$_{30}$N$_3$O$_3$ 456.2282; found 456.2284.

4-((4-Methyl-3-(5-(1-(naphthalen-1-yl)ethyl)-1,2,4-oxadiazol-3-yl)phenyl)amino)benzoic Acid (5g). A mixture of compound 4 (0.4 mmol), 4-bromobenzoic acid (0.5 mmol), BINAP (0.032 mmol), palladium acetate (0.02 mmol), cesium carbonate (0.8 mmol), and toluene (5.0 mL) was heated at 100 °C for 12 h under argon. The mixture was added to 10 mL of water and extracted with 20 mL of CH$_2$Cl$_2$. The organic extract was washed with brine and dried over anhydrous Na$_2$SO$_4$. The solvent was removed by evaporation, and the crude product was purified by flash chromatography on silica gel

(MeOH(0.1% acetic acid)/CH$_2$Cl$_2$ = 0−2:100) to afford the target compound as a white solid, 132 mg, yield 73%, mp 153−154 °C. ^{1}H NMR (400 MHz, CDCl$_3$) δ 8.15 (d, J = 8.5 Hz, 1H), 7.97 (d, J = 8.7 Hz, 2H), 7.89 (d, J = 8.0 Hz, 1H), 7.85−7.78 (m, 2H), 7.60−7.43 (m, 4H), 7.31−7.21 (m, 2H), 6.96 (d, J = 8.8 Hz, 2H), 5.28 (q, J = 7.2 Hz, 1H), 2.59 (s, 3H), 1.97 (d, J = 7.2 Hz, 3H). ^{13}C NMR (100 MHz, CDCl$_3$) δ 181.0, 171.1, 168.5, 149.0, 138.4, 136.0, 134.0, 133.5, 132.5, 132.3, 130.9, 129.1, 128.4, 127.3, 126.7, 125.9, 125.6, 124.7, 123.2, 122.9, 122.7, 119.9, 114.2, 34.1, 21.5, 19.5. HRMS (ESI): m/z [M + H]$^+$ calcd for C$_{28}$H$_{24}$N$_3$O$_3$ 450.1812; found 450.1812.

Methyl 4-((4-methyl-3-(5-(1-(naphthalen-1-yl)ethyl)-1,2,4-oxadiazol-3-yl)phenyl)amino)benzoate (5h). **5h** was synthesized using the same method for **5g**. White solid, 134 mg, yield 72%, mp 68−69 °C. ^{1}H NMR (400 MHz, CDCl$_3$) δ 8.14 (d, J = 8.4 Hz, 1H), 7.94−7.86 (m, 3H), 7.83−7.77 (m, 2H), 7.56 (t, J = 7.6 Hz, 1H), 7.52 (d, J = 7.5 Hz, 1H), 7.50−7.43 (m, 2H), 7.27−7.19 (m, 2H), 6.94 (d, J = 8.7 Hz, 2H), 5.27 (q, J = 7.1 Hz, 1H), 3.87 (s, 3H), 2.58 (s, 3H), 1.96 (d, J = 7.2 Hz, 3H). ^{13}C NMR (100 MHz, CDCl$_3$) δ 181.0, 168.5, 167.0, 148.2, 138.7, 136.0, 134.0, 133.1, 132.4, 131.5, 130.9, 129.1, 128.3, 127.2, 126.7, 125.9, 125.6, 124.7, 122.8, 122.7, 122.5, 121.1, 114.3, 51.7, 34.1, 21.5, 19.5. HRMS (ESI): m/z [M + H]$^+$ calcd for C$_{29}$H$_{26}$N$_3$O$_3$ 464.1969; found 464.1972.

4-(((4-Methyl-3-(5-(1-(naphthalen-1-yl)ethyl)-1,2,4-oxadiazol-3-yl)phenyl)amino)methyl)benzoic Acid (5i). White solid, 143 mg, yield 77%, mp 80−81 °C. ^{1}H NMR (400 MHz, CDCl$_3$) δ 8.14 (d, J = 8.4 Hz, 1H), 8.05 (d, J = 8.4 Hz, 2H), 7.88 (d, J = 7.7 Hz, 1H), 7.83−7.77 (m, 1H), 7.59−7.49 (m, 2H), 7.49−7.43 (m, 4H), 7.39 (s, 1H), 7.09 (d, J = 8.2 Hz, 1H), 6.68 (d, J = 8.3 Hz, 1H), 5.26 (q, J = 7.1 Hz, 1H), 4.45 (s, 2H), 2.48 (s, 3H), 1.96 (d, J = 7.2 Hz, 3H). ^{13}C NMR (100 MHz, CDCl$_3$) δ 180.7, 170.9, 168.9, 146.0, 140.6, 136.1, 134.0, 132.3, 130.9, 130.8, 130.6, 129.1, 128.3, 128.3, 127.7, 126.7, 126.6, 125.8, 125.6, 124.7, 122.8, 116.0, 115.6, 48.8, 34.2, 21.1, 19.6. HRMS (ESI): m/z [M + H]$^+$ calcd for C$_{29}$H$_{26}$N$_3$O$_3$ 464.1969; found 464.1970.

Methyl 4-(((4-methyl-3-(5-(1-(naphthalen-1-yl)ethyl)-1,2,4-oxadiazol-3-yl)phenyl)amino)methyl)benzoate (5j). White solid, 160 mg, yield 84%, mp 69−70 °C. ^{1}H NMR (400 MHz, CDCl$_3$) δ 8.14 (d, J = 8.5 Hz, 1H), 8.01−7.95 (m, 2H), 7.89 (d, J = 7.6 Hz, 1H), 7.84−7.76 (m, 1H), 7.60−7.29 (m, 7H), 7.08 (d, J = 8.2 Hz, 1H), 6.65 (d, J = 11.1 Hz, 1H), 5.26 (q, J = 7.3 Hz, 1H), 4.42 (s, 2H), 3.90 (s, 3H), 2.47 (s, 3H), 1.95 (d, J = 7.2 Hz, 3H). ^{13}C NMR (100 MHz, CDCl$_3$) δ 180.7, 168.9, 166.9, 144.0, 136.1, 134.0, 132.3, 130.9, 130.0, 129.9, 129.3, 129.1, 128.3, 127.5, 126.9, 126.7, 126.6, 125.8, 125.6, 124.7, 122.8, 115.8, 115.4, 52.1, 48.6, 34.2, 21.1, 19.6. HRMS (ESI): m/z [M + H]$^+$ calcd for C$_{30}$H$_{28}$N$_3$O$_3$ 478.2125; found 478.2130.

3-(((4-Methyl-3-(5-(1-(naphthalen-1-yl)ethyl)-1,2,4-oxadiazol-3-yl)phenyl)amino)methyl)benzoic Acid (5k). White solid, 125 mg, yield 67%, mp 136−137 °C. ^{1}H NMR (400 MHz, CDCl$_3$) δ 8.14 (d, J = 8.4 Hz, 1H), 8.10 (s, 1H), 7.99 (d, J = 7.7 Hz, 1H), 7.87 (d, J = 7.2 Hz, 1H), 7.79 (dd, J = 6.9, 2.5 Hz, 1H), 7.60 (d, J = 7.7 Hz, 1H), 7.57−7.38 (m, 5H), 7.35 (d, J = 2.6 Hz, 1H), 7.08 (d, J = 8.3 Hz, 1H), 6.64 (dd, J = 8.2, 2.6 Hz, 1H), 5.26 (q, J = 7.2 Hz, 1H), 4.41 (s, 2H), 2.47 (s, 3H), 1.95 (d, J = 7.3 Hz, 3H). ^{13}C NMR (100 MHz, CDCl$_3$) δ 180.7, 171.5, 169.0, 145.5, 139.8, 136.1, 134.0, 132.9, 132.3, 130.9, 129.7, 129.2, 129.1, 129.0, 128.8, 128.3, 127.4, 126.6, 126.5, 125.8, 125.6, 124.7, 122.8, 115.3, 114.9, 48.2, 34.2, 21.0, 19.6. HRMS (ESI): m/z [M + H]$^+$ calcd for C$_{29}$H$_{26}$N$_3$O$_3$ 464.1969; found 464.1977.

4-(((4-Methyl-3-(5-(1-(naphthalen-1-yl)ethyl)-1,2,4-oxadiazol-3-yl)phenyl)amino)methyl)benzonitrile (5l). White solid, 124 mg, yield 70%, mp 61−62 °C. ^{1}H NMR (400 MHz, CDCl$_3$) δ 8.13 (d, J = 8.4 Hz, 1H), 7.89 (d, J = 8.0 Hz, 1H), 7.84−7.78 (m, 1H), 7.58 (d, J = 8.4 Hz, 2H), 7.56−7.50 (m, 2H), 7.47−7.42 (m, 4H), 7.28 (d, J = 2.7 Hz, 1H), 7.07 (d, J = 8.3 Hz, 1H), 6.58 (dd, J = 8.3, 2.7 Hz, 1H), 5.25 (q, J = 7.2 Hz, 1H), 4.41 (s, 2H), 2.47 (s, 3H), 1.95 (d, J = 7.2 Hz, 3H). ^{13}C NMR (100 MHz, CDCl$_3$) δ 180.7, 168.9, 144.8, 136.1, 134.0, 132.5, 132.4, 132.3, 130.9, 129.1, 129.1, 128.3, 127.9, 126.7, 126.6, 125.8, 125.6, 124.7, 122.7, 118.8, 115.3, 114.9, 111.0, 48.1, 34.2, 21.0, 19.6. HRMS (ESI): m/z [M + H]$^+$ calcd for C$_{29}$H$_{25}$N$_4$O 445.2023; found 445.2029.

4-(((4-Methyl-3-(5-(1-(naphthalen-1-yl)ethyl)-1,2,4-oxadiazol-3-yl)phenyl)amino)methyl)phenol (5m). White solid, 130 mg, yield 75%, mp 71−72 °C. ^{1}H NMR (400 MHz, CDCl$_3$) δ 8.12 (d, J = 8.4 Hz, 1H), 7.87 (d, J = 6.0 Hz, 1H), 7.78 (d, J = 7.8 Hz, 1H), 7.56−7.40 (m, 4H), 7.27 (d, J = 2.6 Hz, 1H), 7.13 (d, J = 8.4 Hz, 2H), 7.07 (d, J = 8.2 Hz, 1H), 6.71 (d, J = 8.5 Hz, 2H), 6.63 (dd, J = 8.2, 2.6 Hz, 1H), 5.27 (q, J = 7.2 Hz, 1H), 4.14 (s, 2H), 2.47 (s, 3H), 1.95 (d, J = 7.2 Hz, 3H). ^{13}C NMR (100 MHz, CDCl$_3$) δ 180.9, 169.0, 155.1, 146.0, 136.0, 134.0, 132.2, 130.9, 130.8, 129.2, 129.1, 128.3, 127.0, 126.7, 126.3, 125.8, 125.6, 124.7, 122.7, 115.5, 115.4, 114.6, 48.1, 34.2, 21.0, 19.5. HRMS (ESI): m/z [M + H]$^+$ calcd for C$_{28}$H$_{26}$N$_3$O$_2$ 436.2020; found 436.2019.

4-Methyl-N-(4-(methylsulfonyl)benzyl)-3-(5-(1-(naphthalen-1-yl)ethyl)-1,2,4-oxadiazol-3-yl)aniline (5n). White solid, 162 mg, yield 81%, mp 68−69 °C. ^{1}H NMR (400 MHz, CDCl$_3$) δ 8.14 (d, J = 8.4 Hz, 1H), 7.93−7.83 (m, 3H), 7.83−7.76 (m, 1H), 7.59−7.49 (m, 4H), 7.46 (d, J = 5.7 Hz, 2H), 7.29 (d, J = 2.7 Hz, 1H), 7.08 (d, J = 8.2 Hz, 1H), 6.59 (dd, J = 8.3, 2.7 Hz, 1H), 5.26 (q, J = 7.2 Hz, 1H), 4.45 (s, 2H), 3.01 (s, 3H), 2.47 (s, 3H), 1.95 (d, J = 7.2 Hz, 3H). ^{13}C NMR (125 MHz, CDCl$_3$) δ 180.8, 168.9, 142.4, 139.6, 136.1, 134.1, 132.4, 130.9, 130.4, 129.5, 129.2, 128.3, 128.2, 127.9, 127.8, 126.8, 126.7, 125.9, 125.6, 124.7, 122.8, 122.2, 44.5, 34.2, 21.8, 21.0, 19.6. HRMS (ESI): m/z [M + H]$^+$ calcd for C$_{29}$H$_{28}$N$_3$O$_3$S 498.1846; found 498.1850.

5-(((4-Methyl-3-(5-(1-(naphthalen-1-yl)ethyl)-1,2,4-oxadiazol-3-yl)phenyl)amino)methyl)furan-2-carboxylic Acid (5o). White solid, 137 mg, yield 76%, mp 132−133 °C. ^{1}H NMR (400 MHz, CDCl$_3$) δ 8.06 (d, J = 8.3 Hz, 1H), 7.82 (d, J = 7.9 Hz, 1H), 7.73 (d, J = 6.7 Hz, 1H), 7.51−7.41 (m, 2H), 7.41−7.33 (m, 2H), 7.16 (s, 1H), 6.93 (d, J = 8.2 Hz, 1H), 6.70−6.66 (m, 1H), 6.51 (d, J = 8.3 Hz, 1H), 5.96 (s, 1H), 5.17 (q, J = 7.1 Hz, 1H), 4.05 (s, 2H), 2.38 (s, 3H), 1.87 (d, J = 7.1 Hz, 3H). ^{13}C NMR (125 MHz, CDCl$_3$) δ 180.9, 169.0, 166.7, 154.6, 148.4, 145.3, 136.1, 134.0, 132.2, 130.9, 129.1, 128.3, 127.7, 126.6, 126.3, 125.8, 125.6, 124.6, 122.7, 116.0, 115.8, 114.7, 109.5, 50.8, 34.1, 20.8, 19.5. HRMS (ESI): m/z [M + H]$^+$ calcd for C$_{27}$H$_{24}$N$_3$O$_4$ 454.1761; found 454.1757.

5-(((4-Methyl-3-(5-(1-(naphthalen-1-yl)ethyl)-1,2,4-oxadiazol-3-yl)phenyl)amino)methyl)thiophene-2-carboxylic Acid (5p). White solid, 121 mg, yield 64%, mp 119−120 °C. ^{1}H NMR (400 MHz, CDCl$_3$) δ 8.15 (d, J = 8.4 Hz, 1H), 7.89 (d, J = 8.9 Hz, 1H), 7.80 (dd, J = 6.7, 2.9 Hz, 1H), 7.72 (d, J = 3.8 Hz, 1H), 7.56 (t, J = 6.8 Hz, 1H), 7.52 (d, J = 7.0 Hz, 1H), 7.50−7.45 (m, 2H), 7.37 (d, J = 2.7 Hz, 1H), 7.11 (d, J = 8.3 Hz, 1H), 7.02 (d, J = 3.8 Hz, 1H), 6.70 (dd, J = 8.2, 2.7 Hz, 1H), 5.27 (q, J = 7.1 Hz, 1H), 4.57 (s, 2H), 2.49 (s, 3H), 1.96 (d, J = 7.3 Hz, 3H). ^{13}C NMR (100 MHz, CDCl$_3$) δ 180.7, 168.9, 166.7, 153.0, 144.9, 136.1, 135.2, 134.0, 132.3, 131.3, 130.9, 129.1, 128.3, 128.1, 126.7, 126.6, 125.8, 125.7, 125.6, 124.7, 122.8, 115.5, 115.1, 44.0, 34.2, 21.1, 19.6. HRMS (ESI): m/z [M + H]$^+$ calcd for C$_{27}$H$_{24}$N$_3$O$_3$S 470.1533; found 470.1534.

5-(1-(Naphthalen-1-yl)ethyl)-3-(3-nitrophenyl)-1,2,4-oxadiazole (7a). Following general procedure A, the target compound was afforded (0.95 g) as a yellow solid, yield 55%. ^{1}H NMR (400 MHz, CDCl$_3$) δ 8.96 (s, 1H), 8.42 (d, J = 7.8 Hz, 1H), 8.35 (d, J = 8.2 Hz, 1H), 8.14 (d, J = 8.5 Hz, 1H), 7.90 (d, J = 8.1 Hz, 1H), 7.86−7.80 (m, 1H), 7.66 (t, J = 9.2 Hz, 1H), 7.62−7.56 (m, 1H), 7.56−7.51 (m, 1H), 7.51−7.45 (m, 2H), 5.30 (q, J = 8.0 Hz, 1H), 1.99 (d, J = 4.8 Hz, 3H).

3-(2-Bromo-5-nitrophenyl)-5-(1-(naphthalen-1-yl)ethyl)-1,2,4-oxadiazole (7b). Following general procedure A, the target compound was afforded (0.98 g) as a yellow solid, yield 46%. ^{1}H NMR (400 MHz, CDCl$_3$) δ 8.77 (d, J = 2.7 Hz, 1H), 8.18−8.12 (m, 2H), 7.91 (dd, J = 8.5, 5.2 Hz, 2H), 7.83 (dd, J = 7.0, 2.3 Hz, 1H), 7.59 (t, J = 8.0 Hz, 1H), 7.55−7.45 (m, 3H), 5.33 (q, J = 8.5 Hz, 1H), 2.00 (d, J = 7.2 Hz, 3H).

5-(1-(Naphthalen-1-yl)ethyl)-3-(3-nitro-5-(trifluoromethyl)phenyl)-1,2,4-oxadiazole (7c). Following general procedure A, the target compound was afforded 1.20 g as yellow solid, yield 58%. ^{1}H NMR (400 MHz, CDCl$_3$) δ 9.13 (s, 1H), 8.68 (s, 1H), 8.60 (s, 1H), 8.12 (d, J = 8.4 Hz, 1H), 7.90 (d, J = 8.0 Hz, 1H), 7.83 (t, J = 4.8 Hz,

1H), 7.59 (t, J = 7.0 Hz, 1H), 7.52 (t, J = 7.2 Hz, 1H), 7.48 (d, J = 4.8 Hz, 2H), 5.32 (q, J = 6.9 Hz, 1H), 2.00 (d, J = 7.2 Hz, 3H).

3-(4-Methyl-3-nitrophenyl)-5-(1-(naphthalen-1-yl)ethyl)-1,2,4-oxadiazole (7d). Following general procedure A, the target compound was afforded (1.11 g) as a yellow solid, yield 62%. ^{1}H NMR (400 MHz, CDCl$_3$) δ 8.69 (s, 1H), 8.19 (d, J = 9.7 Hz, 1H), 8.13 (d, J = 8.5 Hz, 1H), 7.90 (d, J = 8.1 Hz, 1H), 7.84−7.79 (m, 1H), 7.58 (t, J = 8.4 Hz, 1H), 7.52 (t, J = 8.1 Hz, 1H), 7.49−7.43 (m, 3H), 5.28 (q, J = 7.2 Hz, 1H), 2.66 (s, 3H), 1.98 (d, J = 7.2 Hz, 3H).

3-(4-Methoxy-3-nitrophenyl)-5-(1-(naphthalen-1-yl)ethyl)-1,2,4-oxadiazole (7e). Following general procedure A, the target compound was afforded (0.90 g) as a yellow solid, yield 48%. ^{1}H NMR (400 MHz, CDCl$_3$) δ 8.59 (d, J = 2.1 Hz, 1H), 8.25 (dd, J = 8.8, 2.2 Hz, 1H), 8.13 (d, J = 8.5 Hz, 1H), 7.90 (d, J = 8.0 Hz, 1H), 7.84−7.79 (m, 1H), 7.60−7.55 (m, 1H), 7.54−7.49 (m, 1H), 7.47 (d, J = 4.9 Hz, 2H), 7.17 (d, J = 8.8 Hz, 1H), 5.27 (q, J = 7.2 Hz, 1H), 4.03 (s, 3H), 1.97 (d, J = 7.2 Hz, 3H).

3-(5-(1-(Naphthalen-1-yl)ethyl)-1,2,4-oxadiazol-3-yl)aniline (8a). The target compound was afforded following general procedure B. White solid 470 mg, yield 75%. ^{1}H NMR (400 MHz, CDCl$_3$) δ 8.12 (d, J = 8.4 Hz, 1H), 7.88 (d, J = 8.1 Hz, 1H), 7.80 (s, 1H), 7.60−7.38 (m, 6H), 7.28−7.21 (m, 1H), 6.80 (d, J = 7.5 Hz, 1H), 5.25 (q, J = 7.6 Hz, 1H), 1.95 (d, J = 7.3 Hz, 3H).

4-Bromo-3-(5-(1-(naphthalen-1-yl)ethyl)-1,2,4-oxadiazol-3-yl)-aniline (8b). White solid 495 mg, yield 63%. ^{1}H NMR (400 MHz, CDCl$_3$) δ 8.14 (d, J = 8.4 Hz, 1H), 7.89 (d, J = 8.6 Hz, 1H), 7.81 (dd, J = 7.3, 2.2 Hz, 1H), 7.56 (t, J = 6.8 Hz, 1H), 7.52 (d, J = 6.8 Hz, 1H), 7.50−7.43 (m, 3H), 7.20 (d, J = 2.9 Hz, 1H), 6.69 (dd, J = 8.6, 2.9 Hz, 1H), 5.28 (q, J = 7.2 Hz, 1H), 1.97 (d, J = 7.2 Hz, 3H).

3-(5-(1-(Naphthalen-1-yl)ethyl)-1,2,4-oxadiazol-3-yl)-5-(trifluoromethyl)aniline (8c). White solid 450 mg, yield 59%. ^{1}H NMR (400 MHz, CDCl$_3$) δ 8.11 (d, J = 8.4 Hz, 1H), 7.89 (d, J = 8.1 Hz, 1H), 7.83−7.78 (m, 1H), 7.74 (s, 1H), 7.61−7.48 (m, 3H), 7.47−7.44 (m, 2H), 7.01 (s, 1H), 5.26 (q, J = 6.7 Hz, 1H), 1.96 (d, J = 7.2 Hz, 3H).

2-Methyl-5-(5-(1-(naphthalen-1-yl)ethyl)-1,2,4-oxadiazol-3-yl)-aniline (8d). White solid 410 mg, yield 62%. ^{1}H NMR (400 MHz, CDCl$_3$) δ 8.13 (d, J = 8.4 Hz, 1H), 7.88 (d, J = 7.5 Hz, 1H), 7.82−7.75 (m, 3H), 7.59−7.47 (m, 2H), 7.47−7.43 (m, 2H), 6.74 (d, J = 8.2 Hz, 1H), 5.24 (q, J = 7.2 Hz, 1H), 2.22 (s, 3H), 1.94 (d, J = 7.2 Hz, 3H).

2-Methoxy-5-(5-(1-(naphthalen-1-yl)ethyl)-1,2,4-oxadiazol-3-yl)-aniline (8e). White solid 420 mg, yield 61%. ^{1}H NMR (400 MHz, CDCl$_3$) δ 8.13 (d, J = 8.3 Hz, 1H), 7.88 (d, J = 7.9 Hz, 1H), 7.84−7.77 (m, 1H), 7.61−7.42 (m, 6H), 6.84 (d, J = 8.4 Hz, 1H), 5.24 (q, J = 7.3 Hz, 1H), 3.90 (s, 3H), 1.94 (d, J = 7.2 Hz, 3H).

4-(((3-(5-(1-(Naphthalen-1-yl)ethyl)-1,2,4-oxadiazol-3-yl)-phenyl)amino)methyl)benzoic Acid (9a). The target compound was afforded following general procedure C. White solid, 133 mg, yield 74%, mp 130−131 °C. ^{1}H NMR (400 MHz, CDCl$_3$) δ 8.11 (d, J = 8.4 Hz, 1H), 8.04 (d, J = 7.8 Hz, 2H), 7.86 (d, J = 8.0 Hz, 1H), 7.81−7.74 (m, 1H), 7.53 (t, J = 7.5 Hz, 1H), 7.49 (d, J = 7.6 Hz, 1H), 7.47−7.39 (m, 5H), 7.36 (s, 1H), 7.23 (t, J = 8.0 Hz, 1H), 6.67 (d, J = 10.5 Hz, 1H), 5.24 (q, J = 7.2 Hz, 1H), 4.42 (s, 2H), 1.93 (d, J = 7.2 Hz, 3H). ^{13}C NMR (125 MHz, CDCl$_3$) δ 181.7, 171.3, 168.5, 147.9, 145.5, 136.1, 134.0, 130.9, 130.7, 130.6, 129.8, 129.1, 128.3, 127.8, 127.3, 126.7, 125.8, 125.6, 124.7, 122.7, 117.2, 115.5, 111.7, 47.9, 34.3, 19.6. HRMS (ESI): *m/z* [M + H]$^+$ calcd for C$_{28}$H$_{24}$N$_3$O$_3$ 450.1812; found 450.1814.

5-(((3-(5-(1-(Naphthalen-1-yl)ethyl)-1,2,4-oxadiazol-3-yl)-phenyl)amino)methyl)thiophene-2-carboxylic Acid (9b). White solid, 105 mg, yield 58%, mp 224−225 °C. ^{1}H NMR (400 MHz, CDCl$_3$) δ 8.12 (d, J = 8.5 Hz, 1H), 7.88 (d, J = 8.1 Hz, 1H), 7.80 (t, J = 5.1 Hz, 1H), 7.73 (d, J = 3.8 Hz, 1H), 7.60−7.47 (m, 3H), 7.47−7.40 (m, 3H), 7.29 (t, J = 7.9 Hz, 1H), 7.04 (s, 1H), 6.79 (d, J = 8.1 Hz, 1H), 5.26 (q, J = 7.3 Hz, 1H), 4.61 (s, 2H), 1.95 (d, J = 7.2 Hz, 3H). ^{13}C NMR (125 MHz, CDCl$_3$) δ 181.8, 168.4, 166.5, 146.9, 142.9, 136.1, 135.2, 134.0, 131.5, 130.9, 129.9, 129.1, 128.3, 127.9, 126.7, 125.9, 125.8, 125.6, 124.7, 122.7, 118.1, 116.2, 112.3, 43.9, 34.3, 19.6. HRMS (ESI): *m/z* [M + H]$^+$ calcd for C$_{26}$H$_{22}$N$_3$O$_3$S 456.1376; found 456.1374.

5-(((3-(5-(1-(Naphthalen-1-yl)ethyl)-1,2,4-oxadiazol-3-yl)-phenyl)amino)methyl)furan-2-carboxylic Acid (9c). White solid, 123 mg, yield 70%, mp 175−176 °C. ^{1}H NMR (400 MHz, CDCl$_3$) δ 8.12 (d, J = 8.4 Hz, 1H), 7.90 (d, J = 8.0 Hz, 1H), 7.85−7.77 (m, 1H), 7.61−7.48 (m, 2H), 7.48−7.42 (m, 3H), 7.42−7.37 (m, 1H), 7.24 (t, J = 8.0 Hz, 1H), 6.87 (s, 1H), 6.80 (d, J = 8.1 Hz, 1H), 6.28 (s, 1H), 5.28 (d, J = 7.3 Hz, 1H), 4.35 (s, 2H), 1.96 (d, J = 7.2 Hz, 3H). ^{13}C NMR (125 MHz, DMSO-*d*$_6$) δ 181.2, 167.6, 167.1, 151.0, 144.9, 136.5, 133.5, 130.4, 129.5, 129.4, 129.4, 129.3, 128.8, 128.2, 127.9, 127.0, 126.6, 125.9, 125.6, 124.6, 122.9, 113.0, 112.1, 45.6, 33.4, 19.2. HRMS (ESI): *m/z* [M + H]$^+$ calcd for C$_{26}$H$_{22}$N$_3$O$_4$ 440.1605; found 440.1602.

4-(((4-Bromo-3-(5-(1-(naphthalen-1-yl)ethyl)-1,2,4-oxadiazol-3-yl)phenyl)amino)methyl)benzoic Acid (9d). White solid, 116 mg, yield 55%, mp 134−135 °C. ^{1}H NMR (400 MHz, CDCl$_3$) δ 8.14 (d, J = 8.4 Hz, 1H), 8.06 (d, J = 7.9 Hz, 2H), 7.89 (d, J = 8.0 Hz, 1H), 7.81 (d, J = 7.0 Hz, 1H), 7.59−7.49 (m, 2H), 7.49−7.40 (m, 5H), 7.09 (s, 1H), 6.54 (d, J = 8.8 Hz, 1H), 5.27 (q, J = 7.1 Hz, 1H), 4.43 (s, 2H), 1.96 (d, J = 7.2 Hz, 3H). ^{13}C NMR (175 MHz, CDCl$_3$) δ 181.4, 170.3, 168.1, 146.8, 144.8, 135.9, 134.7, 134.0, 130.9, 130.7, 129.1, 128.5, 128.3, 127.2, 126.8, 126.8, 125.8, 125.6, 124.7, 122.8, 116.1, 116.0, 108.9, 47.8, 34.3, 19.6. HRMS (ESI): *m/z* [M + H]$^+$ calcd for C$_{28}$H$_{23}$BrN$_3$O$_3$ 528.0917; found 528.0928.

4-(((3-Trifluoromethyl-5-(5-(1-(naphthalen-1-yl)ethyl)-1,2,4-oxa-diazol-3-yl)phenyl)amino)methyl)benzoic Acid (9e). White solid, 162 mg, yield 78%, mp 94−95 °C, purity 98.54%. ^{1}H NMR (400 MHz, CDCl$_3$) δ 8.10 (d, J = 8.5 Hz, 1H), 8.06 (d, J = 7.8 Hz, 2H), 7.87 (d, J = 8.0 Hz, 1H), 7.84−7.75 (m, 1H), 7.69 (s, 1H), 7.55 (t, J = 7.6 Hz, 1H), 7.50 (d, J = 7.7 Hz, 1H), 7.48−7.39 (m, 5H), 6.90 (s, 1H), 5.26 (q, J = 7.1 Hz, 1H), 4.45 (s, 2H), 1.95 (d, J = 7.1 Hz, 3H). ^{13}C NMR (125 MHz, CDCl$_3$) δ 182.2, 171.0, 167.7, 148.2, 144.5, 135.9, 134.1, 132.5 (q, $^2J_{F,C}$ = 33 Hz), 130.9, 130.8, 129.2, 128.7, 128.6, 128.4, 127.4, 126.7, 125.9, 125.6, 124.7, 123.9 (q, $^1J_{F,C}$ = 271 Hz), 122.6, 114.3, 113.6, 111.5, 47.7, 34.3, 19.6. HRMS (ESI): *m/z* [M + H]$^+$ calcd for C$_{29}$H$_{23}$F$_3$N$_3$O$_3$ 518.1686; found 518.1691.

4-(((2-Methyl-5-(5-(1-(naphthalen-1-yl)ethyl)-1,2,4-oxadiazol-3-yl)phenyl)amino)methyl)benzoic Acid (9f). White solid, 181 mg, yield 88%, mp 185−186 °C. ^{1}H NMR (400 MHz, CDCl$_3$) δ 8.12 (d, J = 8.4 Hz, 1H), 8.07 (d, J = 8.0 Hz, 2H), 7.87 (d, J = 8.0 Hz, 1H), 7.79 (t, J = 4.8 Hz, 1H), 7.59−7.52 (m, 1H), 7.52−7.47 (m, 3H), 7.47−7.41 (m, 3H), 7.34 (s, 1H), 7.18 (d, J = 7.7 Hz, 1H), 5.24 (q, J = 7.2 Hz, 1H), 4.53 (s, 2H), 2.24 (s, 3H), 1.94 (d, J = 7.2 Hz, 3H). ^{13}C NMR (125 MHz, CDCl$_3$) δ 181.5, 170.8, 168.6, 145.4, 140.0, 136.2, 134.0, 130.9, 130.7, 129.6, 129.1, 128.4, 128.2, 127.7, 126.6, 125.8, 125.6, 124.7, 122.8, 121.7, 118.2, 116.7, 112.7, 48.3, 34.3, 19.6, 17.7. HRMS (ESI): *m/z* [M + H]$^+$ calcd for C$_{29}$H$_{26}$N$_3$O$_3$ 464.1969; found 464.1970.

5-(((3-Trifluoromethyl-5-(5-(1-(naphthalen-1-yl)ethyl)-1,2,4-oxa-diazol-3-yl)phenyl)amino)methyl)thiophene-2-carboxylic Acid (9g). White solid, 132 mg, yield 63%, mp 109−110 °C, purity 98.87%. ^{1}H NMR (400 MHz, CDCl$_3$) δ 8.11 (d, J = 8.5 Hz, 1H), 7.89 (d, J = 8.0 Hz, 1H), 7.81 (t, J = 5.0 Hz, 1H), 7.74 (s, 2H), 7.62−7.43 (m, 5H), 7.05 (s, 1H), 6.96 (s, 1H), 5.27 (q, J = 7.2 Hz, 1H), 4.63 (s, 2H), 1.96 (d, J = 7.1 Hz, 3H). ^{13}C NMR (125 MHz, CDCl$_3$) δ 182.3, 167.6, 166.2, 151.0, 147.4, 135.8, 135.3, 134.1, 132.5 (q, $^2J_{F,C}$ = 33 Hz), 131.7, 130.9, 129.2, 128.8, 128.4, 126.7, 126.1, 125.9, 125.6, 124.7, 123.9 (q, $^1J_{F,C}$ = 271 Hz), 122.6, 114.6, 114.3, 111.9, 43.5, 34.3, 19.6. HRMS (ESI): *m/z* [M + H]$^+$ calcd for C$_{27}$H$_{21}$F$_3$N$_3$O$_3$S 524.1250; found 524.1255.

5-(((2-Methyl-5-(5-(1-(naphthalen-1-yl)ethyl)-1,2,4-oxadiazol-3-yl)phenyl)amino)methyl)thiophene-2-carboxylic Acid (9h). White solid, 110 mg, yield 59%, mp 126−127 °C. ^{1}H NMR (400 MHz, CDCl$_3$) δ 8.13 (d, J = 8.4 Hz, 1H), 7.88 (d, J = 8.1 Hz, 1H), 7.83−7.77 (m, 1H), 7.74 (d, J = 3.8 Hz, 1H), 7.59−7.52 (m, 1H), 7.52−7.41 (m, 4H), 7.35 (s, 1H), 7.18 (d, J = 7.8 Hz, 1H), 7.07 (s, 1H), 5.26 (q, J = 7.5 Hz, 1H), 4.67 (s, 2H), 2.23 (s, 3H), 1.95 (d, J = 7.3 Hz, 3H). ^{13}C NMR (125 MHz, CDCl$_3$) δ 181.6, 168.6, 166.3, 152.6, 145.2, 136.2, 135.3, 134.0, 131.4, 130.9, 130.7, 129.1, 128.3, 126.6, 126.0, 126.0, 125.8, 125.7, 125.6, 124.7, 122.8, 117.7, 108.7, 43.7,

34.3, 19.6, 17.7. HRMS (ESI): m/z [M + H]$^+$ calcd for C$_{27}$H$_{24}$N$_3$O$_3$S 470.1533; found 470.1533.

5-(((2-Methoxy-5-(5-(1-(naphthalen-1-yl)ethyl)-1,2,4-oxadiazol-3-yl)phenyl)amino)methyl)thiophene-2-carboxylic Acid (9i). White solid, 120 mg, yield 62%, mp 121−122 °C. ^{1}H NMR (400 MHz, CDCl$_3$) δ 8.13 (d, J = 8.4 Hz, 1H), 7.88 (d, J = 8.0 Hz, 1H), 7.82−7.76 (m, 1H), 7.72 (d, J = 3.6 Hz, 1H), 7.59−7.47 (m, 3H), 7.47−7.43 (m, 2H), 7.36 (s, 1H), 7.07 (d, J = 3.7 Hz, 1H), 6.85 (d, J = 8.3 Hz, 1H), 5.24 (q, J = 7.1 Hz, 1H), 4.65 (s, 2H), 3.91 (s, 3H), 1.94 (d, J = 7.2 Hz, 3H). ^{13}C NMR (175 MHz, CDCl$_3$) δ 181.4, 168.4, 166.3, 152.7, 149.3, 137.0, 136.2, 135.2, 134.0, 131.2, 130.9, 129.1, 128.2, 126.6, 125.9, 125.8, 125.6, 124.7, 122.8, 119.8, 118.0, 109.4, 108.7, 55.7, 43.4, 34.3, 19.6. HRMS (ESI): m/z [M + H]$^+$ calcd for C$_{27}$H$_{24}$N$_3$O$_4$S 486.1482; found 486.1489.

5-(1-(Naphthalen-1-yl)ethyl)-3-(4-nitrophenyl)-1,2,4-oxadiazole (11). Following general procedure A, the target compound was afforded (0.74 g) as a yellow solid, yield 43%. ^{1}H NMR (400 MHz, CDCl$_3$) δ 8.29 (q, J = 8.9 Hz, 4H), 8.12 (d, J = 8.5 Hz, 1H), 7.90 (d, J = 9.4 Hz, 1H), 7.85−7.79 (m, 1H), 7.57 (t, J = 8.4 Hz, 1H), 7.52 (t, J = 7.7 Hz, 1H), 7.47 (d, J = 5.7 Hz, 2H), 5.30 (q, J = 6.9 Hz, 1H), 1.98 (d, J = 7.2 Hz, 3H).

4-(5-(1-(Naphthalen-1-yl)ethyl)-1,2,4-oxadiazol-3-yl)aniline (12). The target compound was afforded following general procedure B. White solid 475 mg, yield 75%. ^{1}H NMR (400 MHz, DMSO-d_6) δ 8.20 (d, J = 8.3 Hz, 1H), 7.99 (d, J = 6.3 Hz, 1H), 7.90 (d, J = 8.1 Hz, 1H), 7.65 (d, J = 8.4 Hz, 2H), 7.64−7.54 (m, 2H), 7.51 (t, J = 7.7 Hz, 1H), 7.42 (d, J = 7.1 Hz, 1H), 6.64 (d, J = 8.6 Hz, 2H), 5.75 (brs, 2H), 5.41 (q, J = 7.0 Hz, 1H), 1.84 (d, J = 7.1 Hz, 3H).

4-(((4-(5-(1-(Naphthalen-1-yl)ethyl)-1,2,4-oxadiazol-3-yl)phenyl)amino)methyl)benzoic Acid (13a). The target compound was afforded following general procedure C. White solid, 111 mg, yield 62%, mp >250 °C. ^{1}H NMR (400 MHz, DMSO-d_6) δ 8.19 (d, J = 8.4 Hz, 1H), 7.98 (d, J = 7.9 Hz, 1H), 7.93−7.87 (m, 3H), 7.69 (d, J = 8.4 Hz, 2H), 7.63−7.53 (m, 2H), 7.50 (t, J = 7.7 Hz, 1H), 7.46 (d, J = 8.0 Hz, 2H), 7.41 (d, J = 7.2 Hz, 1H), 7.02 (t, J = 6.2 Hz, 1H), 6.67 (d, J = 8.5 Hz, 2H), 5.40 (q, J = 7.0 Hz, 1H), 4.43 (d, J = 6.0 Hz, 2H), 1.83 (d, J = 7.0 Hz, 3H). ^{13}C NMR (125 MHz, DMSO-d_6) δ 181.9, 168.0, 148.7, 136.4, 133.5, 130.4, 129.6, 128.9, 128.8, 127.9, 126.6, 126.5, 125.9, 125.7, 125.6, 124.7, 122.9, 114.5, 110.7, 107.8, 107.6, 55.9, 33.5, 19.2. HRMS (ESI): m/z [M + H]$^+$ calcd for C$_{28}$H$_{24}$N$_3$O$_3$ 450.1812; found 450.1814.

5-(((4-(5-(1-(Naphthalen-1-yl)ethyl)-1,2,4-oxadiazol-3-yl)phenyl)amino)methyl)thiophene-2-carboxylic Acid (13b). White solid, 110 mg, yield 60%, mp 179−180 °C, purity 98.64%. ^{1}H NMR (400 MHz, CDCl$_3$) δ 8.13 (d, J = 8.5 Hz, 1H), 7.95−7.85 (m, 3H), 7.82−7.75 (m, 1H), 7.73 (d, J = 4.3 Hz, 1H), 7.59−7.47 (m, 2H), 7.47−7.42 (m, 2H), 7.02 (d, J = 3.8 Hz, 1H), 6.79−6.65 (m, 2H), 5.23 (q, J = 7.3 Hz, 1H), 4.60 (s, 2H), 1.94 (d, J = 7.2 Hz, 3H). ^{13}C NMR (125 MHz, CDCl$_3$) δ 181.3, 167.6, 162.7, 151.7, 150.5, 136.5, 133.5, 133.1, 132.6, 130.4, 128.8, 128.2, 127.9, 126.6, 125.9, 125.7, 125.6, 124.6, 122.9, 113.5, 112.3, 41.5, 33.4, 19.2. HRMS (ESI): m/z [M + H]$^+$ calcd for C$_{26}$H$_{22}$N$_3$O$_3$S 456.1376; found 456.1381.

5-((Methyl(4-(5-(1-(naphthalen-1-yl)ethyl)-1,2,4-oxadiazol-3-yl)phenyl)amino)methyl)thiophene-2-carboxylic Acid (13c). CH$_3$I (0.2 mmol) and K$_2$CO$_3$ (0.2 mmol) were added to a solution of 13b (0.2 mmol) in acetone (5.0 mL). The reaction mixture was refluxed for 2 h. The solvent was removed by evaporation and the crude product was purified by flash chromatography on silica gel (MeOH(0.1% acetic acid)/CH$_2$Cl$_2$ = 0−2:100). White solid, 58 mg, yield 62%, mp 171−172 °C. ^{1}H NMR (400 MHz, CDCl$_3$) δ 8.13 (d, J = 8.4 Hz, 1H), 7.96 (d, J = 8.6 Hz, 2H), 7.88 (d, J = 8.0 Hz, 1H), 7.79 (dd, J = 6.6, 2.9 Hz, 1H), 7.71 (d, J = 3.8 Hz, 1H), 7.55 (t, J = 7.4 Hz, 1H), 7.51 (d, J = 7.6 Hz, 1H), 7.49−7.42 (m, 2H), 6.94 (d, J = 3.8 Hz, 1H), 6.83 (d, J = 8.6 Hz, 2H), 5.24 (q, J = 7.2 Hz, 1H), 4.75 (s, 2H), 3.11 (s, 3H), 1.94 (d, J = 7.2 Hz, 3H). ^{13}C NMR (175 MHz, CDCl$_3$) δ 181.2, 168.2, 166.5, 151.1, 150.4, 136.2, 135.1, 134.0, 131.5, 130.9, 129.1, 128.9, 128.2, 126.6, 125.8, 125.7, 125.6, 124.7, 122.8, 115.7, 112.4, 52.1, 38.7, 34.3, 19.6. HRMS (ESI): m/z [M + H]$^+$ calcd for C$_{27}$H$_{24}$N$_3$O$_3$S 470.1533; found 470.1537.

4-((4-(5-(1-(Naphthalen-1-yl)ethyl)-1,2,4-oxadiazol-3-yl)phenyl)amino)benzoic Acid (13d). To a stirred solution of 15 (0.5 mmol) in toluene (5.0 mL) were added 4-aminobenzoic acid (0.6 mmol), BINAP (0.04 mmol), palladium acetate (0.03 mmol), and cesium carbonate (0.7 mmol). The mixture was heated at 100 °C for 12 h under argon. The reaction mixture was added to 20 mL of water and extracted with 20 mL of CH$_2$Cl$_2$, washed with brine, and then dried over Na$_2$SO$_4$. The solvent was removed by evaporation and the crude product was purified by flash chromatography on silica gel (MeOH(0.1% acetic acid)/CH$_2$Cl$_2$ = 0−2:100) to afford 13d as a white solid, 135 mg, yield 62%, mp 174−175 °C. ^{1}H NMR (400 MHz, DMSO-d_6) δ 9.13 (brs, 1H), 8.21 (d, J = 7.8 Hz, 1H), 7.98 (d, J = 8.0 Hz, 1H), 7.96−7.81 (m, 5H), 7.67−7.47 (m, 3H), 7.47−7.38 (m, 1H), 7.30 (d, J = 5.7 Hz, 2H), 7.20 (d, J = 6.0 Hz, 2H), 5.45 (q, J = 6.7 Hz, 1H), 1.86 (d, J = 4.4 Hz, 3H). ^{13}C NMR (175 MHz, DMSO-d_6) δ 181.9, 167.4, 167.0, 146.5, 144.9, 136.5, 133.6, 131.1, 130.5, 128.9, 128.5, 128.0, 126.7, 126.0, 125.7, 124.7, 123.0, 121.9, 118.0, 117.5, 115.8, 33.5, 19.3. HRMS (ESI): m/z [M + H]$^+$ calcd for C$_{27}$H$_{22}$N$_3$O$_3$ 436.1656; found 436.1657.

General Procedure to Synthesize 13e−l. To a solution of compound 15, 18, or 21 (0.4 mmol) in 1,4-dioxane (2.0 mL) and H$_2$O (0.2 mL) were added aryl boronic acid (0.4 mmol), K$_2$CO$_3$ (0.8 mmol), and Pd(PPh$_3$)$_4$ (0.02 mmol). The reaction mixture was heated at 100 °C for 6 h under argon. The mixture was added to 10 mL of water and extracted with 20 mL of CH$_2$Cl$_2$. The organic extract was washed with brine and dried over anhydrous Na$_2$SO$_4$. The solvent was removed by evaporation and the crude product was purified by flash chromatography on silica gel (MeOH(0.1% acetic acid)/CH$_2$Cl$_2$ = 0−2:100) to obtain 13e−l.

4′-(5-(1-(Naphthalen-1-yl)ethyl)-1,2,4-oxadiazol-3-yl)-[1,1′-biphenyl]-4-carboxylic Acid (13e). White solid, 114 mg, yield 68%, mp >250 °C. ^{1}H NMR (400 MHz, DMSO-d_6) δ 8.24 (d, J = 8.4 Hz, 1H), 8.13 (d, J = 6.4 Hz, 2H), 8.06 (d, J = 6.5 Hz, 2H), 8.01 (d, J = 8.1 Hz, 1H), 7.97−7.86 (m, 5H), 7.67−7.50 (m, 3H), 7.47 (d, J = 7.2 Hz, 1H), 5.52 (q, J = 7.1 Hz, 1H), 1.90 (d, J = 7.1 Hz, 3H). ^{13}C NMR (125 MHz, DMSO-d_6) δ 182.4, 167.2, 167.0, 142.9, 141.7, 136.3, 133.5, 130.4, 130.2, 130.0, 128.9, 128.0, 127.7, 127.6, 126.9, 126.7, 125.9, 125.8, 125.7, 124.7, 122.9, 33.5, 19.2. HRMS (ESI): m/z [M + H]$^+$ calcd for C$_{27}$H$_{21}$N$_2$O$_3$ 421.1547; found 421.1546.

5-(4-(5-(1-(Naphthalen-1-yl)ethyl)-1,2,4-oxadiazol-3-yl)phenyl)thiophene-2-carboxylic Acid (13f). White solid, 94 mg, yield 55%, mp 204−205 °C, purity 98.30%. ^{1}H NMR (400 MHz, DMSO-d_6) δ 8.23 (d, J = 8.4 Hz, 1H), 8.07 (d, J = 8.1 Hz, 2H), 8.00 (d, J = 7.9 Hz, 1H), 7.96−7.89 (m, 3H), 7.76−7.69 (m, 2H), 7.66−7.60 (m, 1H), 7.60−7.54 (m, 1H), 7.52 (d, J = 7.9 Hz, 1H), 7.46 (d, J = 7.2 Hz, 1H), 5.52 (q, J = 7.0 Hz, 1H), 1.89 (d, J = 7.0 Hz, 3H). ^{13}C NMR (125 MHz, DMSO-d_6) δ 182.4, 167.0, 162.6, 148.0, 136.3, 135.5, 134.6, 134.2, 133.5, 130.4, 128.8, 128.0, 127.8, 126.7, 126.4, 126.0, 125.9, 125.7, 125.6, 124.7, 122.9, 33.5, 19.2. HRMS (ESI): m/z [M + H]$^+$ calcd for C$_{25}$H$_{19}$N$_2$O$_3$S 427.1111; found 427.1113.

5-(4-(5-(1-(Naphthalen-1-yl)ethyl)-1,2,4-oxadiazol-3-yl)phenyl)thiophene-2-carbonitrile (13g). White solid, 80 mg, yield 49%, mp 161−162 °C. ^{1}H NMR (400 MHz, CDCl$_3$) δ 8.19−8.12 (m, 3H), 7.90 (d, J = 8.2 Hz, 1H), 7.85−7.79 (m, 1H), 7.70 (d, J = 8.1 Hz, 2H), 7.64−7.50 (m, 3H), 7.50−7.44 (m, 2H), 7.36 (d, J = 3.9 Hz, 1H), 5.29 (q, J = 7.3 Hz, 1H), 1.98 (d, J = 7.2 Hz, 3H). ^{13}C NMR (175 MHz, CDCl$_3$) δ 182.2, 167.6, 150.6, 138.4, 135.9, 134.6, 134.0, 130.9, 129.2, 128.4, 128.3, 127.8, 126.7, 126.6, 125.9, 125.6, 124.7, 124.0, 122.6, 114.2, 109.1, 34.3, 19.6. HRMS (ESI): m/z [M + H]$^+$ calcd for C$_{25}$H$_{18}$N$_3$OS 408.1165; found 408.1166.

N-Methoxy-4′-(5-(1-(naphthalen-1-yl)ethyl)-1,2,4-oxadiazol-3-yl)-[1,1′-biphenyl]-4-carboxamide (13h). White solid, 54 mg, yield 30%, mp 224−225 °C. ^{1}H NMR (400 MHz, DMSO-d_6) δ 8.24 (d, J = 8.4 Hz, 1H), 8.12 (d, J = 8.1 Hz, 2H), 8.00 (d, J = 8.0 Hz, 1H), 7.96−7.90 (m, 3H), 7.90−7.84 (m, 4H), 7.66−7.54 (m, 2H), 7.52 (d, J = 7.8 Hz, 1H), 7.47 (d, J = 7.2 Hz, 1H), 5.52 (q, J = 7.0 Hz, 1H), 3.74 (s, 3H), 1.90 (d, J = 7.1 Hz, 3H). ^{13}C NMR (175 MHz, DMSO-d_6) δ 182.4, 167.2, 163.5, 141.8, 141.7, 136.3, 133.5, 131.6, 130.4, 128.8, 128.0, 127.7, 127.6, 127.5, 126.7, 126.6, 125.9, 125.7, 125.6, 124.7,

122.9, 63.2, 33.5, 19.2. HRMS (ESI): m/z [M + H]$^+$ calcd for C$_{28}$H$_{24}$N$_3$O$_3$ 450.1812; found 450.1812.

5-(4-(3-(1-(Naphthalen-1-yl)ethyl)-1,2,4-oxadiazol-5-yl)phenyl)-thiophene-2-carbonitrile (13i). White solid, 58 mg, yield 36%, mp 175−176 °C. ^{1}H NMR (700 MHz, CDCl$_3$) δ 8.24 (d, J = 8.5 Hz, 1H), 8.15 (d, J = 8.5 Hz, 2H), 7.88 (d, J = 8.1 Hz, 1H), 7.79 (d, J = 8.0 Hz, 1H), 7.70 (d, J = 8.5 Hz, 2H), 7.62 (d, J = 3.9 Hz, 1H), 7.58−7.53 (m, 2H), 7.50 (t, J = 6.9 Hz, 1H), 7.50−7.46 (m, 1H), 7.38 (d, J = 4.0 Hz, 1H), 5.20 (q, J = 7.2 Hz, 1H), 1.92 (d, J = 7.2 Hz, 3H). ^{13}C NMR (175 MHz, CDCl$_3$) δ 174.6, 174.2, 149.8, 138.5, 137.3, 136.0, 134.0, 131.2, 129.1, 129.0, 127.9, 126.7, 126.4, 125.7, 125.6, 124.9, 124.7, 124.6, 123.0, 114.0, 109.7, 33.5, 19.6. HRMS (ESI): m/z [M + H]$^+$ calcd for C$_{25}$H$_{18}$N$_3$OS 408.1165; found 408.1163.

5-(4-(3-(1-(Naphthalen-1-yl)ethyl)-1,2,4-oxadiazol-5-yl)phenyl)-thiophene-2-carboxylic Acid (13j). White solid, 66 mg, yield 39%, mp 181−182 °C. ^{1}H NMR (400 MHz, CDCl$_3$) δ 8.23 (d, J = 8.5 Hz, 1H), 8.09 (s, 2H), 7.87 (d, J = 8.1 Hz, 1H), 7.83 (s, 1H), 7.78 (d, J = 8.1 Hz, 1H), 7.70 (s, 2H), 7.59−7.52 (m, 2H), 7.52−7.42 (m, 2H), 7.36 (s, 1H), 5.19 (q, J = 7.0 Hz, 1H), 1.91 (d, J = 7.1 Hz, 3H). ^{13}C NMR (175 MHz, CDCl$_3$) δ 174.8, 174.1, 137.4, 137.1, 135.7, 134.5, 134.4, 134.0, 131.2, 130.8, 130.7, 129.0, 128.9, 127.8, 126.5, 126.4, 125.6, 125.5, 125.1, 124.7, 123.1, 33.5, 19.6. HRMS (ESI): m/z [M + H]$^+$ calcd for C$_{25}$H$_{19}$N$_2$O$_3$S 427.1111; found 427.1111.

5-(4-(2-(1-(Naphthalen-1-yl)ethyl)oxazol-5-yl)phenyl)thiophene-2-carbonitrile (13k). White solid, 80 mg, yield 49%, mp 121−122 °C. ^{1}H NMR (400 MHz, CDCl$_3$) δ 8.21 (d, J = 8.5 Hz, 1H), 7.89 (d, J = 8.1 Hz, 1H), 7.79 (d, J = 8.1 Hz, 1H), 7.61−7.56 (m, 6H), 7.54−7.48 (m, 1H), 7.48−7.42 (m, 1H), 7.42−7.34 (m, 2H), 7.28−7.25 (m, 2H), 5.16 (q, J = 7.4 Hz, 1H), 1.92 (d, J = 7.0 Hz, 3H). ^{13}C NMR (175 MHz, CDCl$_3$) δ 166.9, 150.9, 150.3, 138.4, 137.7, 134.0, 131.8, 131.1, 129.9, 129.1, 128.9, 127.9, 126.7, 126.4, 125.7, 125.6, 124.8, 124.4, 123.4, 123.0, 114.3, 108.4, 35.6, 19.6. HRMS (ESI): m/z [M + H]$^+$ calcd for C$_{26}$H$_{19}$N$_2$OS 407.1213; found 407.1216.

5-(4-(2-(1-(Naphthalen-1-yl)ethyl)oxazol-5-yl)phenyl)thiophene-2-carboxylic Acid (13l). White solid, 74 mg, yield 43%, mp 152−153 °C. ^{1}H NMR (400 MHz, DMSO-d_6) δ 8.29 (d, J = 8.5 Hz, 1H), 7.97 (d, J = 8.1 Hz, 1H), 7.86 (d, J = 8.2 Hz, 1H), 7.79 (d, J = 8.1 Hz, 2H), 7.75−7.70 (m, 2H), 7.66 (d, J = 8.1 Hz, 2H), 7.63−7.59 (m, 2H), 7.59−7.53 (m, 1H), 7.49 (t, J = 7.7 Hz, 1H), 7.36 (d, J = 7.2 Hz, 1H), 5.28 (q, J = 7.0 Hz, 1H), 1.80 (d, J = 7.0 Hz, 3H). ^{13}C NMR (175 MHz, DMSO-d_6) δ 166.1, 162.6, 149.8, 148.8, 138.0, 134.3, 133.5, 133.4, 132.3, 130.5, 128.7, 127.5, 127.4, 126.4, 126.3, 125.7, 125.6, 124.8, 124.3, 124.2, 123.3, 123.1, 34.7, 19.4. HRMS (ESI): m/z [M + H]$^+$ calcd for C$_{26}$H$_{20}$NO$_3$S 426.1158; found 426.1160.

3-(4-Bromophenyl)-5-(1-(naphthalen-1-yl)ethyl)-1,2,4-oxadiazole (15). Following general procedure A, the target compound was afforded (1.25 g) as a white solid, yield 66%. ^{1}H NMR (400 MHz, CDCl$_3$) δ 8.13 (d, J = 8.5 Hz, 1H), 7.96 (d, J = 8.3 Hz, 2H), 7.89 (d, J = 8.0 Hz, 1H), 7.83−7.78 (m, 1H), 7.60 (d, J = 8.4 Hz, 2H), 7.58−7.48 (m, 2H), 7.48−7.44 (m, 2H), 5.27 (q, J = 7.1 Hz, 1H), 1.96 (d, J = 7.2 Hz, 3H).

N′-Hydroxy-2-(naphthalen-1-yl)propanimidamide (16). The amidoxime compound **16** was synthesized according to the literature method.[31] ^{1}H NMR (400 MHz, DMSO-d_6) δ 9.01 (brs, 1H), 8.26 (d, J = 8.1 Hz, 1H), 7.91 (d, J = 7.1 Hz, 1H), 7.79 (d, J = 8.0 Hz, 1H), 7.56−7.44 (m, 4H), 5.28 (brs, 2H), 4.32 (q, J = 7.1 Hz, 1H), 1.52 (d, J = 7.1 Hz, 3H).

5-(4-Bromophenyl)-3-(1-(naphthalen-1-yl)ethyl)-1,2,4-oxadiazole (18). Following general procedure A, the target compound was afforded (0.92 g) as a white solid, yield 48%. ^{1}H NMR (400 MHz, CDCl$_3$) δ 8.23 (d, J = 8.5 Hz, 1H), 7.95 (d, J = 8.3 Hz, 2H), 7.87 (d, J = 8.1 Hz, 1H), 7.78 (d, J = 8.1 Hz, 1H), 7.62 (d, J = 8.3 Hz, 2H), 7.58−7.48 (m, 3H), 7.48−7.43 (m, 1H), 5.18 (q, J = 7.1 Hz, 1H), 1.90 (d, J = 7.1 Hz, 3H).

N-(2-(4-Bromophenyl)-2-oxoethyl)-2-(naphthalen-1-yl)-propenamide (20). CDI (2.2 mmol) was added to a stirred solution of 2-(naphthalen-1-yl)propanoic acid (2.0 mmol) in dry CH$_2$Cl$_2$ (10.0 mL) at room temperature, followed by 2-amino-1-(4-bromophenyl)ethan-1-one (2.0 mmol) and DIPEA (2.2 mmol). The mixture was stirred at room temperature for 1 h. The solvent was

removed by evaporation, and the crude product was purified by flash chromatography on silica gel (MeOH/CH$_2$Cl$_2$ = 1:100) to obtain *N*-(2-(4-bromophenyl)-2-oxoethyl)-2-(naphthalen-1-yl)propenamide. White solid, 530 mg, yield 67%. ^{1}H NMR (400 MHz, CDCl$_3$) δ 8.07 (d, J = 8.2 Hz, 1H), 7.88 (d, J = 7.8 Hz, 1H), 7.82 (d, J = 8.3 Hz, 1H), 7.72 (d, J = 8.3 Hz, 2H), 7.58 (d, J = 8.2 Hz, 3H), 7.55−7.45 (m, 3H), 6.32 (brs, 1H), 4.61 (d, J = 2.6 Hz, 2H), 4.46 (q, J = 7.2 Hz, 1H), 1.75 (d, J = 7.2 Hz, 3H).

5-(4-Bromophenyl)-2-(1-(naphthalen-1-yl)ethyl)oxazole (21). *N*-(2-(4-Bromophenyl)-2-oxoethyl)-2-(naphthalen-1-yl)propenamide (1.0 mmol) was dissolved in 1.0 mL of pyridine. POCl$_3$ (4.0 mmol) was added to the solution, and the reaction mixture was stirred at room temperature for 2 h. To the resulting reaction mixture was added 20 mL of NaHCO$_3$ aq. and extracted with 20 mL of ethyl acetate. The organic extract was washed with brine and dried over anhydrous Na$_2$SO$_4$. The solvent was removed by evaporation and the crude product was purified by flash chromatography on silica gel (hexane/EtOAc = 4:1) to obtain 5-(4-bromophenyl)-2-(1-(naphthalen-1-yl)ethyl)oxazole. White solid, 240 mg, yield 63%. ^{1}H NMR (400 MHz, CDCl$_3$) δ 8.19 (d, J = 8.5 Hz, 1H), 7.88 (d, J = 8.0 Hz, 1H), 7.78 (d, J = 8.1 Hz, 1H), 7.56 (t, J = 7.7 Hz, 1H), 7.51 (d, J = 7.6 Hz, 1H), 7.49−7.41 (m, 3H), 7.41−7.36 (m, 3H), 7.30 (s, 1H), 5.13 (q, J = 7.2 Hz, 1H), 1.90 (d, J = 7.2 Hz, 3H).

5-(1-([1,1′-Biphenyl]-3-yl)ethyl)-3-(4-methyl-3-nitrophenyl)-1,2,4-oxadiazole (24a). Following general procedure A, the target compound was afforded (1.39 g) as a yellow solid, yield 72%. ^{1}H NMR (500 MHz, CDCl$_3$) δ 8.70 (s, 1H), 8.20 (d, J = 8.0 Hz, 1H), 7.59−7.57 (m, 3H), 7.54−7.52 (m, 1H), 7.47−7.42 (m, 4H), 7.38−7.34 (m, 2H), 4.54 (q, J = 7.2 Hz, 1H), 2.67 (s, 3H), 1.88 (d, J = 7.2 Hz, 3H).

5-(2-([1,1′-Biphenyl]-4-yl)propan-2-yl)-3-(4-methyl-3-nitrophenyl)-1,2,4-oxadiazole (24b). Following general procedure A, the target compound was afforded (0.71 g) as a yellow solid, yield 35%. ^{1}H NMR (400 MHz, CDCl$_3$) δ 8.71 (s, 1H), 8.22 (d, J = 8.0 Hz, 1H), 7.57−7.55 (m, 4H), 7.47−7.41 (m, 5H), 7.36−7.33 (m, 1H), 2.67 (s, 3H), 1.95 (s, 6H).

5-(1-(4-Isobutylphenyl)ethyl)-3-(4-methyl-3-nitrophenyl)-1,2,4-oxadiazole (24c). Following general procedure A, the target compound was afforded (1.04 g) as a yellow solid, yield 57%. ^{1}H NMR (400 MHz, CDCl$_3$) δ 8.82 (s, 1H), 8.33 (dd, J = 8.4 Hz, J = 1.6 Hz, 1H), 7.59 (d, J = 8.0 Hz, 1H), 7.41 (d, J = 8 Hz, 2H), 7.28−7.26 (m, 2H), 4.59 (q, J = 7.2 Hz, 1H), 2.79 (s, 3H), 2.59 (d, J = 7.2 Hz, 2H), 2.02−1.97 (m, 1H), 1.95 (d, J = 7.2 Hz, 3H), 1.03 (d, J = 6.8 Hz, 6H).

3-(4-Methyl-3-nitrophenyl)-5-(1-(3-(thiophen-2-yl)phenyl)ethyl)-1,2,4-oxadiazole (24d). Following general procedure A, the target compound was afforded (1.27 g) as a yellow solid, yield 65%. ^{1}H NMR (400 MHz, CDCl$_3$) δ 8.65 (s, 1H), 8.16 (d, J = 7.6 Hz, 1H), 7.57 (s, 1H), 7.50 (d, J = 7.6 Hz, 1H), 7.42 (d, J = 8.0 Hz, 1H), 7.33 (t, J = 7.6 Hz, 1H), 7.30−7.21 (m, 3H), 7.04−7.03 (m, 1H), 4.47 (q, J = 7.2 Hz, 1H), 2.62 (s, 3H), 1.82 (d, J = 7.2 Hz, 3H).

3-(4-Methyl-3-nitrophenyl)-5-(3-(thiophen-2-yl)benzyl)-1,2,4-oxadiazole (24e). Following general procedure A, the target compound was afforded (1.55 g) as a yellow solid, yield 82%. ^{1}H NMR (400 MHz, CDCl$_3$) δ 8.67 (s, 1H), 8.18 (d, J = 8.0 Hz, 1H), 7.62 (s, 1H), 7.57 (d, J = 8.0 Hz, 1H), 7.46 (d, J = 8.0 Hz, 1H), 7.39 (t, J = 7.6 Hz, 1H), 7.34−7.29 (m, 3H), 7.09−7.08 (m, 1H) 4.34 (s, 2H), 2.66 (s, 3H).

3-(4-Methyl-3-nitrophenyl)-5-(naphthalen-1-yl)-1,2,4-oxadiazole (24f). Following general procedure A, the target compound was afforded (0.71 g) as a yellow solid, yield 43%. ^{1}H NMR (400 MHz, CDCl$_3$) δ 9.24 (d, J = 8.7 Hz, 1H), 8.84 (s, 1H), 8.45 (d, J = 7.4 Hz, 1H), 8.37 (d, J = 7.9 Hz, 1H), 8.13 (d, J = 8.2 Hz, 1H), 7.97 (d, J = 8.2 Hz, 1H), 7.76 (t, J = 7.8 Hz, 1H), 7.64 (t, J = 7.6 Hz, 2H), 7.53 (d, J = 8.0 Hz, 1H), 2.70 (s, 3H).

3-(4-Methyl-3-nitrophenyl)-5-phenyl-1,2,4-oxadiazole (24g). Following general procedure A, the target compound was afforded (0.87 g) as a yellow solid, yield 62%. ^{1}H NMR (400 MHz, CDCl$_3$) δ 8.77 (s, 1H), 8.28 (d, J = 8.0 Hz, 1H), 8.22 (d, J = 7.6 Hz, 2H), 7.67−

7.60 (m, 1H), 7.60–7.53 (m, 2H), 7.50 (d, J = 8.0 Hz, 1H), 2.68 (s, 3H).

5-([1,1'-Biphenyl]-4-yl)-3-(4-methyl-3-nitrophenyl)-1,2,4-oxadiazole (24h). Following general procedure A, the target compound was afforded (0.81 g) as a yellow solid, yield 45%. ^{1}H NMR (400 MHz, DMSO-d_6) δ 8.63 (s, 1H), 8.33–8.27 (m, 2H), 7.99 (d, J = 8.0 Hz, 2H), 7.86–7.77 (m, 3H), 7.77–7.72 (m, 1H), 7.58–7.51 (m, 2H), 7.51–7.43 (m, 1H), 2.64 (s, 3H).

5-Benzhydryl-3-(4-methyl-3-nitrophenyl)-1,2,4-oxadiazole (24i). Following general procedure A, the target compound was afforded (1.41 g) as a white solid, yield 76%. ^{1}H NMR (400 MHz, CDCl$_3$) δ 8.69 (s, 1H), 8.21 (d, J = 8.0 Hz, 1H), 7.46 (d, J = 8.0 Hz, 1H), 7.40–7.29 (m, 10H), 5.82 (s, 1H), 2.67 (s, 3H).

(3-(4-Methyl-3-nitrophenyl)-1,2,4-oxadiazol-5-yl)(phenyl)-methanol (24j). Following general procedure A, the target compound was afforded (0.81 g) as a yellow solid, yield 52%. ^{1}H NMR (400 MHz, CDCl$_3$) δ 8.18 (s, 1H), 7.63 (d, J = 7.8 Hz, 1H), 7.44–7.36 (m, 2H), 7.35–7.28 (m, 3H), 7.14 (d, J = 7.7 Hz, 1H), 6.04 (s, 1H), 2.14 (s, 3H).

(3-(1-(3-(4-Methyl-3-nitrophenyl)-1,2,4-oxadiazol-5-yl)ethyl)-phenyl)(phenyl)methanol (24k). Following general procedure A, the target compound was afforded (1.45 g) as a white solid, yield 70%. ^{1}H NMR (400 MHz, CDCl$_3$) δ 8.66 (brs, 1H), 8.18 (d, J = 8.0 Hz, 1H), 7.47–7.42 (m, 2H), 7.38–7.35 (m, 3H), 7.34–7.27 (m, 5H), 5.85 (s, 1H), 4.45 (q, J = 7.2 Hz, 1H), 3.70 (s, 1H), 2.66 (s, 3H), 1.81 (d, J = 7.2 Hz, 3H).

3-(4-Methyl-3-nitrophenyl)-5-(1-(3-phenoxyphenyl)ethyl)-1,2,4-oxadiazole (24l). Following general procedure A, the target compound was afforded (1.44 g) as a white solid, yield 72%. ^{1}H NMR (400 MHz, DMSO-d_6) δ 8.47 (s, 1H), 8.18 (d, J = 7.6 Hz, 1H), 7.70 (d, J = 8.0 Hz, 1H), 7.39 (t, J = 9.2 Hz, 3H), 7.14 (d, J = 7.2 Hz, 2H), 7.09 (s, 1H), 7.02 (d, J = 8.0 Hz, 2H), 6.90 (dd, J = 8.2, 2.4 Hz, 1H), 4.71 (q, J = 7.2 Hz, 1H), 2.60 (s, 3H), 1.72 (d, J = 7.2 Hz, 3H).

5-(1-(6-Chloro-9H-carbazol-2-yl)ethyl)-3-(4-methyl-3-nitrophenyl)-1,2,4-oxadiazole (24m). Following general procedure A, the target compound was afforded (1.21 g) as a white solid, yield 56%. ^{1}H NMR (400 MHz, DMSO-d_6) δ 11.42 (brs, 1H), 8.51 (d, J = 2.0 Hz, 1H), 8.26–8.18 (m, 2H), 8.14 (d, J = 8.0 Hz, 1H), 7.70 (d, J = 8.0 Hz, 1H), 7.50–7.48 (m, 2H), 7.37 (dd, J = 8.8, 2.0 Hz, 1H), 7.19 (dd, J = 8.0, 1.6 Hz, 1H), 4.86 (q, J = 7.2 Hz, 1H), 2.60 (s, 3H), 1.83 (d, J = 7.2 Hz, 3H).

2-(4-(1-(3-(4-Methyl-3-nitrophenyl)-1,2,4-oxadiazol-5-yl)ethyl)-phenyl)isoindolin-1-one (24n). Following general procedure A, the target compound was afforded (0.84 g) as a white solid, yield 38%. ^{1}H NMR (400 MHz, CDCl$_3$) δ 8.69 (s, 1H), 8.20 (d, J = 8.4 Hz, 1H), 7.93–7.86 (m, 3H), 7.62–7.58 (m, 1H), 7.53–7.49 (m, 2H), 7.47–7.43 (m, 3H), 4.85 (s, 2H), 4.49 (q, J = 7.2 Hz, 1H), 2.66 (s, 3H), 1.84 (d, J = 7.2 Hz, 3H).

5-(1-(6-Methoxynaphthalen-2-yl)ethyl)-3-(4-methyl-3-nitrophenyl)-1,2,4-oxadiazole (24o). Following general procedure A, the target compound was afforded (1.36 g) as a white solid, yield 70%. ^{1}H NMR (400 MHz, CDCl$_3$) δ 8.69 (s, 1H), 8.20 (d, J = 8.0, 1H), 7.75–7.71 (m, 3H), 7.47–7.44 (m, 2H), 7.17–7.14 (m, 1H), 7.12 (s, 1H), 4.61 (q, J = 7.2 Hz, 1H), 3.93 (s, 3H), 2.70 (s, 3H), 1.90 (d, J = 7.2 Hz, 3H).

(R)-5-(1-(6-Methoxynaphthalen-2-yl)ethyl)-3-(4-methyl-3-nitrophenyl)-1,2,4-oxadiazole (24p). Following general procedure A, the target compound was afforded (1.27 g) as a white solid, yield 65%. ^{1}H NMR (400 MHz, CDCl$_3$) δ 8.69 (s, 1H), 8.19 (d, J = 8.0 Hz, 1H), 7.74–7.71 (m, 3H), 7.47–7.44 (m, 2H), 7.18–7.11 (m, 2H), 4.61 (q, J = 7.2 Hz, 1H), 3.92 (s, 3H), 2.66 (s, 3H), 1.90 (d, J = 7.2 Hz, 3H).

(S)-5-(1-(6-Methoxynaphthalen-2-yl)ethyl)-3-(4-methyl-3-nitrophenyl)-1,2,4-oxadiazole (24q). Following general procedure A, the target compound was afforded (1.40 g) as a white solid, yield 72%. ^{1}H NMR (400 MHz, CDCl$_3$) δ 8.69 (s, 1H), 8.20 (d, J = 9.6 Hz, 1H), 7.75–7.71 (m, 3H), 7.46 (d, J = 8.4 Hz, 2H), 7.17–7.12 (m, 2H), 4.61 (q, J = 7.2 Hz, 1H), 3.92 (s, 3H), 2.66 (s, 3H), 1.90 (d, J = 7.2 Hz, 3H).

5-(1-(2-Fluoro-[1,1'-biphenyl]-4-yl)ethyl)-3-(4-methyl-3-nitrophenyl)-1,2,4-oxadiazole (24r). Following general procedure A, the target compound was afforded (1.23 g) as a white solid, yield 61%. ^{1}H

NMR (400 MHz, DMSO-d_6) δ 8.51 (s, 1H), 8.22 (d, J = 8.0 Hz, 1H), 7.71 (d, J = 8.1 Hz, 1H), 7.54 (d, J = 7.8 Hz, 3H), 7.47 (t, J = 7.6 Hz, 2H), 7.44–7.37 (m, 2H), 7.33 (d, J = 8.0 Hz, 1H), 4.80 (q, J = 7.2 Hz, 1H), 2.60 (s 3H), 1.78 (d, J = 6.8 Hz, 3H).

(R)-5-(1-(2-Fluoro-[1,1'-biphenyl]-4-yl)ethyl)-3-(4-methyl-3-nitrophenyl)-1,2,4-oxadiazole (24s). Following general procedure A, the target compound was afforded (1.29 g) as a white solid, yield 64%. ^{1}H NMR (400 MHz, CDCl$_3$) δ 8.70 (s, 1H), 8.21 (d, J = 8.0 Hz, 1H), 7.53 (d, J = 7.6 Hz, 2H), 7.48–7.42 (m, 4H), 7.39–7.37 (m, 1H), 7.24–7.18 (m, 2H), 4.51 (q, J = 7.2 Hz, 1H), 2.67 (s, 3H), 1.87 (d, J = 7.2 Hz, 3H).

(S)-5-(1-(2-Fluoro-[1,1'-biphenyl]-4-yl)ethyl)-3-(4-methyl-3-nitrophenyl)-1,2,4-oxadiazole (24t). Following general procedure A, the target compound was afforded (1.55 g) as a white solid, yield 77%. ^{1}H NMR (400 MHz, CDCl$_3$) δ 8.70 (d, J = 1.8 Hz, 1H), 8.21 (dd, J = 8.0, 1.8 Hz, 1H), 7.56–7.50 (m, 2H), 7.50–7.41 (m, 4H), 7.41–7.34 (m, 1H), 7.25–7.15 (m, 2H), 4.51 (q, J = 7.2 Hz, 1H), 2.67 (s, 3H), 1.87 (d, J = 7.2 Hz, 3H).

5-(5-(1-([1,1'-Biphenyl]-3-yl)ethyl)-1,2,4-oxadiazol-3-yl)-2-methylaniline (25a). The target compound was afforded following general procedure B. White solid 520 mg, yield 73%. ^{1}H NMR (400 MHz, CDCl$_3$) δ 7.58 (d, J = 6.4 Hz, 3H), 7.54–7.48 (m, 1H), 7.46–7.40 (m, 5H), 7.37–7.33 (m, 2H), 7.14 (d, J = 7.7 Hz, 1H), 4.52 (q, J = 7.2 Hz, 1H), 2.22 (s, 3H), 1.86 (d, J = 7.2 Hz, 3H).

5-(5-(2-([1,1'-Biphenyl]-4-yl)propan-2-yl)-1,2,4-oxadiazol-3-yl)-2-methylaniline (25b). White solid 370 mg, yield 50%. ^{1}H NMR (400 MHz, CDCl$_3$) δ 7.60–7.50 (m, 4H), 7.49–7.42 (m, 5H), 7.41 (s, 1H), 7.34–7.32 (m, 1H), 7.15 (d, J = 8.0 Hz, 1H), 2.23 (s, 3H), 1.93 (s, 6H).

5-(5-(1-(4-Isobutylphenyl)ethyl)-1,2,4-oxadiazol-3-yl)-2-methylaniline (25c). White solid 490 mg, yield 73%. ^{1}H NMR (400 MHz, CDCl$_3$) δ 7.44 (d, J = 8 Hz, 1H), 7.42 (s, 1H), 7.28–7.26 (m, 2H), 7.13 (t, J = 8.8 Hz, 3H), 4.43 (q, J = 7.2 Hz, 1H), 2.45 (d, J = 6.4 Hz, 2H), 2.24 (s, 3H), 1.88–1.83 (m, 1H), 1.80 (d, J = 7.2 Hz, 3H), 0.90 (d, J = 6.4 Hz, 6H).

2-Methyl-5-(5-(1-(3-(thiophen-2-yl)phenyl)ethyl)-1,2,4-oxadiazol-3-yl)aniline (25d). White solid 455 mg, yield 63%. ^{1}H NMR (400 MHz, CDCl$_3$) δ 7.60 (s, 1H), 7.53 (d, J = 8.0 Hz, 1H), 7.45–7.41 (m, 2H), 7.35 (t, J = 7.6 Hz, 1H), 7.32–7.23 (m, 3H), 7.14 (d, J = 7.6 Hz, 1H), 7.07 (t, J = 4.4 Hz, 1H), 4.48 (q, J = 7.2 Hz, 1H), 2.22 (s, 3H), 1.84 (d, J = 7.2 Hz, 3H).

2-Methyl-5-(5-(3-(thiophen-2-yl)benzyl)-1,2,4-oxadiazol-3-yl)-aniline (25e). White solid 550 mg, yield 79%. ^{1}H NMR (400 MHz, CDCl$_3$) δ 7.62 (s, 1H), 7.55 (d, J = 8.0 Hz, 1H), 7.43–7.35 (m, 3H), 7.32–7.26 (m, 3H), 7.14 (d, J = 7.6 Hz, 1H), 7.08 (t, J = 4.4 Hz, 1H), 4.31 (s, 2H), 2.21 (s, 3H).

2-Methyl-5-(5-(naphthalen-1-yl)-1,2,4-oxadiazol-3-yl)aniline (25f). White solid 300 mg, yield 50%. ^{1}H NMR (400 MHz, CDCl$_3$) δ 9.26 (d, J = 8.7 Hz, 1H), 8.41 (d, J = 8.6 Hz, 1H), 8.10 (d, J = 8.2 Hz, 1H), 7.96 (d, J = 8.2 Hz, 1H), 7.72 (t, J = 7.7 Hz, 1H), 7.66–7.58 (m, 3H), 7.57 (s, 1H), 7.22 (d, J = 7.7 Hz, 1H), 3.79 (brs, 2H), 2.26 (s, 3H).

2-Methyl-5-(5-phenyl-1,2,4-oxadiazol-3-yl)aniline (25g). White solid 367 mg, yield 73%. ^{1}H NMR (400 MHz, DMSO-d_6) δ 8.17 (d, J = 7.2 Hz, 2H), 7.76–7.71 (m, 1H), 7.71–7.63 (m, 2H), 7.40 (s, 1H), 7.21 (d, J = 7.2 Hz, 1H), 7.12 (d, J = 7.7 Hz, 1H), 5.23 (brs, 2H), 2.13 (s, 3H).

5-(5-([1,1'-Biphenyl]-4-yl)-1,2,4-oxadiazol-3-yl)-2-methylaniline (25h). White solid 490 mg, yield 75%. ^{1}H NMR (400 MHz, DMSO-d_6) δ 8.24 (d, J = 8.1 Hz, 2H), 7.97 (d, J = 8.1 Hz, 2H), 7.80 (d, J = 7.6 Hz, 2H), 7.58–7.51 (m, 2H), 7.50–7.43 (m, 1H), 7.42 (s, 1H), 7.23 (d, J = 7.4 Hz, 1H), 7.13 (d, J = 7.7 Hz, 1H), 5.22 (brs, 2H), 2.14 (s, 3H).

5-(5-Benzhydryl-1,2,4-oxadiazol-3-yl)-2-methylaniline (25i). White solid 457 mg, yield 67%. ^{1}H NMR (400 MHz, CDCl$_3$) δ 7.47–7.43 (m, 2H), 7.38–7.27 (m, 10H), 7.14 (d, J = 7.6 Hz, 1H), 5.79 (s, 1H), 2.23 (s, 3H).

(3-(3-Amino-4-methylphenyl)-1,2,4-oxadiazol-5-yl)(phenyl)-methanol (25j). White solid 298 mg, yield 53%. ^{1}H NMR (400 MHz, DMSO-d_6) δ 7.51 (d, J = 7.2 Hz, 2H), 7.44–7.37 (m, 2H), 7.37–7.32

(m, 1H), 7.11−7.03 (m, 2H), 6.81 (d, J = 5.0 Hz, 1H), 6.09 (d, J = 5.0 Hz, 1H), 2.10 (s, 3H).

(3-(1-(3-(3-Amino-4-methylphenyl)-1,2,4-oxadiazol-5-yl)ethyl)-phenyl)(phenyl)methanol (25k). White solid 560 mg, yield 73%. ^{1}H NMR (400 MHz, CDCl₃) δ 7.50−7.41 (m, 3H), 7.35−7.32(m, 3H), 7.32−7.22 (m, 5H), 7.16 (d, J = 8.0 Hz, 1H), 5.83 (s, 1H), 5.30 (s, 1H), 4.43 (q, J = 7.2 Hz, 1H), 2.26 (s, 3H), 1.78 (d, J = 7.2 Hz, 3H).

2-Methyl-5-(5-(1-(3-phenoxyphenyl)ethyl)-1,2,4-oxadiazol-3-yl)-aniline (25l). White solid 624 mg, yield 84%. ^{1}H NMR (400 MHz, DMSO-d₆) δ 7.43 (s, 1H), 7.37−7.35 (m, 2H), 7.30−7.26 (m, 5H), 7.19−7.18 (m, 2H), 7.12−7.05 (m, 2H), 5.17 (brs, 2H), 4.60 (q, J = 4.0 Hz, 1H), 2.11 (s, 3H), 1.68 (d, J = 4.0 Hz, 3H).

5-(5-(1-(5-Chloro-9H-carbazol-2-yl)ethyl)-1,2,4-oxadiazol-3-yl)-2-methylaniline (25m). White solid 588 mg, yield 73%. ^{1}H NMR (400 MHz, DMSO-d₆) δ 11.42 (brs, 1H), 8.19 (s, 1H), 8.14 (d, J = 8.0 Hz, 1H), 7.50−7.47 (m, 2H), 7.37 (dd, J = 8.8, 2.4 Hz, 1H), 7.31 (s, 1H), 7.18 (d, J = 8.4 Hz, 1H), 7.13−7.06 (m, 2H), 5.17 (brs, 2H), 4.79 (q, J = 7.2 Hz, 1H), 2.10 (s, 3H), 1.80 (d, J = 7.2 Hz, 3H).

2-(4-(1-(3-(3-Amino-4-methylphenyl)-1,2,4-oxadiazol-5-yl)-ethyl)phenyl)isoindolin-1-one (25n). White solid 590 mg, yield 72%. ^{1}H NMR (400 MHz, CDCl₃) δ 7.91 (d, J = 8.0 Hz, 1H), 7.85 (d, J = 8.4 Hz, 2H), 7.60−7.56 (m, 1H), 7.51−7.47 (m, 2H), 7.45−7.38 (m, 4H), 7.13 (d, J = 7.6 Hz, 1H), 4.82 (s, 2H), 4.46 (q, J = 7.2 Hz, 1H), 2.20 (s, 3H), 1.81 (d, J = 7.2 Hz, 3H).

5-(5-(1-(6-Methoxynaphthalen-2-yl)ethyl)-1,2,4-oxadiazol-3-yl)-2-methylaniline (25o). White solid 600 mg, yield 83%. ^{1}H NMR (400 MHz, CDCl₃) δ 7.72−7.69 (m, 3H), 7.46−7.43 (m, 3H), 7.16−7.05 (m, 3H), 4.58 (q, J = 7.6 Hz, 1H), 3.91 (s, 3H), 2.23 (s, 3H), 1.88 (d, J = 7.6 Hz, 3H).

(R)-5-(5-(1-(6-Methoxynaphthalen-2-yl)ethyl)-1,2,4-oxadiazol-3-yl)-2-methylaniline (25p). White solid 610 mg, yield 85%. ^{1}H NMR (400 MHz, CDCl₃) δ 7.73−7.69 (m, 3H), 7.48−7.44 (m, 3H), 7.16−7.10 (m, 3H), 4.58 (q, J = 7.2 Hz, 1H), 3.91 (s, 3H), 2.25 (s, 3H), 1.88 (d, J = 7.2 Hz, 3H).

(S)-5-(5-(1-(6-Methoxynaphthalen-2-yl)ethyl)-1,2,4-oxadiazol-3-yl)-2-methylaniline (25q). White solid 550 mg, yield 77%. ^{1}H NMR (400 MHz, CDCl₃) δ 7.72−7.69 (m, 3H), 7.46−7.41 (m, 3H), 7.16−7.11 (m, 3H), 4.58 (q, J = 7.2 Hz, 1H), 3.91 (s, 3H), 2.22 (s, 3H), 1.88 (d, J = 7.2 Hz, 3H).

5-(5-(1-(2-Fluoro-[1,1′-biphenyl]-4-yl)ethyl)-1,2,4-oxadiazol-3-yl)-2-methylaniline (25r). White solid 620 mg, yield 83%. ^{1}H NMR (400 MHz, CDCl₃) δ 7.53 (d, J = 9.2 Hz, 2H), 7.46−7.34 (m, 4H), 7.39−7. 34 (m, 2H), 7.23−7.15 (m, 3H), 4.49 (q, J = 7.2 Hz, 1H), 2.24 (s, 3H), 1.84 (d, J = 7.2 Hz, 3H).

(R)-5-(5-(1-(2-Fluoro-[1,1′-biphenyl]-4-yl)ethyl)-1,2,4-oxadiazol-3-yl)-2-methylaniline (25s). White solid 610 mg, yield 82%. ^{1}H NMR (400 MHz, DMSO-d₆) δ 7.55−7.46 (m, 5H), 7.42−7.37 (m, 2H), 7.32−7.29 (m, 2H), 7.13−7.06 (m, 2H), 5.17 (s, 2H), 4.73 (q, J = 7.2 Hz, 1H), 2.10 (s, 3H), 1.75 (d, J = 7.2 Hz, 3H).

(S)-5-(5-(1-(2-Fluoro-[1,1′-biphenyl]-4-yl)ethyl)-1,2,4-oxadiazol-3-yl)-2-methylaniline (25t). White solid 575 mg, yield 77%. ^{1}H NMR (400 MHz, CDCl₃) δ 7.53 (d, J = 7.6 Hz, 2H), 7.46 (s, 1H), 7.45−7.35 (m, 5H), 7.23−7.21 (m, 2H), 7.18−7.14 (m, 1H), 4.49 (q, J = 7.2 Hz, 1H), 2.23 (s, 3H), 1.84 (d, J = 7.2 Hz, 3H).

5-(((5-(5-(1-([1,1′-Biphenyl]-3-yl)ethyl)-1,2,4-oxadiazol-3-yl)-2-methylphenyl)amino)methyl)thiophene-2-carboxylic Acid (26a). The target compound was afforded following general procedure C. White solid, 145 mg, yield 73%, mp 130−131 °C. ^{1}H NMR (400 MHz, DMSO-d₆) δ 7.66−7.55 (m, 5H), 7.47 (s, 3H), 7.39−7.33 (m, 2H), 7.17 (d, J = 6.9 Hz, 2H), 7.10−7.08 (m, 2H), 6.12 (brs, 1H), 4.70 (q, J = 7.2 Hz, 1H), 4.60 (s, 2H), 2.20 (s, 3H), 1.75 (d, J = 7.2 Hz, 3H). ^{13}C NMR (125 MHz, DMSO-d₆) δ 181.6, 168.2, 163.0, 146.2, 141.2, 140.9, 140.0, 133.3, 130.7, 129.7, 129.2, 129.1, 127.9, 127.8, 126.9, 126.5, 126.5, 126.2, 126.0, 125.5, 124.7, 115.7, 107.5, 42.4, 37.6, 19.9, 18.0. HRMS (ESI): *m/z* [M + H]⁺ calcd for C₂₉H₂₆N₃O₃S 496.1689; found 496.1694.

5-(((5-(5-(2-([1,1′-Biphenyl]-4-yl)propan-2-yl)-1,2,4-oxadiazol-3-yl)-2-methylphenyl)amino)methyl)thiophene-2-carboxylic Acid (26b). White solid, 98 mg, yield 48%, mp 184−185 °C. ^{1}H NMR (400 MHz, DMSO-d₆) δ 7.64 (d, J = 8.0 Hz, 4H), 7.56 (s, 1H), 7.47−7.34 (m, 5H), 7.22−7.16 (m, 2H), 7.14−7.11 (m, 2H), 6.13

(brs, 1H), 4.60 (d, J = 5.6 Hz, 2H), 2.21 (s, 3H), 1.84 (s, 6H). ^{13}C NMR (125 MHz, DMSO-d₆) δ 184.3, 167.9, 152.4, 146.1, 143.3, 142.8, 139.6, 139.0, 132.9, 130.5, 128.9, 127.5, 127.1, 127.0, 126.7, 126.3, 126.2, 125.3, 124.5, 115.6, 107.4, 42.3, 40.4, 27.3, 17.9. HRMS (ESI): *m/z* [M + H]⁺ calcd for C₃₀H₂₈N₃O₃S 510.1846; found 510.1854.

5-(((5-(5-(1-(4-Isobutylphenyl)ethyl)-1,2,4-oxadiazol-3-yl)-2-methylphenyl)amino)methyl)thiophene-2-carboxylic Acid (26c). White solid, 86 mg, yield 45%, mp 177−178 °C. ^{1}H NMR (400 MHz, DMSO-d₆) δ 12.90 (brs, 1H), 7.58 (d, J = 4.0 Hz, 1H), 7.24 (d, J = 8.0 Hz, 2H), 7.20−7.17 (m, 2H), 7.14−7.10 (m, 4H), 6.13 (brs, 1H), 4.61 (d, J = 5.4 Hz, 2H), 4.55 (q, J = 7.2 Hz, 1H), 2.41 (d, J = 7.2 Hz, 2H), 2.21 (s, 3H), 1.85−1.75 (m, 1H), 1.67 (d, J = 7.2 Hz, 3H), 0.84 (d, J = 6.4 Hz, 6H). ^{13}C NMR (125 MHz, DMSO-d₆) δ 181.5, 167.8, 162.7, 152.6, 145.9, 140.1, 137.5, 133.1, 132.3, 130.3, 129.2, 126.9, 126.1, 125.2, 124.4, 115.3, 107.2, 44.0, 42.1, 36.8, 29.4, 21.9, 19.5, 17.7. HRMS (ESI): *m/z* [M + H]⁺ calcd for C₂₇H₃₀N₃O₃S 476.2002; found 476.2009.

5-(((2-Methyl-5-(5-(1-(3-(thiophen-2-yl)phenyl)ethyl)-1,2,4-oxa-diazol-3-yl)phenyl)amino)methyl)thiophene-2-carboxylic Acid (26d). White solid, 80 mg, yield 50%, mp 103−104 °C. ^{1}H NMR (400 MHz, DMSO-d₆) δ 12.89 (brs, 1H), 7.67 (s, 1H), 7.59−7.53 (m, 4H), 7.41 (t, J = 7.7 Hz, 1H), 7.28 (d, J = 7.7 Hz, 1H), 7.21−7.14 (m, 3H), 7.11−7.09 (m, 2H), 6.13 (brs, 1H), 4.67 (q, J = 7.2 Hz, 1H), 4.61 (d, J = 5.7 Hz, 2H), 2.21 (s, 3H), 1.73 (d, J = 7.2 Hz, 3H). ^{13}C NMR (125 MHz, DMSO-d₆) δ 181.4, 168.0, 162.9, 152.8, 146.0, 142.9, 141.3, 134.3, 133.3, 132.4, 130.5, 129.7, 128.5, 126.5, 126.3, 125.9, 125.3, 124.6, 124.6, 124.5, 124.1, 115.5, 107.4, 42.3, 37.3, 19.7, 17.8. HRMS (ESI): *m/z* [M + H]⁺ calcd for C₂₇H₂₄N₃O₃S₂ 502.1254; found 502.1258.

5-(((2-Methyl-5-(5-(3-(thiophen-2-yl)benzyl)-1,2,4-oxadiazol-3-yl)phenyl)amino)methyl)thiophene-2-carboxylic Acid (26e). White solid, 90 mg, yield 46%, mp 140−141 °C. ^{1}H NMR (400 MHz, DMSO-d₆) δ 7.69 (s,1H), 7.60 (d, J = 8.0 Hz, 1H), 7.57−7.52 (m, 3H), 7.41 (t, J = 7.6 Hz, 1H), 7.30 (d, J = 8.0 Hz, 1H), 7.16−7.14 (m, 3H), 7.09−7.07 (m, 2H), 6.12 (brs, 1H), 4.60 (d, J = 6.0 Hz, 2H), 4.44 (s, 2H), 2.20 (s, 3H). ^{13}C NMR (125 MHz, DMSO-d₆) δ 178.2, 168.2, 162.9, 152.7, 146.0, 142.9, 135.1, 134.2, 131.9, 133.2, 130.5, 129.6, 128.5, 128.3, 126.3, 126.2, 125.9, 125.3, 124.5, 124.4, 123.9, 115.4, 107.4, 42.2, 31.8, 17.8. HRMS (ESI): *m/z* [M + H]⁺ calcd for C₂₆H₂₂N₃O₃S₂ 488.1087; found 488.1100.

5-(((2-Methyl-5-(5-(naphthalen-1-yl)-1,2,4-oxadiazol-3-yl)-phenyl)amino)methyl)thiophene-2-carboxylic Acid (26f). White solid, 62 mg, yield 35%, mp 227−228 °C. ^{1}H NMR (700 MHz, DMSO-d₆) δ 9.15−9.11 (m, 1H), 8.41 (d, J = 5.9 Hz, 1H), 8.32 (d, J = 8.2 Hz, 1H), 8.14 (d, J = 6.9 Hz, 1H), 7.82 (t, J = 7.0 Hz, 1H), 7.77−7.74 (m, 1H), 7.71 (t, J = 6.9 Hz, 1H), 7.64 (d, J = 3.8 Hz, 1H), 7.38 (d, J = 5.7 Hz, 1H), 7.29 (s, 1H), 7.25 (d, J = 7.6 Hz, 1H), 7.21 (d, J = 3.8 Hz, 1H), 4.69 (s, 2H), 2.26 (s, 3H). ^{13}C NMR (175 MHz, DMSO-d₆) δ 174.7, 168.4, 162.8, 152.9, 146.0, 133.8, 133.4, 133.2, 132.3, 130.5, 129.9, 129.3, 128.9, 128.4, 126.8, 126.3, 125.3, 125.2, 125.0, 124.4, 119.7, 115.3, 107.7, 42.3, 17.8. HRMS (ESI): *m/z* [M + H]⁺ calcd for C₂₅H₂₀N₃O₃S 442.1220; found 442.1218.

5-(((2-Methyl-5-(5-phenyl-1,2,4-oxadiazol-3-yl)phenyl)amino)-methyl)thiophene-2-carboxylic Acid (26g). White solid, 68 mg, yield 43%, mp 174−175 °C. ^{1}H NMR (400 MHz, DMSO-d₆) δ 8.15 (d, J = 7.6 Hz, 2H), 7.76−7.70 (m, 1H), 7.70−7.62 (m, 2H), 7.58 (s, 1H), 7.30 (d, J = 7.7 Hz, 1H), 7.24−7.18 (m, 2H), 7.15 (s, 1H), 6.16 (brs, 1H), 4.64 (d, J = 5.8 Hz, 2H), 2.23 (s, 3H). ^{13}C NMR (175 MHz, DMSO-d₆) δ 174.9, 168.6, 162.8, 146.0, 141.1, 133.1, 130.4, 129.4, 127.7, 126.7, 126.3, 125.2, 125.1, 124.3, 123.4, 115.4, 107.3, 42.2, 17.8. HRMS (ESI): *m/z* [M + H]⁺ calcd for C₂₁H₁₈N₃O₃S 392.1063; found 392.1054.

5-(((5-(5-([1,1′-Biphenyl]-4-yl)-1,2,4-oxadiazol-3-yl)-2-methylphenyl)amino)methyl)thiophene-2-carboxylic Acid (26h). White solid, 79 mg, yield 42%, mp 224−225 °C. ^{1}H NMR (400 MHz, DMSO-d₆) δ 8.23 (d, J = 8.3 Hz, 2H), 8.00−7.94 (m, 3H), 7.83−7.77 (m, 3H), 7.60 (d, J = 3.8 Hz, 1H), 7.54 (t, J = 7.5 Hz, 3H), 7.47 (d, J = 7.4 Hz, 1H), 7.31 (d, J = 7.6 Hz, 1H), 7.23 (s, 2H), 7.16 (d, J = 3.7 Hz, 1H), 4.66 (d, J = 5.6 Hz, 2H). ^{13}C NMR (175 MHz,

DMSO-d_6) δ 174.7, 168.6, 162.9, 147.2, 146.0, 144.4, 138.5, 130.5, 129.1, 128.5, 128.4, 127.6, 126.9, 126.3, 125.3, 124.4, 122.2, 115.4, 114.7, 111.8, 107.4, 42.2, 17.8. HRMS (ESI): m/z [M + H]$^+$ calcd for $C_{27}H_{22}N_3O_3S$ 468.1376; found 468.1374.

5-(((5-(5-Benzhydryl-1,2,4-oxadiazol-3-yl)-2-methylphenyl)-amino)methyl)thiophene-2-carboxylic Acid (26i). White solid, 106 mg, yield 55%, mp 127−128 °C. ^{1}H NMR (400 MHz, DMSO-d_6) δ 12.91 (brs, 1H), 7.57 (d, J = 3.6 Hz, 1H), 7.42−7.34 (m, 8H), 7.33−7.27 (m, 2H), 7.19−7.15 (m, 2H), 7.12−7.09 (m, 2H), 6.16 (t, J = 5.2 Hz, 1H), 6.09 (s, 1H), 4.60 (d, J = 5.2 Hz, 2H), 2.21 (s, 3H). ^{13}C NMR (125 MHz, DMSO-d_6) δ 179.7, 168.4, 163.0, 152.9, 146.2, 138.9, 133.4, 132.5, 130.7, 128.9, 128.6, 127.7, 126.6, 125.5, 124.5, 115.6, 107.7, 48.2, 42.5, 18.0. HRMS (ESI): m/z [M + H]$^+$ calcd for $C_{28}H_{24}N_3O_3S$ 482.1533; found 482.1540.

5-(((5-(5-(Hydroxy(phenyl)methyl)-1,2,4-oxadiazol-3-yl)-2-methylphenyl)amino)methyl)thiophene-2-carboxylic Acid (26j). White solid, 86 mg, yield 51%, mp 170−171 °C. ^{1}H NMR (400 MHz, DMSO-d_6) δ 7.57 (d, J = 3.7 Hz, 1H), 7.50 (d, J = 7.6 Hz, 2H), 7.40 (t, J = 7.4 Hz, 2H), 7.37−7.31 (m, 1H), 7.17 (s, 2H), 7.12−7.06 (m, 2H), 6.80 (d, J = 5.0 Hz, 1H), 6.13 (t, J = 6.2 Hz, 1H), 6.08 (d, J = 4.0 Hz, 1H), 4.60 (d, J = 5.6 Hz, 2H), 2.20 (s, 3H). ^{13}C NMR (175 MHz, DMSO-d_6) δ 180.0, 167.9, 162.8, 152.6, 145.9, 139.1, 133.1, 132.4, 130.4, 128.4, 128.2, 126.5, 126.3, 125.2, 124.2, 115.4, 107.2, 67.5, 42.1, 17.7. HRMS (ESI): m/z [M + H]$^+$ calcd for $C_{22}H_{20}N_3O_4S$ 422.1169; found 422.1173.

5-(((5-(5-(1-(3-(Hydroxy(phenyl)methyl)phenyl)ethyl)-1,2,4-oxadiazol-3-yl)-2-methylphenyl)amino)methyl)thiophene-2-carboxylic Acid (26k). White solid, 58 mg, yield 21%, mp 71−72 °C. ^{1}H NMR (400 MHz, DMSO-d_6) δ 12.89 (brs, 1H), 7.58 (s, 1H), 7.42−7.34 (m, 3H), 7.29−7.23 (m, 4H), 7.22−7.14 (m, 4H), 7.13−7.07 (m, 2H), 6.13 (brs, 1H), 5.68 (m, 1H), 4.66−4.50 (m, 3H), 2.21 (s, 3H), 1.66 (d, J = 7.2 Hz, 3H). ^{13}C NMR (125 MHz, DMSO-d_6) δ 181.5, 168.0, 162.9, 152.8, 146.4, 146.0, 145.4, 140.2, 133.3, 132.4, 130.5, 128.6, 128.1, 126.8, 126.3, 125.7, 125.4, 125.3, 125.2, 124.5, 115.6, 107.3, 74.1, 42.3, 37.4, 19.7, 17.8. HRMS (ESI): m/z [M + H]$^+$ calcd for $C_{30}H_{28}N_3O_4S$ 526.1795; found 526.1774.

5-(((2-Methyl-5-(5-(1-(3-phenoxyphenyl)ethyl)-1,2,4-oxadiazol-3-yl)phenyl)amino)methyl)thiophene-2-carboxylic Acid (26l). White solid, 104 mg, yield 51%, mp 135−136 °C, purity 99.11%. ^{1}H NMR (400 MHz, DMSO-d_6) δ 12.89 (brs, 1H), 7.57 (d, J = 4.0 Hz, 1H), 7.40−7.35 (m, 3H), 7.17−7.14 (m, 3H), 7.12−7.09 (m, 3H), 7.05−7.01 (m, 3H), 6.89 (d, J = 8.4 Hz, 1H), 6.13 (brs,1H), 4.64−4.59 (m, 3H), 2.21 (s, 3H), 1.67 (d, J = 7.2 Hz, 3H). ^{13}C NMR (125 MHz, DMSO-d_6) δ 181.2, 168.0, 162.9, 156.9, 156.3, 152.7, 146.0, 142.5, 133.2, 130.5, 130.5, 130.1, 126.3, 125.3, 124.5, 123.7, 122.3, 118.8, 117.7, 117.2, 115.6, 110.9, 107.3, 42.3, 37.1, 19.7, 17.9. HRMS (ESI): m/z [M + H]$^+$ calcd for $C_{29}H_{26}N_3O_4S$ 512.1639; found 512.1645.

5-(((5-(5-(1-(6-Chloro-9H-carbazol-2-yl)ethyl)-1,2,4-oxadiazol-3-yl)-2-methylphenyl)amino)methyl)thiophene-2-carboxylic Acid (26m). White solid, 87 mg, yield 40%, mp 182−183 °C. ^{1}H NMR (400 MHz, DMSO-d_6) δ 11.62 (brs, 1H), 8.18 (s, 1H), 8.12 (d, J = 8.0 Hz, 1H), 7.49 (d, J = 8.4 Hz, 1H), 7.45 (s, 2H), 7.36 (d, J = 8.8 Hz, 1H), 7.20−7.16 (m, 4H), 7.04 (s, 1H), 6.09 (brs, 1H), 4.76 (q, J = 7.2 Hz, 1H), 4.57 (d, J = 5.6 Hz, 2H), 2.20 (s, 3H), 1.77 (d, J = 7.2 Hz, 3H). ^{13}C NMR (125 MHz, DMSO-d_6) δ 181.9, 168.2, 147.7, 146.3, 144.3, 140.8, 138.9, 138.7, 131.8, 130.6, 128.8, 126.4, 125.5, 125.2, 124.7, 123.6, 123.1, 121.3, 121.0, 119.9, 118.6, 115.5, 112.7, 110.0, 107.7, 42.4, 37.9, 20.3, 18.0. HRMS (ESI): m/z [M + H]$^+$ calcd for $C_{29}H_{24}N_4O_3SCl$ 543.1252; found 543.1262.

5-(((2-Methyl-5-(5-(1-(4-(1-oxoisoindolin-2-yl)phenyl)ethyl)-1,2,4-oxadiazol-3-yl)phenyl)amino)methyl)thiophene-2-carboxylic Acid (26n). White solid, 95 mg, yield 43%, mp 165−166 °C. ^{1}H NMR (400 MHz, DMSO-d_6) δ 12.88 (brs, 1H), 7.90 (d, J = 8.0 Hz, 2H), 7.78 (d, J = 7.6 Hz, 1H), 7.70−7.67 (m, 2H), 7.58−7.53 (m, 2H), 7.43 (d, J = 8.4 Hz, 2H), 7.18 (q, J = 7.7 Hz, 2H), 7.11 (s, 2H), 6.13 (brs, 1H), 5.02 (s, 2H), 4.64−4.60 (m, 3H), 2.21 (s, 3H), 1.71 (d, J = 7.2 Hz, 3H). ^{13}C NMR (125 MHz, DMSO-d_6) δ 181.7, 168.2, 166.8, 163.0, 146.2, 141.2, 138.9, 136.1, 134.9, 133.4, 132.5, 132.5, 130.7, 128.4, 128.2, 126.5, 126.1, 125.5, 124.7, 123.5, 123.4, 119.8, 115.7,

107.6, 50.6, 42.5, 37.0, 19.8, 18.0. HRMS (ESI): m/z [M + H]$^+$ calcd for $C_{31}H_{27}N_4O_4S$ 551.1748; found 551.1755.

5-(((5-(5-(1-(6-Methoxynaphthalen-2-yl)ethyl)-1,2,4-oxadiazol-3-yl)-2-methylphenyl)amino)methyl)thiophene-2-carboxylic Acid (26o). White solid, 84 mg, yield 42%, mp 147−148 °C. ^{1}H NMR (400 MHz, DMSO-d_6) δ 12.83 (brs, 1H), 7.82 (s, 1H), 7.80 (s, 2H), 7.55 (d, J = 3.6 Hz, 1H), 7.45 (d, J = 9.2 Hz, 1H), 7.30 (d, J = 2.4 Hz, 1H), 7.23−7.12 (m, 3H), 7.13−7.06 (m, 2H), 6.12 (t, J = 6.0 Hz, 1H), 4.72 (q, J = 7.2 Hz, 1H), 4.60 (d, J = 5.6 Hz, 2H), 3.86 (s, 3H), 2.20 (s, 3H), 1.76 (d, J = 7.2 Hz, 3H). ^{13}C NMR (125 MHz, DMSO-d_6) δ 181.8, 168.2, 163.1, 157.6, 152.9, 146.2, 135.5, 133.7, 133.3, 132.5, 130.7, 129.4, 128.6, 127.5, 126.4, 126.2, 125.9, 125.5, 124.7, 119.1, 115.7, 107.6, 105.9, 55.4, 42.4, 37.5, 19.8, 18.0. HRMS (ESI): m/z [M + H]$^+$ calcd for $C_{28}H_{26}N_3O_4S$ 500.1639; found 500.1642.

(R)-5-(((5-(5-(1-(6-Methoxynaphthalen-2-yl)ethyl)-1,2,4-oxadiazol-3-yl)-2-methylphenyl)amino)methyl)thiophene-2-carboxylic Acid (26p). White solid, 88 mg, yield 44%, mp 148−149 °C. ^{1}H NMR (400 MHz, DMSO-d_6) δ 7.81 (d, J = 9.6 Hz, 3H), 7.52 (s, 1H), 7.45 (d, J = 8.4 Hz, 1H), 7.30 (s, 1H), 7.19−7.16 (m, 3H), 7.11 (s, 1H), 7.08 (s, 1H), 6.11 (brs, 1H), 4.72 (q, J = 7.2 Hz, 1H), 4.59 (d, J = 5.6 Hz, 2H), 3.86 (s, 3H), 2.20 (s, 3H), 1.77 (d, J = 7.2 Hz, 3H). ^{13}C NMR (125 MHz, DMSO-d_6) δ 181.6, 168.0, 162.9, 157.4, 152.8, 146.0, 135.4, 133.5, 133.3, 132.5, 130.5, 129.3, 128.4, 127.4, 126.3, 126.0, 125.8, 125.3, 124.5, 118.9, 115.5, 107.4, 105.8, 55.2, 42.3, 37.4, 19.6, 17.8. HRMS (ESI): m/z [M + H]$^+$ calcd for $C_{28}H_{26}N_3O_4S$ 500.1639; found 500.1642.

(S)-5-(((5-(5-(1-(6-Methoxynaphthalen-2-yl)ethyl)-1,2,4-oxadiazol-3-yl)-2-methylphenyl)amino)methyl)thiophene-2-carboxylic Acid (26q). White solid, 80 mg, yield 40%, mp 150−151 °C. ^{1}H NMR (400 MHz, DMSO-d_6) δ 7.81 (d, J = 9.2 Hz, 3H), 7.51 (s, 1H), 7.45 (d, J = 8 Hz,1H), 7.31 (s, 1H), 7.20−7.06 (m, 5H), 6.10 (brs, 1H), 4.72 (q, J = 7.2 Hz, 1H), 4.59 (d, J = 6 Hz, 2H), 3.86 (s, 3H), 2.20 (s, 3H), 1.77 (d, J = 7.2 Hz, 3H). ^{13}C NMR (125 MHz, DMSO-d_6) δ 181.8, 168.2, 163.1, 157.2, 152.9, 146.2, 135.5, 133.7, 133.4, 132.7, 130.7, 129.4, 128.6, 127.5, 126.5, 126.2, 125.9, 125.5, 124.7, 119.1, 115.7, 107.6, 105.9, 55.4, 42.5, 37.5, 19.8, 18.0. HRMS (ESI): m/z [M + H]$^+$ calcd for $C_{28}H_{26}N_3O_4S$ 500.1639; found 500.1642.

5-(((5-(5-(1-(2-Fluoro-[1,1′-biphenyl]-4-yl)ethyl)-1,2,4-oxadiazol-3-yl)-2-methylphenyl)amino)methyl)thiophene-2-carboxylic Acid (26r). White solid, 78 mg, yield 38%, mp 168−169 °C, purity 99.31%. ^{1}H NMR (400 MHz, DMSO-d_6) δ 12.89 (brs, 1H), 7.55−7.53 (m, 4H), 7.48 (t, J = 6.8 Hz, 2H), 7.42−7.36 (m, 2H), 7.29 (d, J = 8.0 Hz, 1H), 7.21−7.15 (m, 2H), 7.11 (s, 2H), 6.14 (brs, 1H), 4.70 (q, J = 7.2 Hz, 1H), 4.61 (d, J = 5.6 Hz, 2H), 2.21 (s, 3H), 1.73 (d, J = 7.2 Hz, 3H). ^{13}C NMR (125 MHz, DMSO-d_6) δ 180.8, 167.9, 162.7, 158.9 (d, $J_{F,C}$ = 245 Hz), 152.7, 145.9, 141.9, 134.5, 133.1, 132.3, 131.0, 130.3, 128.6, 128.6, 127.8, 127.2, 126.2, 125.2, 124.3, 123.8, 115.3, 115.1, 107.2, 42.1, 36.6, 19.2, 17.6. HRMS (ESI): m/z [M + H]$^+$ calcd for $C_{29}H_{25}N_3O_4FS$ 514.1595; found 514.1600.

(R)-5-(((5-(5-(1-(2-Fluoro-[1,1′-biphenyl]-4-yl)ethyl)-1,2,4-oxadiazol-3-yl)-2-methylphenyl)amino)methyl)thiophene-2-carboxylic Acid (26s). White solid, 88 mg, yield 43%, mp 170−171 °C. ^{1}H NMR (400 MHz, DMSO-d_6) δ 12.84 (s, 1H), 7.58 (d, J = 3.6 Hz, 1H), 7.56−7.53 (m, 3H), 7.51−7.46 (m, 2H), 7.43−7.36 (m, 2H), 7.29 (dd, J = 8.0, 1.6 Hz, 1H), 7.22−7.16 (m, 2H), 7.12 (s, 2H), 6.15 (t, J = 5.6 Hz, 1H), 4.71 (q, J = 7.2 Hz, 1H), 4.61 (d, J = 5.6 Hz, 2H), 2.21 (s, 3H), 1.73 (d, J = 7.2 Hz, 3H). ^{13}C NMR (125 MHz, DMSO-d_6) δ 180.9, 168.1, 162.9, 158.9 (d, $J_{F,C}$ = 245 Hz), 152.8, 146.0, 142.0, 134.7, 133.3, 132.5, 131.2, 130.5, 128.8, 128.6, 127.9, 127.3, 126.4, 125.4, 124.4, 124.0, 115.3, 115.2, 107.4, 42.3, 36.8, 19.4, 17.9. HRMS (ESI): m/z [M + H]$^+$ calcd for $C_{29}H_{25}N_3O_4FS$ 514.1595; found 514.1600.

(S)-5-(((5-(5-(1-(2-Fluoro-[1,1′-biphenyl]-4-yl)ethyl)-1,2,4-oxadiazol-3-yl)-2-methylphenyl)amino)methyl)thiophene-2-carboxylic Acid (26t). White solid, 78 mg, yield 38%, mp 169−170 °C. ^{1}H NMR (400 MHz, DMSO-d_6) δ 12.90 (brs, 1H), 7.56−7.52 (m, 4H), 7.47 (t, J = 7.6 Hz, 2H), 7.42−7.36 (m, 2H), 7.29 (d, J = 8.0 Hz, 1H), 7.18 (q, J = 6.8 Hz, 2H), 7.12 (s, 2H), 6.14 (t, J = 5.6 Hz, 1H), 4.71 (q, J = 7.2 Hz, 1H), 4.61 (d, J = 5.6 Hz, 2H), 2.21 (s, 3H), 1.73 (d, J = 7.2 Hz, 3H). ^{13}C NMR (125 MHz, DMSO-d_6) δ 180.9, 168.1, 162.9, 158.9 (d, $J_{F,C}$ = 245 Hz), 152.9, 146.0, 142.1, 134.7, 133.3, 132.4,

131.2, 130.5, 128.8, 128.6, 127.9, 127.3, 126.4, 125.4, 124.4, 124.0, 115.5, 115.2, 107.4, 42.3, 36.9, 19.4, 17.9. HRMS (ESI): m/z [M + H]$^+$ calcd for $C_{29}H_{25}N_3O_4FS$ 514.1595; found 514.1600.

Plasmid Construction, Protein Expression, and Purification. The gene sequences of PLpro encompassing SARS-CoV-2 PLpro, SARS-CoV PLpro, and MERS PLpro were synthesized, and codon-optimized. Then, SARS-CoV-2 PLpro was cloned into the pET28a-Sumo vector, while the other two variants were integrated into pET28a through homologous recombination. All three plasmid constructs were transformed into C3016H competent cells (New England Biolabs) and expressed as published previously.[29] Briefly, competent cells carrying recombinant plasmids were cultured in Luria−Bertani medium at 37 °C until the OD600 reached 0.8−1.0 and protein expression was induced by adding a final concentration of 0.5 mM IPTG (isopropyl-β-D-thiogalactopyranoside) at 18 °C overnight. The cells were harvested by centrifugation at 6000g. The cell pellets were resuspended in lysis buffer (20 mM HEPESPH = 7.4, 300 mM NaCl, 10 mM imidazole, 20 mM β-mercaptoethanol, and 1 mM PMSF) and lysed by ultrasonication. The lysate was centrifuged at 10,000g for 1 h at 4 °C, and the supernatant was loaded onto a pre-equilibrated Ni-NTA column (Qiagen). Then, the beads were washed twice with wash buffer (same composition as lysis buffer) and the protein was eluted with elution buffer (20 mM HEPES pH = 7.4, 300 mM NaCl, 300 mM imidazole, 20 mmol/L β-mercaptoethanol) and processed differently. SCoV-2 PLpro underwent cleavage by Ulp1 peptidase, and the other two PLpros with thrombin peptidase overnight at 4 °C in dialysis buffer (20 mM HEPES pH = 7.4, 100 mM NaCl, 10 mM dithiothreitol (DTT)). A second affinity step using a pre-equilibrated Ni-column was performed to collect flow through sample and further purification was achieved using a Superdex 200 10/300 size exclusion column (Cytiva) equilibrated with buffer (20 mM HEPES pH = 7.4, 100 mM NaCl, 10 mM DTT). The purified protein was then concentrated to 10 mg/mL and stored at −80 °C for subsequent analyses.

Fluorescence-Based PLpro Enzymatic Inhibition Assays. The fluorogenic substrate was designed and synthesized to test the ubiquitin C-terminal hydrolases (UCHs) to perform the PLpro enzymatic inhibition assays. PLpro could release the fluorogenic 7-amido-4-methylcoumarin (AMC) from the peptidomimetic probes Z-RLRGG-AMC, which harbored a conserved RLRGG sequence homologous to the C-terminal pentapeptide of Ubiquitin. The time-resolved fluorescence signal generated by cleaved AMC was quantified using SpectraMax iD5 (Molecular Devices, San Jose, CA) for 30 min. All assays were performed at room temperature with a 96-well coster blk/clrbtm plate (corning). The final reaction volume was 0.1 mL in the assay buffer (25 mM HEPES pH = 7.4, 100 mM NaCl, 10 mM DTT). The assays were assembled as follows: 0.1 μM SARS-CoV-2 PLpro was first incubated with different inhibitor concentrations at multiple dilution rations ranging from 0 to 50 mM at 37 °C for 10 min and the reactions were initiated by adding 1 μL of 300 μM fluorogenic substrate in assay buffer, shaken vigorously for 20 s before measuring fluorescence emission intensity at an absorption wave-length of 345 nm and an emission wavelength of 445 nm. The relative fluorescence values were reported, and the IC$_{50}$ value of the inhibitor was determined based on both the inhibitor concentration and the reaction rate of SARS-CoV-2 PLpro. The same assay was employed to assess the IC$_{50}$ of inhibitor against SARS-CoV PLpro and MERS PLpro. The initial hydrolysis rate was plotted as a function of inhibitor concentration, and IC$_{50}$ value was calculated using the dose−response−inhibition function in GraphPad Prism with [inhibitor] vs response equation. GRL0617 served as a positive control throughout the experiments.

Biotinylation of SARS-CoV-2 PLpro. Purified SARS-CoV-2 PLpro was subjected to biotinylation using the Biotin Quick Labeling Kit (Frdbbio, ARL0020K) as described before.[34] Briefly, ultrafiltration concentration was used to substitute the buffer of 1 mg protein to the marking buffer and 10 μL of biotin (10 mM) was added to incubate with 1 mg of protein at 37 °C for 30 min. Then, the redundant biotin was removed through multiple concentrating-diluting cycles utilizing ultrafiltration concentration tubs. Finally, biotin-SARS-CoV-2 PLpro

was divided into appropriate aliquots and stored at −80 °C for subsequent use.

Binding Kinetic Analysis by Biolayer Interferometry. The binding activity of SARS-CoV-2 PLpro with synthesized inhibitors was assessed via biointerference (BLI) using ForteBio Octet RED96e Analysis System. All inhibitors dissolved in 100% dimethyl sulfoxide (DMSO) were evaluated for the interaction with 50 ng/μL Biotin-SARS-CoV-2 PLpro immobilized on SSA biosensors for 1800 s in 1× PBS and dipped into inhibitors with 2-fold serial dilution ratio. After association for 100 s, dissociation was carried out in 1× PBS for 150 s. To avoid the nonspecific binding, extra SSA sensors were employed for double reference subtraction. All BLI experiments were carried out at 25 °C. Data recording and analysis were performed using ForteBio Data analysis v11.1 software. The obtained data underwent reference well subtraction and global fitting with a 1:1 model.

Thermal Shift Assay. The melting temperature of the protein-inhibitor complex was assessed by monitoring the exposure of hydrophobic amino acids as the temperature increased. First, the SARS-CoV-2 PLpro protein was incubated with different inhibitors at a 1:10 molar ratio at 4 °C overnight. Then, the reaction system was constituted by mixing 0.15 μL of 1× SYPRO Orange (Invitrogen), 0.6 μL (0.2 mg/mL) protein-inhibitor complex, and 29.25 μL 1× PBS (pH = 7.4) in white-bottom multiwell plates 96 (Roche). The plates were sealed with highly transparent optical-clear quality sealing tape (Roche) and centrifuged at 4 °C at 2000 rpm for 1 min before experiments. The plates were heated in a CFX96 Real-Time System (Bio-Rad) from 4 to 95 °C with increments of 1 °C per minute. Fluorescence changes (excitation 470 nm, emission 570 nm) in each well were recorderd in real time. Bio-Rad CFX Manager 3.0 software was employed to calculate melting temperatures. All data were recorded in triplicate and in at least two independent experiments.

Gel-Based Ub Chain Cleavage Assay. Cleavage of K48-linked diubiquitin was assessed through gel-based assays using SDS-PAGE and SYPRO Ruby staining (Invitrogen, S12001). 1 mg/mL PLpro was incubated with inhibitors at a molar ratio of 1:10, and the protein-inhibitor complex (10 μL) was then added to the reaction mixture containing 2 μL of K48-linked diubiquitin (1 mg/mL) in buffer (25 mM HEPES pH = 7.4, 100 mM NaCl, and 10 mM DTT). The reaction proceeded at 37 °C overnight and was stopped by adding 5 μL SDS loading buffer into a 20 μL mixture. Then, samples were analyzed by 15% SDS-PAGE and SYPRO Ruby staining on a rocking platform at a slow speed. Gel imaging was performed using the Bio-Rad ChemiDoc imaging system.

Cell Lines and SARS-CoV-2 Viruses. Vero E6 cells were cultured in DMEM (gibco) supplemented with 10% FBS, 1 mg/mL G418 Sulfate, and 1% penicillin streptomycin at 37 °C and 5% CO$_2$, ensuring freedom from mycoplasma contamination. SARS-CoV-2 2019-nCoV (Genbank: MT093631) and BA.1 (Genbank: OM095411) were obtained from the Institute of Laboratory Animals Sciences, Chinese Academy of Medical Sciences (CAMS). The viruses were amplified using Vero E6 cells, and virus titers were determined using 50% tissue-culture infectious doses (TCID50). Experiments were conducted in the Institute's BSL-3 laboratory, adhering to safety and security regulations.

Cytotoxicity Assay. The cytotoxicity of inhibitors was assessed in Vero E6 cells as described previously.[34] Briefly, cells (2×10^4 cells per well) were seeded on a 96-well plate, and inhibitions with serial dilution molar ratio were added into the culture for 48 h. The cell availability was assessed by measuring the absorbance of the solubilized formazan product at a specific wavelength (570 nm) with SpectraMax iD5 (Molecular Devices, San Jose, CA). The absorbance was directly proportional to the metabolic activity and viability of the cells, with higher absorbance values indicating increased cell viability. The relative cell viability at different inhibitor concentrations was analyzed by the dose−response−inhibition function in GraphPad Prism with [inhibitor] vs response equation.

Antiviral Activity Assay. The antiviral activity of inhibitors was measured by detecting the viral load reduction in the cell culture supernatant. Vero E6 cells were incubated with DMEM-containing inhibitors at different concentrations (2-fold serial dilution from 100

μM) for 1 h, followed by SARS-CoV-2 virus infection at a multiplicity of infection (MOI) of 0.1. The mixture was removed after 2 h, and fresh DMEM mixed with inhibitors were added for 48 h. The viral copies in the culture supernatant were detected by qRT-PCR with a CFX96 Real-Time System (Bio-Rad). All of the data were recorded in quartic, and the viral load reduction at different inhibitor concentrations was analyzed by the dose−response−inhibition function in GraphPad Prism with [inhibitor] vs response equation.

Hepatocyte Stability Assay. The assay was performed with hepatocytes from male mouse (Bioreclamation IVT) and pooled human (Bioreclamation IVT). Compounds were tested at 1 μM with a final hepatocyte concentration of 1 million cells/mL. The reaction was initiated by the addition of prewarmed hepatocyte working solution (2 million cells/mL) to the compound working solution (2 μM). Reaction mixtures were incubated for up to 30 min at 37 °C in a CO_2 incubator at 100 rpm. At each time point (0 and 30 min), 30 μL of the reaction mixtures were removed, and the reaction was terminated by the addition of 300 μL of ice-cold acetonitrile containing internal standard. Samples were mixed well and then were centrifuged at 4000 rpm at 4 °C for 15 min. 100 μL supernatants were removed and samples were analyzed on an AB SCIEX Q Trap 4500 employing a Kinetex C_{18} 100 Å (3.0 mm × 30 mm, 2.6 μm). Use the equation of first-order kinetics to calculate $t_{1/2}$ and CL_{int}.

Liver Microsome Stability Assay. The assay was performed with liver microsomes from male CD-1 mouse (Bioreclamation IVT) and pooled human (Corning). Compounds of interest were tested at 1 μM with a final concentration of microsomal protein of 1 mg/mL. 1.5 μL of control/test compound working solution was added to 238.5 μL of liver microsome working solution that was preincubated at 37 °C for 5 min. The reaction was started by adding 60 μL of NADPH working solution. At 0 and 30 min, 30 μL of the reaction mixture was removed to 300 μL of quenching solution. The solution was vortexed vigorously for 1 min and centrifuged at 4000 rpm at 4 °C for 15 min, and the supernatants were analyzed by liquid chromatography and tandem mass spectrometry (LC-MS/MS). The metabolic stability of compounds was evaluated using an assay by measuring the amount of parent remaining to test compounds with or without NADPH cofactor.

Pharmacokinetic Study. All animal protocols were approved by Institute Animal Care and Use Committee. The pharmacokinetic properties of compounds in mice were determined as follows. The selected compounds were subjected to pharmacokinetic studies in Balb/c mouse (male) weighing 23−25 g with three mice in the oral administration group and three mice in the intravenous injection group. The compound was administered intravenously as a solution in DMSO/PEG400/normal saline (1:4.5:4.5, v/v/v) at 5 mg/kg or oral as a suspension of 0.5% carboxymethyl cellulose at 50 mg/kg. Serial blood samples were collected by orbital venous plexus for 48 h (0.033, 0.083, 0.25, 0.5, 1, 2, 3, 4, 6, 8, 24, 48 h). Plasma samples were extracted with acetonitrile containing terfenadine as an internal standard using a 20:1 extractant-to-plasma ratio. Analyte quantitation was performed by an LC/MS/MS (Thermo Vanquish liquid chromatograph-TSQ mass spectrum). Chromatographic separation using a linear gradient was performed on a Zorbax SB C_{18} (2.1 mm × 100 mm, 3.5 μm, Agilent) with a flow rate of 0.2 mL/min at 35 °C. Mobile phase A was water and mobile phase B was methanol. Compound detection on the mass spectrometer was performed in electrospray negative ionization mode. The pharmacokinetic parameters were calculated using WinNonlin software version (Version 8.0, Pharsight, Mountain View, CA). The oral bioavailability was calculated as the ratio between the area under the curve (AUC) following intravenous administration corrected for dose ($F = (AUC_{p.o.} \times dose_{i.v.})/(AUC_{i.v.} \times dose_{p.o.}) \times 100\%$).

ASSOCIATED CONTENT

Ⓢ Supporting Information

The Supporting Information is available free of charge at https://pubs.acs.org/doi/10.1021/acs.jmedchem.4c00534.

NMR spectra of all compounds; IC_{50} test of selected 19 compounds against SARS-CoV-2 PLpro; K_D test of selected 19 compounds binding to SARS-CoV-2 PLpro; IC_{50} test of selected 4 compounds against SARS-CoV PLpro and MERS PLpro; and HPLC chromatograms of compounds **9e**, **9g**, **13b**, **13f**, **26l**, and **26r** (PDF)

Molecular formula strings (CSV)

AUTHOR INFORMATION

Corresponding Authors

Peng Li − *Beijing Key Laboratory of Active Substance Discovery and Druggability Evaluation, Institute of Materia Medica, Peking Union Medical College and Chinese Academy of Medical Sciences, Beijing 100050, P. R. China;* Ⓞ orcid.org/0000-0003-1626-3385; Email: qwerlik@imm.ac.cn

Jiangning Liu − *National Center of Technology Innovation for Animal Models, NHC Key Laboratory of Human Disease Comparative Medicine, Institute of Laboratory Animal Science, Chinese Academy of Medical Sciences and Comparative Medicine Center, Peking Union Medical College, Beijing 100021, P. R. China;* Email: liujn@cnilas.org

Sheng Cui − *NHC Key Laboratory of Systems Biology of Pathogens, National Institute of Pathogen Biology, Peking Union Medical College and Chinese Academy of Medical Sciences, Beijing 100730, P. R. China; State Key Laboratory of Respiratory Health and Multimorbidity, Peking Union Medical College and Chinese Academy of Medical Sciences, Beijing 100730, P. R. China;* Ⓞ orcid.org/0000-0001-6329-3582; Email: cui.sheng@ipb.pumc.edu.cn

Haihong Huang − *Beijing Key Laboratory of Active Substance Discovery and Druggability Evaluation, Institute of Materia Medica, Peking Union Medical College and Chinese Academy of Medical Sciences, Beijing 100050, P. R. China; State Key Laboratory of Respiratory Health and Multimorbidity, Peking Union Medical College and Chinese Academy of Medical Sciences, Beijing 100730, P. R. China;* Email: joyce@imm.ac.cn

Authors

Bo Qin − *NHC Key Laboratory of Systems Biology of Pathogens, National Institute of Pathogen Biology, Peking Union Medical College and Chinese Academy of Medical Sciences, Beijing 100730, P. R. China*

Chengwei Wu − *Beijing Key Laboratory of Active Substance Discovery and Druggability Evaluation, Institute of Materia Medica, Peking Union Medical College and Chinese Academy of Medical Sciences, Beijing 100050, P. R. China*

Binbin Zhao − *National Center of Technology Innovation for Animal Models, NHC Key Laboratory of Human Disease Comparative Medicine, Institute of Laboratory Animal Science, Chinese Academy of Medical Sciences and Comparative Medicine Center, Peking Union Medical College, Beijing 100021, P. R. China*

Gang Li − *Beijing Key Laboratory of Active Substance Discovery and Druggability Evaluation, Institute of Materia Medica, Peking Union Medical College and Chinese Academy of Medical Sciences, Beijing 100050, P. R. China; State Key Laboratory of Respiratory Health and Multimorbidity, Peking Union Medical College and Chinese Academy of Medical Sciences, Beijing 100730, P. R. China;* Ⓞ orcid.org/0000-0003-0924-7950

Baolian Wang − *Beijing Key Laboratory of Active Substance Discovery and Druggability Evaluation, Institute of Materia Medica, Peking Union Medical College and Chinese Academy of Medical Sciences, Beijing 100050, P. R. China*

Mengdie Ou − *NHC Key Laboratory of Systems Biology of Pathogens, National Institute of Pathogen Biology, Peking Union Medical College and Chinese Academy of Medical Sciences, Beijing 100730, P. R. China*

Ziheng Li − *NHC Key Laboratory of Systems Biology of Pathogens, National Institute of Pathogen Biology, Peking Union Medical College and Chinese Academy of Medical Sciences, Beijing 100730, P. R. China*

Xuli Lang − *Beijing Key Laboratory of Active Substance Discovery and Druggability Evaluation, Institute of Materia Medica, Peking Union Medical College and Chinese Academy of Medical Sciences, Beijing 100050, P. R. China*

Complete contact information is available at:
https://pubs.acs.org/10.1021/acs.jmedchem.4c00534

Author Contributions

[⊥]B.Q., C.W., and B.Z. contributed equally to this study.

Notes

The authors declare no competing financial interest.

ABBREVIATIONS USED

AcOH, acetic acid; CDI, *N,N*′-carbonyldiimidazole; CDMT, 2-chloro-4,6-dimethoxy-1,3,5-triazine; DMSO, dimethyl sulfoxide; NMM, *N*-methylmorpholine; PAGE, polyacrylamide gel electrophoresis; PLpro, papain-like protease; SAR, structure−activity relationships; SDS, sodium dodecyl sulfate; Tm, melting temperatures

REFERENCES

(1) World Health Organization. *COVID-19 Epidemiological Update.* 2023. (accessed. Dec 17th, 2023). https://www.who.int/publications/m/item/covid-19-epidemiological-update---22-december-2023.

(2) Altmann, D. M.; W, E. M.; Liu, S.; Arachchillage, D. J.; Boyton, R. J. The immunology of long COVID. *Nat. Rev. Immunol.* 2023, 23, 618−634.

(3) Li, T.; Chu, C.; Wei, B.; Lu, H. Immunity debt: Hospitals need to be prepared in advance for multiple respiratory diseases that tend to co-occur. *BioSci. Trends* 2023, 17 (6), 499−502.

(4) Velikova, T.; Georgiev, T. SARS-CoV-2 vaccines and autoimmune diseases amidst the COVID-19 crisis. *Rheumatol. Int.* 2021, 41 (3), 509−518.

(5) Hause, A. M.; Baggs, J.; Gee, J.; Marquez, P.; Myers, T. R.; Shimabukuro, T. T.; Shay, D. K. Safety Monitoring of an Additional Dose of COVID-19 Vaccine - United States, August 12-September 19, 2021. *MMWR. Morb. Mortal. Wkly. Rep.* 2021, 70 (39), 1379−1384.

(6) Li, D.; Sempowski, G. D.; Saunders, K. O.; Acharya, P.; Haynes, B. F. SARS-CoV-2 Neutralizing Antibodies for COVID-19 Prevention and Treatment. *Annu. Rev. Med.* 2022, 73 (1), 1−16.

(7) Jayk Bernal, A.; Gomes da Silva, M. M.; Musungaie, D. B.; Kovalchuk, E.; Gonzalez, A.; Delos Reyes, V.; Martín-Quirós, A.; Caraco, Y.; Williams-Diaz, A.; Brown, M. L.; et al. Molnupiravir for Oral Treatment of Covid-19 in Nonhospitalized Patients. *N. Engl. J. Med.* 2022, 386 (6), 509−520.

(8) Hammond, J.; Leister-Tebbe, H.; Gardner, A.; Abreu, P.; Bao, W.; Wisemandle, W.; Baniecki, M.; Hendrick, V. M.; Damle, B.; Simón-Campos, A.; et al. Oral Nirmatrelvir for High-Risk, Non-hospitalized Adults with Covid-19. *N. Engl. J. Med.* 2022, 386 (15), 1397−1408.

(9) Gammeltoft, K. A.; Zhou, Y.; Ryberg, L. A.; Pham, L. V.; Binderup, A.; Hernandez, C. R. D.; Offersgaard, A.; Fahnoe, U.; Peters, G. H. J.; Ramirez, S.; et al. Substitutions in SARS-CoV-2 Mpro Selected by Protease Inhibitor Boceprevir Confer Resistance to Nirmatrelvir. *Viruses* 2023, 15 (9), 1970.

(10) Hashemian, S. M. R.; Sheida, A.; Taghizadieh, M.; Memar, M. Y.; Hamblin, M. R.; Bannazadeh Baghi, H.; Sadri Nahand, J.; Asemi, Z.; Mirzaei, H. Paxlovid (Nirmatrelvir/Ritonavir): A new approach to Covid-19 therapy? *Biomed. Pharmacother.* 2023, 162, No. 114367.

(11) McLean, G.; Kamil, J.; Lee, B.; Moore, P.; Schulz, T. F.; Muik, A.; Sahin, U.; Tureci, O.; Pather, S. The Impact of Evolving SARS-CoV-2 Mutations and Variants on COVID-19 Vaccines. *mBio* 2022, 13 (2), e0297921.

(12) Zhao, T.; Hu, C.; Ahmed, M. A.; et al. Warnings regarding the potential coronavirus disease 2019 (COVID-19) transmission risk: Vaccination is not enough. *Infect. Control Hosp. Epidemiol.* 2022, 43 (5), 679−680.

(13) Tam, D.; Lorenzo-Leal, A. C.; Hernandez, L. R.; Bach, H. Targeting SARS-CoV-2 Non-Structural Proteins. *Int. J. Mol. Sci.* 2023, 24 (16), 13002.

(14) Santos-Mendoza, T. The Envelope (E) Protein of SARS-CoV-2 as a Pharmacological Target. *Viruses* 2023, 15 (44) 1000.

(15) Ton, A.-T.; Pandey, M.; Smith, J. R.; Ban, F.; Fernandez, M.; Cherkasov, A. Targeting SARS-CoV-2 papain-like protease in the postvaccine era. *Trends Pharmacol. Sci.* 2022, 43 (11), 906−919.

(16) Shin, D.; Mukherjee, R.; Grewe, D.; Bojkova, D.; Baek, K.; Bhattacharya, A.; Schulz, L.; Widera, M.; Mehdipour, A. R.; Tascher, G.; et al. Papain-like protease regulates SARS-CoV-2 viral spread and innate immunity. *Nature* 2020, 587 (7835), 657−662.

(17) Ratia, K.; Pegan, S.; Takayama, J.; Sleeman, K.; Coughlin, M.; Baliji, S.; Chaudhuria, R.; Fu, W.; Prabhakard, B. S.; Johnson, M. E.; Baker, S. C.; Ghoshb, A. K.; Mesecara, A. D. A noncovalent class of papain-like protease/deubiquitinase inhibitors blocks SARS virus replication. *Proc. Natl. Acad. Sci. U.S.A.* 2008, 105, 16119−16124.

(18) Ratia, K.; Saikatendu, K. S.; Santarsiero, B. D.; Barretto, N.; Baker, S. C.; Stevens, R. C.; Mesecar, A. D. Severe acute respiratory syndrome coronaviruspapain-like protease: Structure of a viraldeubiquitinating enzyme. *Proc. Natl. Acad. Sci. U.S.A.* 2006, 103, 5717−5722.

(19) Ghosh, A. K.; Takayama, J.; Rao, K. V.; Ratia, K.; Chaudhuri, R.; Mulhearn, D. C.; Lee, H.; Nichols, D. B.; Baliji, S.; Baker, S. C.; et al. Severe Acute Respiratory Syndrome Coronavirus Papain-like Novel Protease Inhibitors: Design, Synthesis, Protein−Ligand X-ray Structure and Biological Evaluation. *J. Med. Chem.* 2010, 53 (13), 4968−4979.

(20) Subissi, L.; Imbert, I.; Ferron, F.; Collet, A.; Coutard, B.; Decroly, E.; Canard, B. SARS-CoV ORF1b-encoded nonstructural proteins 12−16: Replicative enzymes as antiviral targets. *Antiviral Res.* 2014, 101, 122−130.

(21) Valipour, M. Chalcone-amide, a privileged backbone for the design and development of selective SARS-CoV/SARS-CoV-2 papain-like protease inhibitors. *Eur. J. Med. Chem.* 2022, 240, 114572.

(22) Shen, Z.; Ratia, K.; Cooper, L.; Kong, D.; Lee, H.; Kwon, Y.; Li, Y.; Alqarni, S.; Huang, F.; Dubrovskyi, O.; et al. Design of SARS-CoV-2 PLpro Inhibitors for COVID-19 Antiviral Therapy Leveraging Binding Cooperativity. *J. Med. Chem.* 2022, 65 (4), 2940−2955.

(23) Ghosh, A. K.; Takayama, J.; Aubin, Y.; Ratia, K.; Chaudhuri, R.; Baez, Y.; Sleeman, K.; Coughlin, M.; Nichols, D. B.; Mulhearn, D. C.; et al. Structure-Based Design, Synthesis, and Biological Evaluation of a Series of Novel and Reversible Inhibitors for the Severe Acute Respiratory Syndrome−Coronavirus Papain-Like Protease. *J. Med. Chem.* 2009, 52 (16), 5228−5240.

(24) Zhao, Y.; Du, X.; Duan, Y.; Pan, X.; Sun, Y.; You, T.; Han, L.; Jin, Z.; Shang, W.; Yu, J.; et al. High-throughput screening identifies established drugs as SARS-CoV-2 PLpro inhibitors. *Protein & Cell* 2021, 12 (11), 877−888.

(25) Klemm, T.; Ebert, G.; Calleja, D. J.; Allison, C. C.; Richardson, L. W.; Bernardini, J. P.; Lu, B. G.; Kuchel, N. W.; Grohmann, C.; Shibata, Y.; et al. Mechanism and inhibition of the papain-like protease, PLpro, of SARS-CoV-2. *EMBO J.* **2020**, *39* (18), e106275.

(26) Freitas, B. T.; Durie, I. A.; Murray, J.; Longo, J. E.; Miller, H. C.; Crich, D.; Hogan, R. J.; Tripp, R. A.; Pegan, S. D. Characterization and Noncovalent Inhibition of the Deubiquitinase and deISGylase Activity of SARS-CoV-2 Papain-Like Protease. *ACS Infect. Dis.* **2020**, *6* (8), 2099−2109.

(27) Fu, Z.; Huang, B.; Tang, J.; Liu, S.; Liu, M.; Ye, Y.; Liu, Z.; Xiong, Y.; Zhu, W.; Cao, D.; et al. The complex structure of GRL0617 and SARS-CoV-2 PLpro reveals a hot spot for antiviral drug discovery. *Nat. Commun.* **2021**, *12* (1), 488.

(28) Cho, H.; Kim, Y. J.; Chae, J. W.; Meyer, M. R.; Kim, S. K.; Ryu, C. S. *In vitro* metabolic characterization of the SARS-CoV-2 papain-like protease inhibitors GRL0617 and HY-17542. *Front. Pharmacol.* **2023**, *14*, 1067408.

(29) Gao, X.; Qin, B.; Chen, P.; Zhu, K.; Hou, P.; Wojdyla, J. A.; Wang, M.; Cui, S. Crystal structure of SARS-CoV-2 papain-like protease. *Acta Pharm. Sin. B* **2021**, *11* (1), 237−245.

(30) Welker, A.; Kersten, C.; Müller, C.; Madhugiri, R.; Zimmer, C.; Müller, P.; Zimmermann, R.; Hammerschmidt, S.; Maus, H.; Ziebuhr, J.; et al. Structure-Activity Relationships of Benzamides and Isoindolines Designed as SARS-CoV Protease Inhibitors Effective against SARS-CoV-2. *ChemMedChem* **2021**, *16* (2), 340−354.

(31) Wang, Z.; Zhang, H.; Jabeen, F.; Gopinathan-Pillai, G.; Arami, J. A.; Killian, B. J.; Stiegler, K. D.; Yudewitz, D. S.; Thiemann, P. L.; Turk, J. D.; et al. Synthesis and Properties of Energetic 1,2,4-Oxadiazoles. *Eur. J. Org. Chem.* **2015**, *2015* (34), 7468−7474.

(32) Ramu, T.; Prasanthi, S.; Mangarao, N.; Basha, G. M.; Srinuvasarao, R.; Siddaiah, V. A Simple and Straightforward Protocol to 3,5-Disubstituted 1,2,4-Oxadiazoles from Carboxylic Acids. *Chem. Lett.* **2013**, *42* (7), 722−724.

(33) Xiang, Y.; Hirth, B.; Kane, J. L.; Liao, J.; Noson, K. D.; Yee, C.; Asmussen, G.; Fitzgerald, M.; Klaus, C.; Booker, M. Discovery of novel sphingosine kinase-1 inhibitors. Part 2. *Bioorg. Med. Chem. Lett.* **2010**, *20* (15), 4550−4554.

(34) Qin, B.; Li, Z.; Tang, K.; Wang, T.; Xie, Y.; Aumonier, S.; Wang, M.; Yuan, S.; Cui, S. Identification of the SARS-unique domain of SARS-CoV-2 as an antiviral target. *Nat. Commun.* **2023**, *14* (1), 3999.